

1-1-2007

# Association of Smooth Muscle Myosin and its Carboxyl Isoforms with Actin Isoforms in Aorta Smooth Muscle

Jason Edward Black

Follow this and additional works at: <http://mds.marshall.edu/etd>



Part of the [Musculoskeletal, Neural, and Ocular Physiology Commons](#)

---

## Recommended Citation

Black, Jason Edward, "Association of Smooth Muscle Myosin and its Carboxyl Isoforms with Actin Isoforms in Aorta Smooth Muscle" (2007). *Theses, Dissertations and Capstones*. Paper 489.

**Association of Smooth Muscle Myosin and its Carboxyl  
Isoforms with Actin Isoforms in Aorta Smooth Muscle**

**By**

**Jason Edward Black**

**Dissertation submitted to  
the Graduate College  
of  
Marshall University  
in partial fulfillment of the requirements  
for the degree of**

**Doctor of Philosophy  
in  
Biomedical Sciences**

**Approved by**

**Elizabeth C. Bryda  
Todd L. Green  
William McCumbee  
Michael Moore  
Gary L. Wright, Committee Chairperson**

**Department of Pharmacology, Physiology, and Toxicology**

# **ABSTRACT**

## **Association of Smooth Muscle Myosin and its Carboxyl Isoforms with Actin**

### **Isoforms in Aorta Smooth Muscle**

**By Jason Edward Black**

The contraction mechanism of smooth muscle is not fully understood. The primary interaction that leads to the formation of tension, the myosin-actin crossbridge, has been studied extensively. However, even this aspect of the contraction has proven not to be as simple as it might seem. There are several isoforms of smooth muscle myosin and actin, and the differences in the activities of these isoforms and their interactions during the contractile process are largely unknown. The studies to be discussed are directed at the determination of the interaction of these isoforms during the contraction of rat aortic smooth muscle. Chapter II describes the association of smooth muscle myosin with two of the actin isoforms found in smooth muscle,  $\alpha$ -actin and  $\beta$ -actin, using a novel method of fluorescence resonance energy transfer (FRET) to examine this association in both the A7r5 cell model and in intact tissue. We show that the contractile apparatus undergoes significant remodeling during contraction and that the interaction of myosin with  $\alpha$ -actin and  $\beta$ -actin is different at the various time points of contraction. In Chapter III, we describe more detailed experiments examining the two different myosin tail isoforms, SM1 and SM2. The results of these studies confirm our findings of remodeling of the cytoskeleton and the contractile apparatus during contraction and show that  $\alpha$ -actin and  $\beta$ -actin interact differently with these myosin isoforms. The results provide the first direct evidence of contractile remodeling in smooth muscle and suggest that complex changes in actin-myosin interaction may be important in the contraction of this muscle type.

## **DEDICATION**

True to my nickname (Church Guy) that Dr. Wright gave me, I want first and foremost to thank my gracious and loving Savior, Jesus, for His patience that He shows and strength that He gives day after day. I would have no life without Him.

I want to thank my wonderful parents who raised four very different children and enabled each of us to embrace our individual personalities and to pursue the goals we wanted. With this degree I will finally move out of their house. Thanks for your patience!

I am thankful for my siblings and their families. They help to remove my mind from the ivory tower every now and then and place me in everyday life. They have given me great models of how I would like my future family to be, if ever it happens.

I finally want to thank the two churches, Crown City Community Church and Crew Community Church, that I was a part of during my time in graduate school and the friends that I made during my time there. Thank you for showing me how to live and challenging me to strive to make the world a better place. A special thanks to Rich, thanks for encouraging me to keep asking questions in search of the truth.

## ACKNOWLEDGEMENTS

I feel like I have attended graduate school twice during my time at Marshall. I want to thank my first lab, the Bryda lab, for introducing me to the world of research. Thanks Dustin for teaching me Western blotting, among other things. Thanks Sarah for encouraging me to be a better researcher and showing me how. Thanks Josh and Jennifer for being friends. Also, Thanks to Ian for being the best lab technician I have worked with. Also, thanks to those in the Microbiology Department for all the ways to helped me and taught me even after I had changed labs.

Thanks Brandi, my second favorite lab tech, and to Ryan for helping with the ApoA1 project, although not much came of it.

Thanks to Ava, Sean and Dawn for making my transition into the Wright lab as easy as possible.

Thanks for all your help and your friendship. Thanks to Aileen for knocking some sense into me every now and then. Thanks Kan, Nancy, and the many other graduate students, technicians, etc. that were always ready to help me or to talk about whatever, thanks so much.

Thanks to my committee:

Dr. Moore, thanks for kind words and challenging questions

Dr. McCumbee for all your help in the ApoA1 world, but also for challenging life questions

Dr. Green, thanks for all the things you let me borrow, I hope you forgive my tab

Dr. Bryda, thanks for being a great mentor in the beginning and a great friend through it all

Finally, Dr. Wright thanks for challenging and mentoring me and for giving me a lab to join when I needed to make a big change. I at least owe the last half of my Graduate career to you!

## Table of Contents

<b>ABSTRACT.....</b>	<b>ii</b>
<b>DEDICATION.....</b>	<b>iii</b>
<b>ACKNOWLEDGEMENTS.....</b>	<b>iv</b>
<b>TABLE OF CONTENTS.....</b>	<b>v</b>
<b>LIST OF FIGURES.....</b>	<b>vii</b>
<b>LIST OF TABLES.....</b>	<b>ix</b>
<b>LIST OF SYMBOLS/ABBREVIATIONS.....</b>	<b>xi</b>
<b>CHAPTER I.....</b>	<b>1</b>
GENERAL INTRODUCTION.....	1
DISSERTATION ORGANIZATION.....	1
SMOOTH MUSCLE CONTRACTION.....	1
CYTOSKELETAL REMODELING.....	10
MYOSIN REMODELING.....	12
THE FAMILIES OF MYOSIN.....	14
SMOOTH MUSCLE MYOSIN.....	17
FUNCTION OF MYOSIN ISOFORMS.....	28
FLUORESCENCE RESONANCE ENERGY TRANSFER (FRET).....	32
REFERENCES.....	36
<b>CHAPTER II.....</b>	<b>51</b>
FRET ANALYSIS OF ACTIN/MYOSIN INTERACTION IN CONTRACTING RAT AORTIC SMOOTH MUSCLE.....	51
ABSTRACT.....	52

INTRODUCTION.....	53
METHODS.....	55
RESULTS.....	60
DISCUSSION.....	76
REFERENCES.....	79
<b>CHAPTER III.....</b>	<b>84</b>
MYOSIN ISOFORM INTERACTION WITH ACTIN ISOFORMS IN A7R5 CELLS AND RAT AORTA SMOOTH MUSCLE.....	84
ABSTRACT.....	85
INTRODUCTION.....	86
METHODS.....	88
RESULTS.....	94
DISCUSSION.....	109
REFERENCES.....	112
<b>CHAPTER IV.....</b>	<b>117</b>
SUMMARY AND CONCLUSION.....	117
GENERAL DISCUSSION.....	117
FUTURE WORK.....	119
CURRICULUM VITAE.....	121

## LIST OF FIGURES

### CHAPTER I. GENERAL INTRODUCTION

Figure 1. Model of proposed smooth muscle ‘sarcomere’	2
Figure 2. Smooth muscle contraction mechanism	4
Figure 3. Myosin/actin interaction during crossbridge cycling	6
Figure 4. Smooth muscle relaxation mechanism	7
Figure 5. Proposed model for role of HSP27 in smooth muscle contraction	8
Figure 6. Model of formation of myosin filaments by myosin monomers	13
Figure 7. Structure of myosin II	15
Figure 8. Diagram of smooth muscle myosin heavy chain isoforms	26

### CHAPTER II. FRET ANALYSIS OF ACTIN/MYOSIN INTERACTION IN CONTRACTING RAT AORTIC SMOOTH MUSCLE

Figure 1. Time intervals selected for FRET analysis of rat aortic smooth muscle	64
Figure 2. Dual immunostaining of $\alpha$ -actin and myosin in A7r5 cells	65
Figure 3. FRET analysis of $\alpha$ -actin/myosin complex in A7r5 cells	66
Figure 4. Dual immunostaining of $\beta$ -actin and myosin in A7r5 cells	67
Figure 5. FRET analysis of $\beta$ -actin/myosin complex in A7r5 cells	68
Figure 6. Rat aortic smooth muscle dual stained with phalloidin and TO-PRO-3 iodide	69
Figure 7. Dual staining of a control tissue section for $\alpha$ -actin and myosin	70
Figure 8. FRET analysis of $\alpha$ -actin/myosin in aortic tissue section	71
Figure 9. FRET images showing $\alpha$ -actin/myosin structure in relation to cell nuclei	72



### **CHAPTER III. MYOSIN ISOFORM INTERACTION WITH ACTIN ISOFORMS IN A7R5**

#### **CELLS AND RAT AORTA SMOOTH MUSCLE**

Figure 1. Dual immunostaining of $\alpha$ -actin and SM2 in A7r5 cells	97
Figure 2. Dual immunostaining of $\beta$ -actin and SM2 in A7r5 cells	98
Figure 3. Dual immunostaining of $\alpha$ -actin and SM1 in A7r5 cells	99
Figure 4. Dual immunostaining of $\beta$ -actin and SM1 in A7r5 cells	100
Figure 5. Dual immunostaining of $\alpha$ -actin and SM2 in aorta tissue	101
Figure 6. Dual immunostaining of $\beta$ -actin and SM2 in aorta tissue	102
Figure 7. Dual immunostaining of $\alpha$ -actin and SM1 in aorta tissue	103
Figure 8. Dual immunostaining of $\beta$ -actin and SM1 in aorta tissue	104
Figure 9. Western blot of $\alpha$ -actin co-immunoprecipitation	105
Figure 10. Western blot of $\beta$ -actin co-immunoprecipitation	106

## LIST OF TABLES

### CHAPTER II. FRET ANALYSIS OF ACTIN/MYOSIN INTERACTION IN CONTRACTING RAT AORTIC SMOOTH MUSCLE

- Table 1. Fluorescence resonance energy transfer (FRET) analysis of the association of myosin with  $\alpha$ - and  $\beta$ -actin in Control and PDBu-stimulated A7r5 cells 73
- Table 2. FRET analysis of the association of myosin with  $\alpha$ - and  $\beta$ -actin in rat aortic smooth muscle 74
- Table 3. F-actin content of tissue sections obtained from aortic segments before contraction with PDBu, at the beginning of force development, approximately midway through the contraction, and after the plateau in force development 75

### CHAPTER III. MYOSIN ISOFORM INTERACTION WITH ACTIN ISOFORMS IN A7R5 CELLS AND RAT AORTA SMOOTH MUSCLE

- Table 1. Fluorescence resonance energy transfer (FRET) analysis of the association of SM2 myosin with  $\alpha$ - and  $\beta$ -actin in Control and PDBu-stimulated A7r5 cells. 107
- Table 2. Fluorescence resonance energy transfer (FRET) analysis of the association of SM1 myosin with  $\alpha$ - and  $\beta$ -actin in Control and PDBu-stimulated A7r5 cells. 107

Table 3. Fluorescence resonance energy transfer (FRET) analysis of the association of SM2 myosin with  $\alpha$ - and  $\beta$ -actin in Control, Beginning, Midpoint, and Endpoint time points of PDBu-stimulated rat aorta smooth muscle tissue. 108

Table 4. Fluorescence resonance energy transfer (FRET) analysis of the association of SM1 myosin with  $\alpha$ - and  $\beta$ -actin in Control, Beginning, Midpoint, and Endpoint time points of PDBu-stimulated rat aorta smooth muscle tissue. 108

Table 5. Co-immunoprecipitation experiment results. 109

## LIST OF SYMBOLS/ABBREVIATIONS

<b>Å</b>	angstrom
<b>ADP</b>	adenosine diphosphate
<b>ANOVA</b>	analysis of variance
<b>ATP</b>	adenosine triphosphate
<b>AVM</b>	arteriovenous malformations
<b>CaM</b>	calmodulin
<b>CaP</b>	calponin
<b>CCD</b>	charge coupled device
<b>cDNA</b>	complementary DNA
<b>CO<sub>2</sub></b>	carbon dioxide
<b>CPI-17</b>	protein kinase C-dependent phosphatase inhibitor – 17 kDa
<b>DAG</b>	diacylglycerol
<b>DMEM</b>	Dulbecco's modified Eagle's medium
<b>E</b>	transfer efficiency
<b>EB</b>	esophageal body
<b>ELC</b>	essential light chain
<b>ERK</b>	Extracellular-signal-regulated kinase
<b>F-actin</b>	filamentous actin
<b>F<sub>d</sub></b>	fluorescence of the donor in the absence of the acceptor
<b>F<sub>da</sub></b>	fluorescence of the donor in the presence of the acceptor
<b>FRET</b>	fluorescence resonance energy transfer
<b>GTP</b>	guanosine triphosphate

<b>HSP20</b>	heat shock protein – 20 kDa
<b>HSP27</b>	heat shock protein – 27 kDa
<b>IP<sub>3</sub></b>	inositol, 1,4,5-trisphosphate
<b>J</b>	overlap integral between donor emission spectrum and acceptor absorption spectrum
<b>k</b>	dipole orientation factor
<b>LES</b>	lower esophageal sphincter
<b>LC17</b>	17 kDa light chain – essential light chain
<b>MAPK</b>	mitogen-activated protein kinase
<b>MHC</b>	myosin heavy chain
<b>MLC</b>	myosin light chain
<b>MLCK</b>	myosin light chain kinase
<b>MLCP</b>	myosin light chain phosphatase
<b>mRNA</b>	messenger RNA
<b>n</b>	refractive index of the medium
<b>NM-A</b>	non-muscle myosin A
<b>NM-B</b>	non-muscle myosin B
<b>NMMHC</b>	non-muscle myosin heavy chain
<b>nt</b>	nucleotide
<b>PBOO</b>	partial bladder outlet obstruction
<b>PBS</b>	phosphate-buffered saline
<b>PDBu</b>	phorbol-12, 13-dibutyrate

<b>PKA</b>	protein kinase A
<b>PKC</b>	protein kinase C
<b>PKG</b>	protein kinase G
<b>PMA</b>	phorbol 12-myristate 13-acetate
<b>PVDF</b>	polyvinylidene fluoride
<b>Q<sub>o</sub></b>	quantum yield of the donor
<b>r</b>	distance between two donor and acceptor in FRET system
<b>R<sub>o</sub></b>	Förster distance
<b>RLC</b>	regulatory light chain
<b>ROCK</b>	Rho-associated kinase
<b>SR</b>	sarcoplasmic reticulum
<b>SDS-PAGE</b>	sodium dodecyl sulfate polyacrylamide gel electrophoresis
<b>SEM</b>	standard error of the mean
<b>Sm1</b>	204 kDa smooth muscle myosin tail isoform
<b>Sm2</b>	200 kDa smooth muscle myosin tail isoform
<b>SM-A</b>	smooth muscle myosin heavy chain head isoform without insert
<b>SM-B</b>	smooth muscle myosin heavy chain head isoform with insert
<b>SMC</b>	smooth muscle cells
<b>SMHC</b>	smooth muscle myosin heavy chain
<b>TL</b>	tailless
<b>V<sub>max</sub></b>	maximum enzymatic velocity
<b>WT</b>	wild type
<b>ZIP</b>	zipper-interacting protein kinase

# Chapter I

## General Introduction

### Dissertation Organization

This dissertation will be presented in four chapters. The first chapter is a review of the relevant topics that will be addressed in the chapters that follow. Chapter two is a manuscript that has been submitted to *Acta Physiologica* and is currently under review at the time of this writing. This chapter addresses the remodeling of myosin in both the A7r5 cell model and in rat aortic smooth muscle and myosin's interaction with actin isoforms. We found that myosin does appear to remodel during contraction and that its interaction with  $\alpha$ -actin appears to be quite different from its interaction with  $\beta$ -actin. The third chapter is a manuscript that will soon be submitted that examines the remodeling of the smooth muscle myosin tail isoforms and their association with actin isoforms in both cell and tissue models. The myosin isoforms were found to interact differently with the two actin isoforms studied. Both studies used confocal microscopy and a novel fluorescent resonance energy transfer technique developed in our laboratory. The final chapter examines and discusses the results of the two manuscripts and addresses the possible future studies that could be performed.

### Smooth muscle contraction

Smooth muscle contraction is an integral part of mammalian physiology. It is responsible for the motility of food through the digestive tract as well as the transport of blood and the regulation of blood pressure throughout the cardiovascular system. It is

also present in hollow organs such as the urinary bladder and in the air passages of the respiratory system.

There are many differences between smooth muscle contraction and that of skeletal or cardiac muscle. Striated muscle derives its name from the presence of repetitive structures (sarcomeres) which are absent in smooth muscle. Some studies have suggested the presence of repetitive sarcomere-like structures (Figure 1) in smooth muscle (Herrera et al. 2005). In this structure, dense bodies replace the Z-bands that are seen in skeletal muscle, but actin remains the primary component of the thin filaments and myosin remains the primary component of the thick filaments. The contractile filaments are thought to be arranged in parallel to the longitudinal axis in smooth muscle with the actin filaments attached to dense plaques at the cell membrane. These in turn are attached to other dense plaques in adjacent cells, allowing these cells to act as a mechanical syncytium and to function as a group (Kuo and Seow 2004). However, it should be noted that this model remains speculative and conclusive evidence for its validity remains to be obtained.

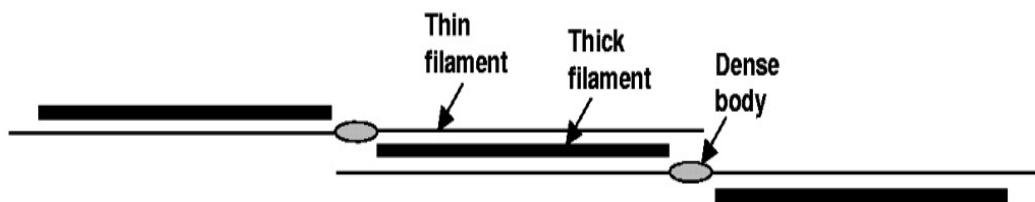


**Figure 1:** Model of the proposed smooth muscle ‘sarcomere’ with dense bodies replacing the more well-known Z-bands that are seen in the sarcomere of skeletal muscle. Modified from Herrera et al. (2005).



Skeletal muscle responds much more quickly (milliseconds) to stimuli than smooth muscle, which takes one to three seconds to respond (Guyton and Hall 2000). However, smooth muscle has been shown to better maintain contraction with less energy expenditure than skeletal muscle (Paul 1983). Another difference is that for contraction to occur in skeletal muscle, the apparatus needs to be de-inhibited, but in smooth muscle the apparatus must be activated. The average force exerted by smooth muscle myosin has been found to be three times that exerted by the myosin of skeletal muscle (VanBuren et al. 1994). Smooth muscle contraction in its entirety may not be as well understood as that of skeletal muscle, but several components and pathways have been described.

The primary pathway of smooth muscle contraction (Figure 2) is initiated by the influx of  $\text{Ca}^{2+}$  into the cytosol of smooth muscle cells (Vorotnikov et al. 2002; Webb 2003). The influx of these ions is from the extracellular space and is caused by the opening of ligand-operated calcium channels in the membrane. The resulting increase in intracellular calcium is supplemented with  $\text{Ca}^{2+}$  released from the sarcoplasmic reticulum. The neural agonist, norepinephrine, binds to a receptor which increases the activity of phospholipase C in the cell membrane in conjunction with a G protein. RhoA plays a significant role in mediating this G protein pathway (Fujihara et al. 1997), which results in the production of inositol 1,4,5-trisphosphate ( $\text{IP}_3$ ) and diacylglycerol (DAG) from phosphatidylinositol 4,5-bisphosphate.  $\text{IP}_3$  signals the sarcoplasmic reticulum to release  $\text{Ca}^{2+}$  and DAG activates the protein kinase C (PKC) pathway (Webb 2003).

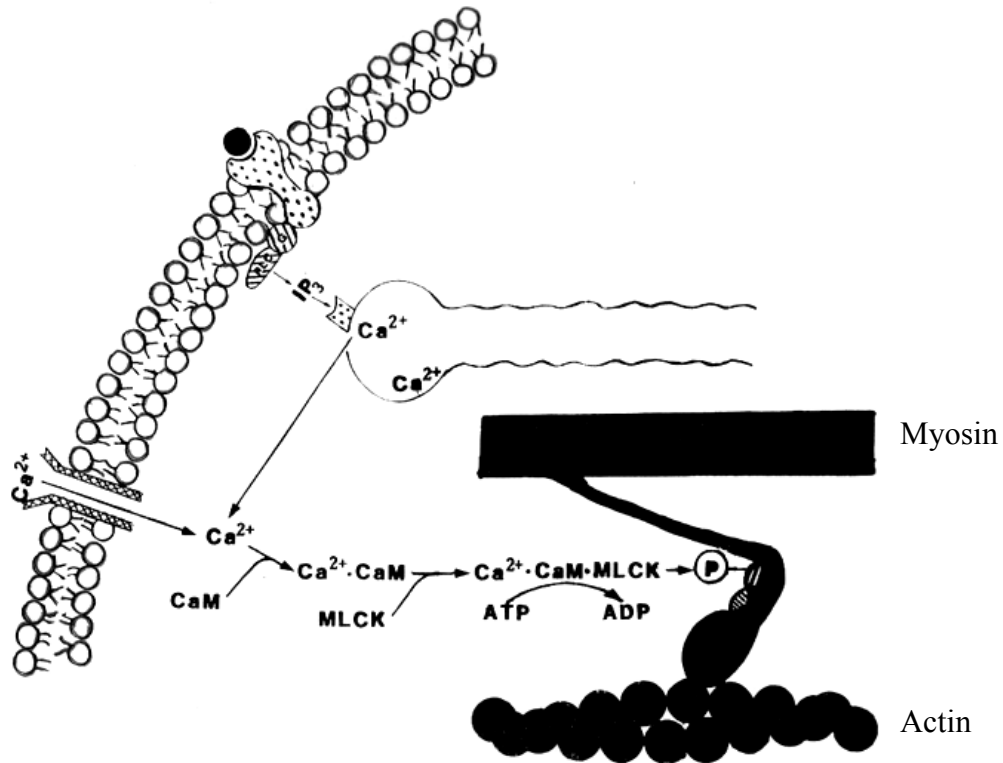
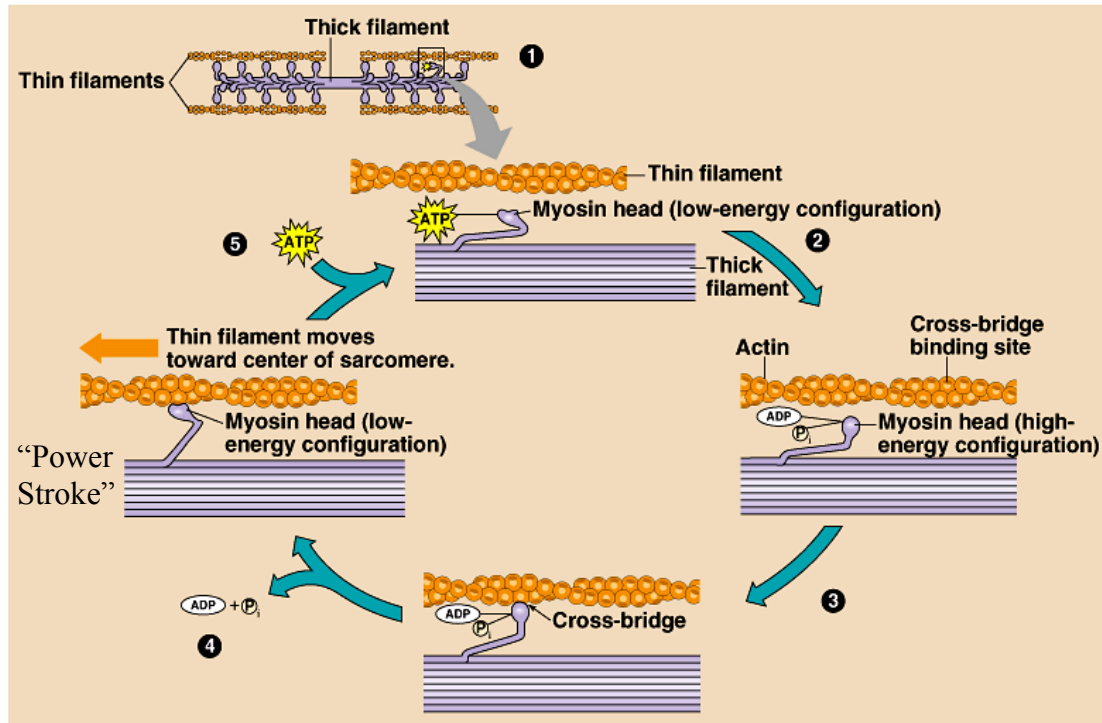


**Figure 2:** Contraction mechanism of smooth muscle showing the result of extracellular  $\text{Ca}^{2+}$  and the agonist activation of contraction.  $\text{Ca}^{2+}$  enters the cytoplasm mostly from the extracellular space; however, some enters from the sarcoplasmic reticulum (SR). An agonist binds to a receptor that is associated with a G-protein and phospholipase C catalyzes the production of  $\text{IP}_3$  and DAG (not shown) and  $\text{IP}_3$  causes release of  $\text{Ca}^{2+}$  from the SR.  $\text{Ca}^{2+}$  binds to CaM, that complex binds to and activates MLCK. This complex phosphorylates the myosin RLC, activating myosin to bind actin. Modified from Barany (1996).

Calmodulin (CaM) is activated when four  $\text{Ca}^{2+}$  ions are bound forming Ca/CaM, and this complex then activates myosin light chain kinase (MLCK) by binding to it. The Ca/CaM/MLCK complex is responsible for phosphorylating the regulatory light chain (RLC) of smooth muscle myosin II. This phosphorylation activates the myosin and enables it to bind to actin filaments. Work in our laboratory also suggests that MLCK

plays a structural role, keeping myosin and actin filaments in register, and then allowing the filaments to slide during contraction. (Thatcher, et al. in review)

Ca/CaM may also aid in preparing the actin filaments for myosin binding by de-inhibiting the actin filament via alterations in caldesmon (Vorotnikov et al. 2002). Caldesmon is a protein that has been shown to bind to actin thin filaments. Caldesmon also has domains that bind to another thin filament protein, tropomyosin. Caldesmon has also been shown to bind to myosin (Gusev 2001) and to inhibit its ATPase activity (Gorenne et al. 2004) as a result of its secondary binding to actin filaments (Borovikov et al. 2004). How this inhibition mechanism operates has been a matter of debate, but may center around the ability of this molecule to engage the tropomyosin molecule in opposition to myosin movement (Graceffa and Mazurkie 2005). Together these results suggest that although the full effect of caldesmon on smooth muscle contraction is not known, the molecule does have a role in the association of myosin with actin and the resulting contraction. Once myosin is activated by the phosphorylation of at least one of the RLCs (Rovner et al. 2006), the myosin head then binds to actin and forms the actin-myosin crossbridge. Myosin will stay attached to the actin filament until ATP binds to the myosin head. Myosin hydrolyzes ATP into ADP and Pi and converts this chemical energy into mechanical energy. The myosin head binds to the actin filament and with the release of the ADP and Pi from the myosin molecule performs the “power stroke” pulling actin. Figure 3 illustrates this myosin/actin crossbridge cycle. Contraction is terminated once myosin is inactivated by the dephosphorylation of the regulatory light chain by myosin light chain phosphatase (MLCP).



Copyright © Pearson Education, Inc., publishing as Benjamin Cummings.

**Figure 3:** The interaction of myosin with actin fibers during crossbridge cycling in muscle contraction. [fig.cox.miami.edu/~cmallery/150/neuro/c49x33muscle-cycle.jpg](http://fig.cox.miami.edu/~cmallery/150/neuro/c49x33muscle-cycle.jpg)

MLCP is the primary phosphatase for removing the phosphate from the regulatory light chain of myosin and initiating relaxation of the smooth muscle cell (Figure 4). MLCP is regulated in multiple ways. CPI-17, which is activated by PKC, is the primary inhibitor of MLCP. MLCP can also be inhibited by Rho kinase via the ZIP kinase pathway. The inhibition of MLCP results in the myosin light chain remaining phosphorylated longer which increases contraction of the smooth muscle cell.

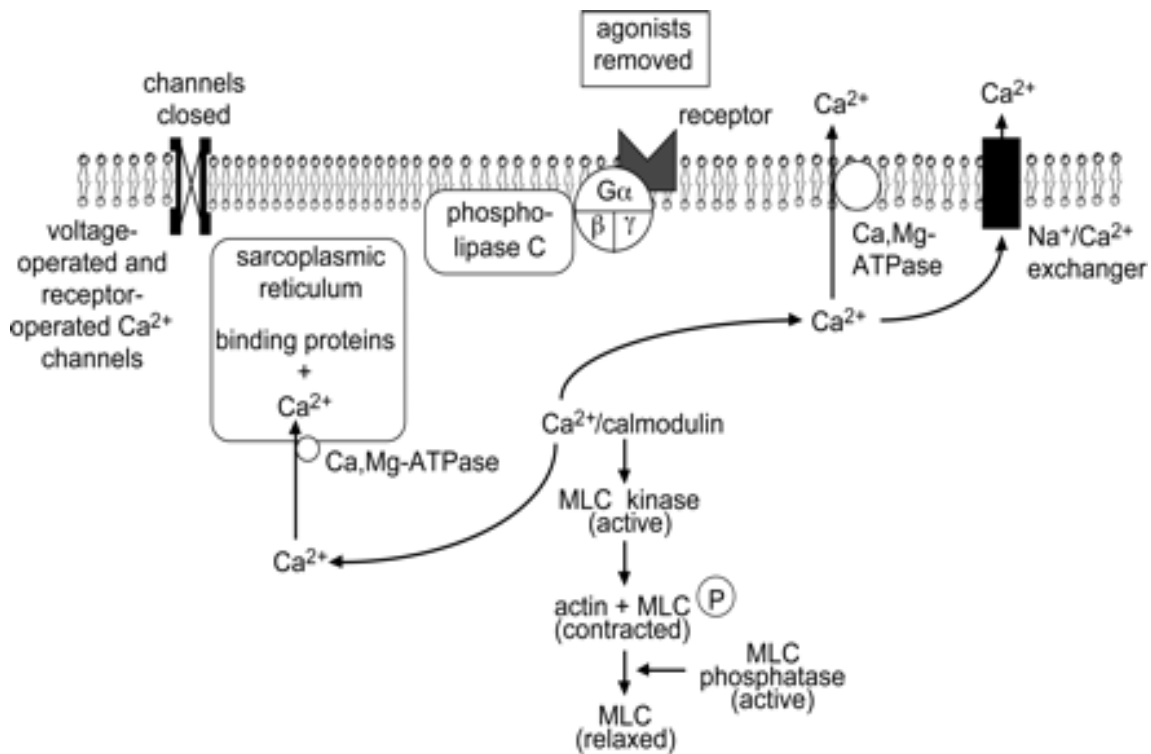


**Figure 4:** Smooth muscle relaxation mechanism illustrating the expelling of Ca<sup>2+</sup> from the intercellular space and the activity of MLCP dephosphorylating MLC. (Webb 2003).

The activity of PKC can also lead directly to the activation of myosin. PKC can phosphorylate MAP kinase, which can then activate MLCK. MAP kinase can also phosphorylate and deactivate caldesmon, preparing actin for myosin binding. PKC has also been shown to induce actin rearrangements (Brandt et al. 2002). In studies using myosin II heavy chain knockout mice, cerebral arteries were only able to contract when treated with PMA, which works through the PKC pathway, but did not contract when treated with K<sup>+</sup>. However, control vessels contracted under both treatments (Lohn et al. 2002). Based on these observations, the authors suggested that another motor protein operates under the influence of the PKC pathway.

There are potentially other proteins that play roles in the contraction of smooth muscle that are not yet fully understood. Heat shock proteins (HSPs) HSP27 and HSP20 have been found to be involved in contraction and relaxation, respectively, of smooth muscle. HSP27 can be phosphorylated by PKC and can lead to the contraction of smooth muscle (Bitar et al. 1991). HSP20 is phosphorylated by PKA and PKG and this activation has been found to lead to relaxation of smooth muscle (Brophy et al. 1999; Brophy et al. 1999). How these molecules perform these actions is not fully understood. HSP27 has been found to form filaments and it is thought that these may bind to actin and tropomyosin (Somara and Bitar 2004) helping to inhibit myosin attaching to the actin filament (Figure 5). In rabbit colon smooth muscle cells, HSP27 has been shown to maintain MLC phosphorylation by mediating the association of RhoA with ROCK-II. HSP20 has structural similarities to troponin I, which inhibits myosin-actin binding in skeletal muscle.

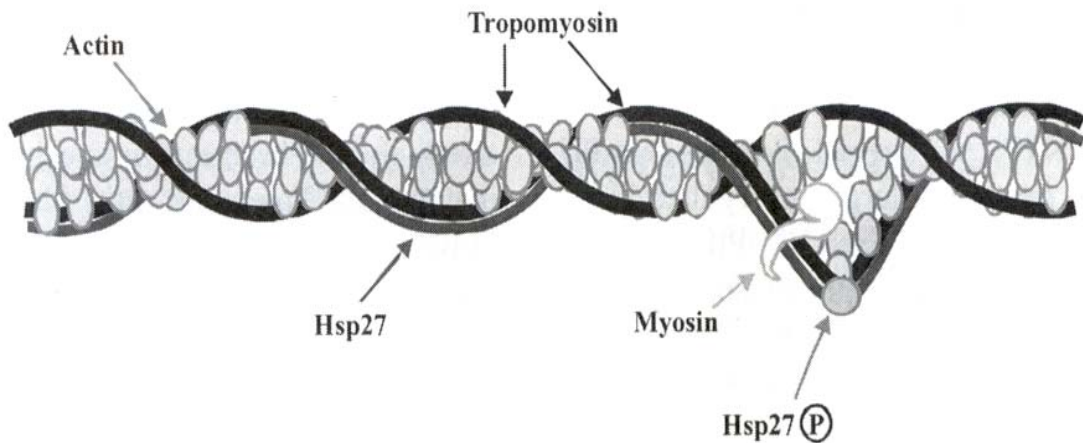


**Figure 5:** Proposed model for the role of HSP27 in smooth muscle contraction demonstrating that phosphorylation of HSP27 results in actin being exposed to myosin binding. Modified from Bitar (2003).

RhoA is a ras-related GTP-binding protein. It has been shown that the activation of rho can induce the phosphorylation of MLC and the formation of stress fibers (Chrzanowska-Wodnicka and Burridge 1996). RhoA has been shown to translocate to the membrane when rabbit portal vein cells were sensitized with  $Ca^{2+}$ . From this position, rhoA can be readily activated to initiate a signaling cascade involved in smooth muscle contraction (Gong et al. 1997). RhoA has been shown to be activated by stretch with evidence that the signaling cascade activated may include ERK (Numaguchi et al. 1999). However, this rhoA-mediated  $Ca^{2+}$  sensitization played a greater role in smooth muscle contraction induced by an agonist in rat pulmonary artery than in aorta (Hyvelin et al. 2004). Also, when rhoA activity was decreased in A7r5 cells by addition of the rho inhibitor Y-27632, actin fibers were seen to disassemble (Brandt et al. 2002). In rabbit aortic smooth muscle cells, rhoA was shown to promote the contractile phenotype (Worth et al. 2004). Rho kinase was also found to bind to non-muscle myosin fibers (Kawabata et al. 2004). All of these studies suggest that rho plays a very active role in smooth muscle contraction.

Another molecule that may play an important role in smooth muscle contraction is calponin (CaP). Evidence has been found for an inhibitory role of CaP in the myosin ATPase. Studies have also suggested that CaP may play a role in signaling cascades. CaP has been shown to associate with ERK and PKC (Morgan and Gangopadhyay 2001).

Taken together, the existing data suggests an extraordinarily complex mechanism of biochemical regulation of contraction in smooth muscle.

## **Cytoskeletal Remodeling**

The mechanism underlying the ability of smooth muscle to maintain contraction with minor energy expenditure has been a central issue of debate. One hypothesis known as the latch state proposes that the crossbridges between myosin and actin somehow begin to cycle slowly, causing the cell to remain contracted. Mathematical models have been developed to support this hypothesis, in which actin-binding proteins are proposed as regulators of actin and myosin association (Hai and Murphy 1992; Hai and Kim 2005). In addition, it has also been found that myosin can continue to be functional even if only one of its two RLCs is phosphorylated, thereby reducing the amount of ATP needed to maintain the activation of a myosin molecule (Rovner et al. 2006). However, direct experimental evidence to support the latch hypothesis has not yet been reported. An alternate hypothesis to explain the characteristics of smooth muscle contraction is that the contractile apparatus and supporting cytoskeleton may undergo remodeling (Battistella-Patterson et al. 1997; Li et al. 2001).

According to the cytoskeletal remodeling hypothesis of contraction, the actin cytoskeleton within a smooth muscle cell changes form, or remodels, to allow the contractile apparatus to maintain optimal mechanical advantage throughout the contraction. This hypothesis further proposes that the tension maintenance at low energy cost is due to cross-linking of actin filaments to hold the cell in the contracted configuration. In A7r5 embryonic rat aorta cells, the transfer of actin into structures known as podosomes has been demonstrated when a stimulus of phorbol-12, 13-dibutyrate (PDBu) has been administered (Fultz et al. 2000). This compound is a DAG analogue and activates the PKC pathway which leads to contraction. During this



contraction, actin forms columns of filaments on the edge of the cell (Fultz et al. 2000). This hypothesis has been tested in rat aorta tissue with the use of cytochalasin, a compound that inhibits the formation of actin filaments. Cytochalasin reduces smooth muscle contraction, and it is thought that this reduction is due to the inhibition of actin remodeling (Wright and Hurn 1994).

One of the key elements of this hypothesis is the proposed differences in the  $\alpha$ -actin and  $\beta$ -actin isoforms which are found in vascular smooth muscle. Studies have shown that the  $\alpha$ -actin isoform is the first to enter the podosome while  $\beta$ -actin remains in filaments for a longer period (Fultz et al. 2000; Brown et al. 2006). This suggests that tension is maintained by myosin binding to  $\beta$ -actin filaments until  $\alpha$ -actin is remodeled in such a way as to maintain tension. The podosome structures seen in cell culture have not been shown in contracting tissue, so it is unknown if a similar structure plays this role in tissue. The isoforms of actin studied in our laboratory are very similar in structure. These proteins are of identical molecular weight with the difference traced to a few amino acid residues that result in  $\alpha$ -actin being more acidic than  $\beta$ -actin (Owens and Thompson 1986; Khaitlina 2001).

Evidence supporting the cytoskeletal remodeling hypothesis include studies in canine trachealis smooth muscle in which actin polymerization was stimulated by contractile activation and this actin polymerization directly contributed to force development (Mehta and Gunst 1999). These authors also suggested that actin remodeling contributes to the length sensitivity of canine tracheal smooth muscle contractility.

## **Myosin Remodeling**

In addition to actin cytoskeleton remodeling, a few studies have shown that the thick filaments of smooth muscle may also be remodeled. It has been shown that myosin, when it is not activated, is in a folded conformation (Trybus et al. 1982; Trybus and Lowey 1984). This folded conformation has been examined by x-ray crystallography and it was found that portions of the “blocked” head and parts of the catalytic and converter domains and the ELC of the “free” head interacted, blocking actin binding (Liu et al. 2003). This conformation inhibits myosin from interacting with actin or forming filaments (Sweeney 1998). The ability of myosin molecules to polymerize into thick filaments and to depolymerize from such filaments in different conditions suggests that myosin can remodel similarly to actin. Early studies in canine airway smooth muscle revealed that, upon a quick change of muscle length, the ability of the muscle to contract was decreased (Gerthoffer and Gunst 2001). Earlier studies showed that smooth muscle tissue can adapt to new lengths if the tissue remains at the new length for an adequate amount of time (Pratusevich et al. 1995). Based on these findings it was suggested that contractile units in canine tracheal muscle are able to move and reform to allow for change in the optimal length of contraction. Further, they proposed that this adaptation takes time and that only about 20% of the contractile units in the tissue are fixed. Other studies have confirmed this slow reformation of the contractile apparatus (Mehta et al. 1996). In addition, airway smooth muscle tissue has also been shown to maintain some memory of past optimal lengths (Chan et al. 2000), which supports the time requirement for a new optimal length to develop. Hence, the data suggest that the actin-myosin contractile apparatus is plastic in nature and can adapt to changes in the external

environment, including rearrangement in response to stretch (Gerthoffer and Gunst 2001). The ability of smooth muscle to adapt its working length could allow for hollow organs to maintain appropriate functions with myosin remodeling dependent on actin structure (Seow 2005). Figure 6 shows a model proposed to demonstrate how myosin monomers can use actin thin filaments to organize the location of the new thick filament.

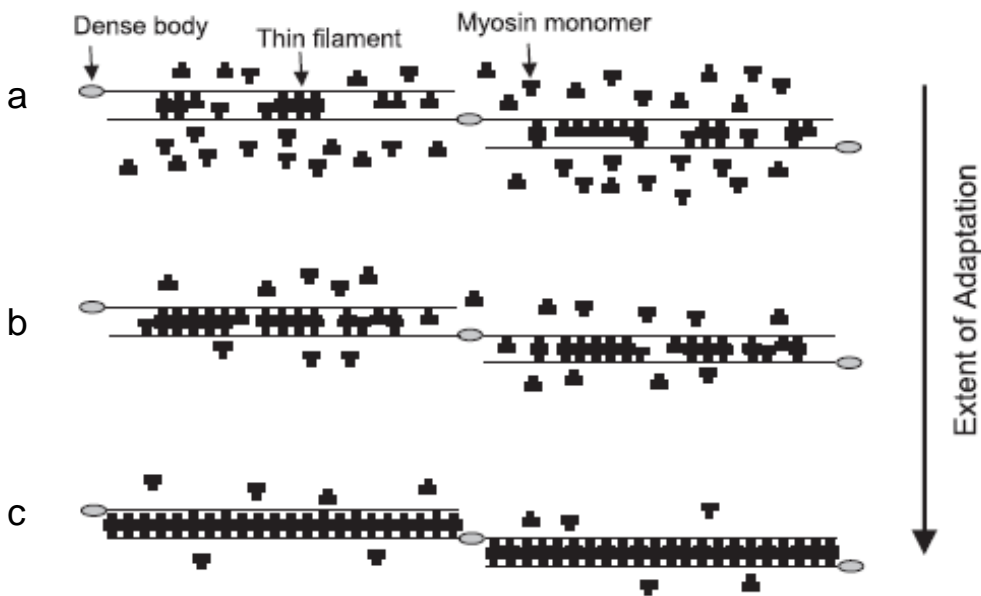


**Figure 6:** Model illustrating the possible model showing the formation of myosin thick filaments by myosin monomers which are using actin thin filaments as a guide during airway smooth muscle cell length adaptation. (Seow 2005).

There is significant experimental evidence supporting myosin contractile remodeling. In porcine tracheal smooth muscle, activation of the muscle resulted in a 144% increase in the density of myosin thick filaments (Herrera et al. 2002). They also found that if  $\text{Ca}^{2+}$  was removed during the resting state, thick filament density decreased by 35%. The authors state that there is an equilibrium that exists in these tissues of filamentous myosin with monomeric myosin. This creates the conditions for myosin remodeling not only during changes in optimal tissue length, but also during contraction.

In addition, stimulated porcine airway smooth muscle demonstrated an increase in thick filament formation (Smolensky et al. 2007), which was blocked by inhibition of MLC phosphorylation even when  $\text{Ca}^{2+}$  levels remained at stimulated levels. Myosin remodeling has also been demonstrated in A7r5 cells in our laboratory (Fultz and Wright 2003) showing that such activity can likely occur in the smooth muscle cells of rat aorta.

### **The Families of Myosin**

The motor protein that contracts muscle is myosin. However, there is a great complexity of myosin isoforms and several forms of myosin may be found within a specific smooth muscle type. Seventeen different families of myosin have been reported (Kendrick-Jones et al. 2001), however, another reports that there are eighteen classes (Berg et al. 2001). These have been broken down into two categories of conventional and unconventional myosin. Conventional myosin consists of the family of myosins called myosin II which was the first myosin protein to be reported by Kuehne back in 1864 (Spudich 1989). Myosin II exists as a hexamer of two heavy chains and four light chains. The largest component of these myosins, called the heavy chain, is comprised of a globular head region and an elongated tail. The tails of two of these heavy chains combine in a coiled-coil configuration. This complex therefore has two head regions and two tail regions. Members of the myosin II class have two myosin chains which are associated via an  $\alpha$ -helix of their tails and two light chains per heavy chain combining to form each myosin molecule (Figure 7). The two heads of smooth muscle myosin II have been shown to work together during contraction to enable myosin to perform the optimum level of force development (Tyska et al. 1999; Lidke and Thomas 2002).

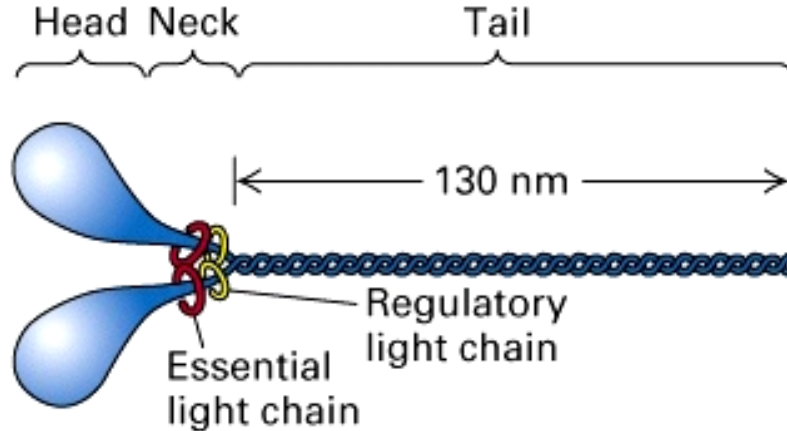


**Figure 7:** Structure of the myosin II molecule. Notice the two heavy chains interconnected by the long tail region and the two large globular heads. Also seen here are the two essential light chains and the two regulatory light chains and their approximate locations

[www.cella.cn/book/09/images/image009.jpg](http://www.cella.cn/book/09/images/image009.jpg).

The other 16 classes of myosin proteins are known as the unconventional myosins (Kendrick-Jones et al. 2001). Not as much is known about these other classes. Nine of these have been classified as having a single heavy chain which tends to be much shorter than in the conventional myosins (Kendrick-Jones et al. 2001). The other seven do have regions of coiled-coil interactions and do form a complex containing two heavy chains (Kendrick-Jones et al. 2001). All myosins possess an ATP-hydrolyzing motor domain that moves along actin filaments (Hasson and Mooseker 1996). It is not known if all of the unconventional myosins have light chains, but a few have been found that do. However, these light chains are not always like those of myosin II. In some cases calmodulin or calmodulin-like molecules bind to the heavy chain neck regions and act as  $\text{Ca}^{2+}$ -binding light chains (Kendrick-Jones et al. 2001). Not all of these myosin molecules are found in mammals. The members of myosin families VIII, XI, and XIII

have only been found in plants with Myosin IV isolated only in amoebas and myosin XII only reported in *C. elegans* (Berg et al. 2001; Kendrick-Jones et al. 2001). Myosin XIV has been found in parasitological protists, and myosin XVII has only been found in fungi (Berg et al. 2001; Kendrick-Jones et al. 2001). Very little is known about myosin X and XVI, although both have been found in humans (Berg et al. 2001). The remaining families have been found in mammals (Kendrick-Jones et al. 2001), and we will discuss them in more detail.

Myosins have been proposed to play a multitude of important roles. Myosin I has been subdivided into four subclasses with the differences being the amount of IQ binding motifs (regions where light chains can bind) and differences in the tail region (Kendrick-Jones et al. 2001). Myosin I proteins have only one heavy chain. Several functions have been proposed for the myosin I molecules: cell crawling, chemotaxis, and phagocytosis (Kendrick-Jones et al. 2001). Subclass 1 molecules have one or two IQ motifs. Subclass 2 proteins are found at the cell membrane and contain 3-6 IQ motifs. A very important member of this subclass is found in the microvilli (Hasson and Mooseker 1996). Another member has been found in stereocilia and plays a role in hearing (Cyr et al. 2002). Subclass 3 proteins contain 3 IQ motifs and have been found in several tissues (Kendrick-Jones et al. 2001). They contain a tail region that can bind phospholipids. Subclass 4 is similar to 3 but only has 2 IQ motifs (Kendrick-Jones et al. 2001). There is still much to be resolved about the myosin I family of myosins, including their regulation within the cell (Kendrick-Jones et al. 2001).

Myosin III has an N-terminal kinase domain, which is different from all other myosins (Kendrick-Jones et al. 2001). This class of myosins has been found in the retina and could play a role in vision (Berg et al. 2001).

Myosin V molecules are dimeric (Hasson and Mooseker 1996) and serve as transport molecules within the cell which literally “walk” along the actin filament (Kendrick-Jones et al. 2001). Myosin VI is similar to myosin V, although V binds several more light chains (Kendrick-Jones et al. 2001). However, myosin VI is very different from other myosins. All other myosins move toward the plus end of the actin filament; whereas, this class of myosin contains what has been called a reverse gear and can move toward the minus end of the actin filament (Diwan 2006). Myosin VI also performs a role in the transport of items within the cell (Kendrick-Jones et al. 2001; Diwan 2006).

Along with myosin VI, VII and XV have been found to play roles in genetic deafness (Hasson and Mooseker 1996; Berg et al. 2001). Several disorders have been linked to either the mutations or absence of these myosins within the ear, specifically affecting the stereocilia (Kendrick-Jones et al. 2001).

Myosin IX molecules are single-chained proteins expressed in several tissues. A role has been proposed for myosin IX as a signaling molecule negatively regulating the Rho signaling pathways (Bahler 2000).

### **Smooth Muscle Myosin**

Smooth muscle myosin is one of the conventional myosins. However, it is still a protein that has diverse forms. This section will examine the isoforms of not only the

smooth muscle myosin heavy chain but also the isoforms of the light chains. The difference in function of these different isoforms has been a matter of controversy. I will trace the research of these isoforms from their discovery through the debate of their different functions.

The discovery of two myosin heavy chain isoforms was reported in 1986 (Rovner et al. 1986). Of the two, the larger one in molecular weight was designated Sm1 while the smaller was designated Sm2 (Rovner et al. 1986). SDS-PAGE was used to examine several protein extracts from multiple smooth muscle tissues in which a 1:1 ratio of Sm1 to Sm2 was observed in most tissues. The authors suggested that these isoforms of myosin could form either heterodimers or homodimers, but were unable to determine which was dominant. In a later study, researchers were able to separate the heavier isoform from the lighter using an antibody specific only for the 204kDa heavy chain (Kelley et al. 1992). These investigators found that immunoprecipitations of Sm1 did not contain any Sm2 in either bovine aortic cells or in turkey gizzard suggesting the isoforms existed as homodimers. Another study, focusing on aorta muscle cells from the rat (Kawamoto and Adelstein 1987) found using protein gels three bands in the 200kDa region. 2-D peptide maps showed the 204 and 200kDa bands to be very similar while the 196kDa protein was largely different from the two heavier bands. They did not find a 1:1 ratio of the two heavier bands, presumably Sm1 and Sm2, but found Sm1 to be 59% of the additive total of the two bands and Sm2 to be 41%. The authors also found differences in expression depending on the state of the cell culture (log phase, postconfluent, etc.). The 196kDa protein was much more highly expressed than the other two, and the 200kDa protein was expressed very little. In the log phase of the culture no



200kDa protein was expressed. Hence, not only are there different myosin isoforms, but the expression levels may change. So, two tail isoforms have been reported which exist as homodimers and are variable in expression. A major question emerging from these studies is, despite the great similarity in the protein sequences of Sm1 and Sm2, could they be involved in different functions of the cell?

To answer this question a later study utilized a rabbit uterine cDNA library, in which SMHC29 was used as a probe (Nagai et al. 1989). The authors had previously determined that this clone encoded for tail region of smooth muscle myosin (Nagai et al. 1988). Positive clones were examined further and it was found that three were positive for SMHC29, but eight were positive for clones of larger sizes. These were called SMHC40 and were found to encode for a myosin chain with 43 unique amino acids in a region of the protein in which SMHC29 encoded for 9 unique amino acids. S1 nuclease mapping determined that SMHC40 was expressed in all smooth muscle tissue examined. However, neither was expressed in skeletal muscle or brain tissue and only slightly expressed in cardiac muscle. Antibodies were isolated that were specific to synthetic peptides encoded by SMHC40 or SMHC29. The antibodies raised against SMHC40 bound to the Sm1 band in rabbit aorta and the antibodies to SMHC29 bound specifically to the Sm2 band in Western blot analysis. The authors claimed to see this in stomach, intestine, and urinary bladder as well. They concluded that the difference between SMHC40 and SMHC29 was a 39nt insert and they concluded that mRNA that contains this 39nt insert encodes for Sm2, while the mRNA without the insert encodes for Sm1. A study published the same year examined a rat aorta cDNA library and found two cDNAs for myosin heavy chain (Babij and Periasamy 1989). The only difference observed was

in the carboxy terminus. These authors also determined that one cDNA encoded 43 unique amino acids and that another encoded nine in the tail region because of a 39nt insert. The authors also determined that on each side of this insert were a 2600nt intron and a 2700nt intron, claiming that this was the first time that alternative RNA processing was shown in vertebrate myosin production. Hence, it was concluded that the same gene encodes for these two tail isoforms. The authors also found this mRNA to be present in both vascular and non-vascular tissue. These studies show that the difference between the smooth muscle myosin tail isoforms results from alternative splicing of the mRNA. This alternative splicing of mRNA results in an insert of 39nt in the message for Sm2, and a shorter protein.

Myosin tail isoforms have been shown to be present in different smooth muscle tissues. Several studies have been done to further examine this. One such study examined two myosin heavy chain isoforms, but these authors determined the molecular weights to be 207kDa, which they called MHC1, and 204kDa, called MHC2 (Schildmeyer and Seidel 1989). They compared several smooth muscle types in several species. They did find differences in expression between species, which was not surprising. Specifically, in examining rat aorta tissue they determined the ratio of MHC1 to MHC2 to be 55:45. They also determined that the reaction of a monoclonal antibody against MHC was different between rat aorta and rat uterus. Another study saw differences when comparing tissue from different aged rats (Eddinger and Murphy 1991). In young rats, the ratio of Sm1 to Sm2 was 0.5 in aorta and 2.7 in bladder. Those ratios changed in older animals to 1.2 and 1.7, respectively. Research has also shown a difference in Sm1 and Sm2 expression between fetal and adult tissue (Kuro-o et al.

1989). Sm1 was seen by immunohistochemistry to be expressed in the fetus (25-28 days gestation) up to 30 days after birth. Sm2 was not visualized until 20 days after birth, suggesting that the expression of these isoforms is developmentally regulated. These authors also used gel electrophoresis to examine Sm1 and Sm2 expression. They found two bands running where Sm1 and Sm2 would be expected to run in samples taken from fetal animals to those four months after birth. The band migrating at 204kDa reacted with the Sm1 antibody. The band migrating at 200kDa, however, did not react with the antibody specific to Sm2, suggesting that this protein band is different than the Sm2 protein. Another study found a similar protein band (Babij et al. 1992). This study combined RNase protection assays with protein gel electrophoresis to determine that aorta tissue expressed more Sm1 and Sm2 than isolated cells. With the RNase protection assay, these researchers found the ratio to be 80:20 of Sm1 to Sm2 in intact aorta. The expression of each decreased in isolated cells, but the decrease of Sm2 was greater than that seen of Sm1. The study also found that another isoform of myosin, non-muscle myosin heavy chain A (NMMHC-A) increased in cell culture when compared to intact aorta, changes also seen with protein gels. The protein studies did reveal a protein band that migrated to about 200kDa but only reacted with the Sm1 antibody. The authors reasoned that this band could be a result of the increased amount of NMMHC-A, which raises the problem of the specificity of the Sm1 antibody. These studies show that the myosin tail isoforms are developmentally regulated and that non-muscle myosins do exist and play active roles even in smooth muscle tissue.

The possible different roles of each of the tail isoforms are still being studied. A very interesting experiment was performed on individual smooth muscle cells (SMCs)

from rabbit arteries (Meer and Eddinger 1997). The cells were contracted and mRNA was extracted from each cell. A large variation was seen in the Sm2/Sm1 ratio ranging from 0.03 to 0.55. When several parameters of the cells were measured and compared to the isoform content, only final cell length showed any significant correlation with the Sm2/Sm1 ratio. As the amount of Sm2 increased the final length of the cell decreased. This suggests that the tail isoforms may differentially affect the structure of myosin filaments thereby affecting overall cell length. Another study examined the affect of different smooth muscle myosin tail lengths on myosin filaments (Rovner et al. 2002). The authors started with chicken gizzard Sm1, and from that constructed Sm2 by replacing the chicken Sm1 tailpiece with that of Sm2 from rabbit. They also constructed another form of the myosin tail that they denoted as tailless (TL) by placing a stop codon as the last codon before the alternative splice site. All proteins were visible when analyzed by gel eletrophoresis. Paracrystals of each isoform were examined with electron microscopy. The crystals formed by each isoform were different although Sm2 and TL were the most similar. Repeating light and dark bands were visualized and the size of these bands were different when comparing the Sm1 crystals to those of Sm2 and TL. The overall length of filaments formed was also different, with TL forming by far the longest filaments (801nm), with Sm1 (526nm) and Sm2 (512nm) being much shorter. It is surprising that with the Sm2 and TL crystals looking similar the length of the filaments was not more similar. It was even more surprising that the length of Sm1 filaments fell between that of TL and Sm2. The tendency for each of these isoforms to form filaments was also examined. TL was the most likely to form filaments followed by Sm1 and then Sm2. The authors used viruses to infect insect cells with the Sm1 and Sm2

and found that homodimers of each isoform were preferred over heterodimers. However, homodimers of Sm1 and Sm2 could copolymerize into thick filaments. An earlier study found that the longer tail region of Sm1 contains a serine that is not present in Sm2 and that this serine can be phosphorylated by casein kinase II (Kelley and Adelstein 1990). This phosphorylation could play a role in filament formation (Babu et al. 2000). So, myosin tail isoforms appear to play a role in filament length and cell structure.

Another way to examine the function of a protein is to look at it in pathophysiological conditions. One such study examined the content of several myosin isoforms (nonmuscle and smooth muscle) in damaged left carotid arteries in Sprague-Dawley rats compared to that of undamaged right carotids (Gallagher et al. 2000). Sm1 levels remained unchanged. Sm2 levels decreased beginning at 24 hours after injury and remained reduced through seven days. Non-muscle myosin A (NM-A) increased while non-muscle myosin B (NM-B) remained unchanged. Microscopic examination revealed a change in where certain isoforms were expressed as well. Cells expressing the two non-muscle isoforms were seen more in the intima and adventitia, while Sm1 expression seems unchanged overall and Sm2 expression was decreased overall. One explanation is that changes in myosin isoform expression are important in cell dedifferentiation and migration from media into the damaged areas of the artery. Hence, NM-A may be important for migrating cells. Sm1 and NM-B are expressed in embryonic smooth muscle, but Sm2 is not. These changes would be expected if such dedifferentiation and migration was taking place. Another study looked at the results of a high cholesterol diet and certain drugs on the expression of myosin isoforms in rats (Itoh et al. 2002). Sm1 levels were unchanged, but Sm2 levels were decreased when compared to controls. It

was also shown that within cells Sm2 levels decreased as oxidative stress increased. The authors suggest that examination of Sm2 levels and oxidative stress may be a way of determining vascular dysfunction. They further suggested that upregulating Sm2 may be a therapeutic way to lessen atherosclerosis. Another study examined arteriovenous malformations (AVMs) from humans and compared them to normal arteries and veins (Hoya et al. 2003). They found Sm1 and Sm2 present in internal carotid arteries, middle cerebral arteries and arteries greater than 30 $\mu$ m in diameter as well as in superficial middle cerebral veins and the transverse sinus. The arterial component of the AVMs showed similar staining patterns to those of normal arteries. However, the venous component often (from cerebral veins) showed staining patterns more like cerebral arteries and earned the name arterialized veins. Changes in smooth muscle myosin tail isoform expression were seen in association with damage to blood vessels in rat, but not so clearly in humans. However, this latter study only looked at whether or not Sm1 or Sm2 was expressed and not at the increase or decrease of expression levels as was examined in the two rat studies. These studies show that smooth muscle myosin tail isoforms are expressed at different levels during different points of cell differentiation.

In addition to the complexity engendered by two tail isoforms, studies have found that the myosin heavy chain also has two other isoforms which differ in the head domain. The discovery of the myosin head isoforms was reported in the early 1990's (Hamada et al. 1990). Rabbit uterus smooth muscle myosin cDNA was examined, and the deduced protein sequences were compared to the known protein sequence of chicken gizzard smooth muscle myosin heavy chain (Babij et al. 1991). The authors found that there was a difference of 13 amino acids including a 7 amino acid insert between the rabbit uterus

and chicken gizzard myosin heavy chains. The difference was seen at the 25/50kDa junction in the myosin head region which is near the putative  $Mg^{2+}$ -ATPase domain. The authors also found that transcription for each isoform begins from a single site in the smooth muscle myosin heavy chain gene. In another study (White et al. 1993), a fetal rat smooth muscle library was constructed and analyzed using smooth muscle heavy chain cDNA obtained from a rat stomach plasmid library as a probe. The authors found two distinct cDNA smooth muscle heavy chain clones separated by only 21nt at the 25/50kDa junction in the S1 head region, strongly supporting the conclusions of Babij et al. (1991). White et al. named these two isoforms as SM1A (no insert) and SM1B (with insert), indicating their studies looked only at the SM1 tail isoform. In addition, they determined the percentage of each isoform in several smooth muscle tissues. In aorta 96% of the myosin content was the non-inserted form. Vein, uterus, lung and stomach showed 70% or more SM1A content, small and large intestine showed a majority of SM1B and bladder showed 83% of the inserted isoform. In another study, none of the inserted isoform was found in vascular tissue, leading the authors to term the isoforms as vascular (non-inserted) and visceral (inserted) (Babij 1993). According to Babij (1993), by examination of cDNA clones, the inserted isoform was only seen with Sm1. He further suggested a method of alternative splicing for the head isoforms in which exon 5a is joined to exon 6 in the non-inserted isoform. The insert comes from an exon denoted as exon 5b. Exon 5a is joined to 5b and then to 6 in the inserted mRNA. To summarize these studies, the myosin heavy chain has another alternative splice site in the head region and this site generates two more heavy chain isoforms.

The question of whether or not the inserted head isoform could be found in either of the tail isoforms was addressed by Low et al. (1999). They examined airway smooth muscle as well as small blood vessels in rat lung tissue. SM-B was found in airway smooth muscle as well as in small blood vessels. Large vessels with elastic laminae did not express SM-B; however, Sm1 and Sm2 were expressed in all the vessels examined. Septal tips and peripheral vessels showed a heterogeneous expression of SM-B and only expression of Sm1. Tracheal smooth muscle expressed SM-B, Sm1 and Sm2. The authors used an antibody specific for SM-B and found that SM-B was expressed in both Sm1 and Sm2. So, as seen in figure 8 the smooth muscle myosin heavy chain can have four different isoforms that result from the two sites of alternative splicing of the mRNA from the one smooth muscle myosin gene.

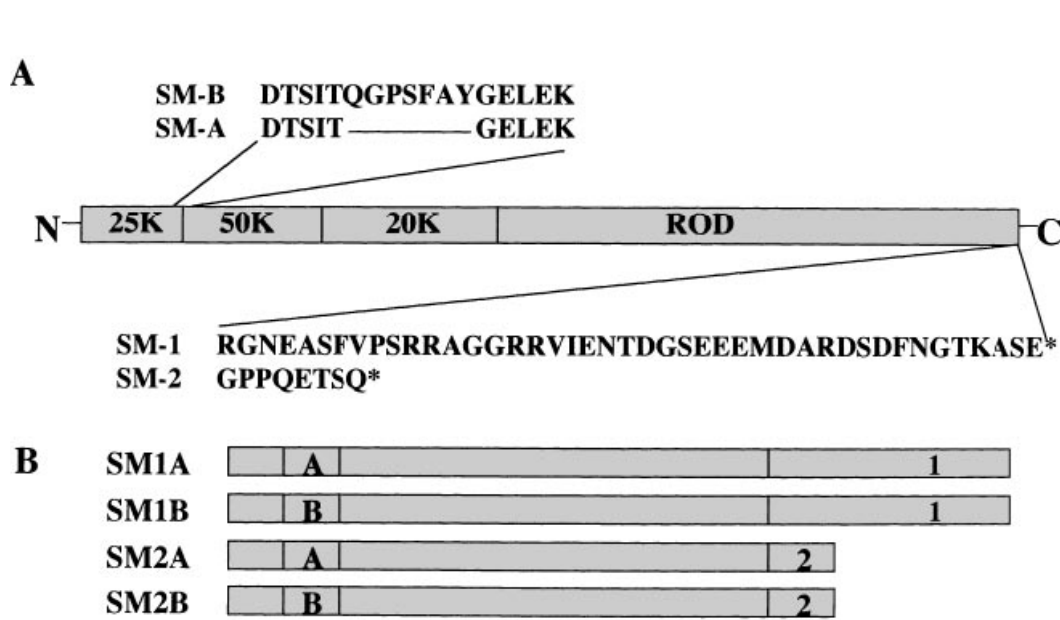


**Figure 8:** Schematic diagram of smooth muscle myosin heavy chain isoforms. *A*: encoded regions involved in splicing of alternative exons and unique amino acids encoded by exons. *B*: 4 possible isoforms generated by alternative splicing at regions encoding carboxy terminus and junction of 25- and 50-kDa tryptic peptides. \*, Stop codon (White et al. 1998).



Other myosin isoforms can be seen in the 17kDa essential light chain (LC17) that binds to the myosin heavy chain neck region and is thought to help stabilize the myosin heavy chain in this region (Lowey and Trybus 1995). Two isoforms of LC17 have been isolated (Cavaille et al. 1986; Nabeshima et al. 1987). The two isoforms were designated LC17a (acidic) and LC17b (basic) because of their isoelectric points at 4.13 and 4.19, respectively (Helper et al. 1988). Tissues expressed each isoform in differing amounts (Helper et al. 1988) with the results only slightly different in comparisons of tissues between species. However, when different tissue was compared within the same species, large differences were noted. For example, porcine stomach was found to contain 100% LC17a, while aorta contained only 60% LC17a, and carotid artery had only 16% LC17a. Other laboratories examined individual SMCs for differences in SM2 and LC17 expression. Cells from rabbit carotid arteries had a lower percentage of SM2 mRNA than those from saphenous arteries (Sherwood and Eddinger 2002). However, saphenous cells showed a lower percentage of LC17b mRNA than cells from carotid or femoral arteries. The authors also found that expression SM1/SM2 and LC17a/LC17b are not coregulated in the SMCs examined. These studies show that other myosin isoforms exist as a result of alternative splicing of the mRNA for the ELC.

Together, these studies indicate a complexity of smooth muscle myosin heavy and light chains that may give rise to multiple protein hexamers within the smooth muscle cell. Several studies have looked at the expression of these proteins in different tissues, and based on the type of smooth muscle (e.g. tonic vs. phasic) tried to determine the characteristics of each isoform. However, the question remains as to the function of multiple myosin isoforms.

## **Function of Myosin Isoforms**

Myosin has different forms throughout the different types of muscle. In the early eighties a study was performed to examine the effects of the different myosin light chains on the enzymatic activity of different myosins (Wagner 1981). Wagner examined cardiac and skeletal muscle myosin and was able to induce an exchange of essential light chains (ELC) between the two different myosins. He determined that the  $V_{max}$  did not change significantly when ELCs were exchanged, but the affinity for ATP was altered by these exchanges. This suggests a possible link of the ELC to the affinity of the myosin ATPase. However, ATPase velocity is thought to be regulated by the heavy chain. Throughout the years there has been much discussion about the different myosin heavy chain isoforms and their roles in smooth muscle. The myosin tail isoforms have been found in both vascular and non-vascular muscle tissue (Babij and Periasamy 1989; Nagai et al. 1989). However, Babij (1993) reported that the inserted head isoform was only present in non-vascular muscle, and that the non-inserted isoform was seen in both vascular and visceral muscle in studies in which only the Sm1 isoform was the inserted isoform examined. On the other hand, White et al. (1993) did find small amounts of both head isoforms in vascular and visceral muscle tissue in similar studies examining the Sm1 isoform. In rats, a wide range of percentages of the SmA and SmB isoforms were seen in the different tissues examined. However, in a later study, the authors could not find the inserted isoform in cultured rat aortic cells, even though Sm1 and Sm2 were present in all tissues examined other than trachea (White et al. 1998). However, others did find that the inserted head isoform existed in either of the tail isoforms (Kelley et al. 1993). These authors also determined that this insert had an effect on the  $V_{max}$  of the

myosin Mg-ATPase. In studies of turkey gizzard and aortic tissues, only the gizzard muscle contained the inserted head isoform and the  $V_{max}$  of its ATPase was nearly two fold higher than that of aorta which had no detectable levels of insert isoform. In agreement with the earlier results of Wagner (1981), the authors suggested that this seven amino acid insert, being near the ATP binding region in the myosin heavy chain, is specific for affecting the actin-activated Mg-ATPase of the myosin protein. A doubling of the  $V_{max}$  was confirmed in a later study by Rovner et al. (1997). However, they did not find that variation in the ELC isoforms changed the function of myosin.

In rabbit, thoracic and abdominal aorta did not contain detectable amounts of the inserted isoform, but femoral and saphenous arteries contained both SM-B and SM-A isoforms (DiSanto et al. 1997). These studies also showed that the  $V_{max}$  of the myosin ATPase in saphenous artery was twice that of aorta. Both tail isoforms were detected in aorta and the femoral-saphenous samples. Another characteristic that these authors examined was RLC phosphorylation. They found that phosphorylation levels were similar in aorta, femoral-saphenous, and bladder samples. In these same tissues, the percentage of LC17b was 45%, 18% and 4%, respectively. In aggregate, the results suggest that LC17 isoform differences do not affect RLC phosphorylation.

To this point, all of these studies described have compared tonic and phasic muscles from different systems (arteries compared to bladder compared to intestines). However, a study was done that compared in the same tissue tonic lower esophageal sphincter (LES) muscle to that of phasic esophageal body (EB) circular muscle (Szymanski et al. 1998). They found the amounts of Sm1 and Sm2 to be similar in these two muscles. However, EB contained 2-3 times more of the head insert than LES. They

also found that there was 3-4 times more LC17a in EB than in LES. Another group of researchers did something similar by examining rabbit bladder (phasic) in comparison with tissue from urethra (tonic) (Hypolite et al. 2001). The authors also divided the bladder into three sections, dome, midbody, and base. They did not find any difference in the expression of Sm1 and Sm2 mRNA in any of these bladder regions, but there was a significant difference in the Sm2:Sm1 ratio when comparing dome (2:1) to urethra (1.5:1.0). The head isoforms were also examined showing that SM-B isoform mRNA copy numbers were much higher than those for SM-A in both bladder and urethra tissue. The authors also found significant differences in RLC phosphorylation levels when comparing dome, midbody, base, and urethra in resting tissue. After contraction with  $K^+$ , bladder and urethra tissue RLC phosphorylation increased up to 50% of force development. This leveled off for urethra tissue between 80% and 100% of force. However, bladder muscle showed only a slight increase between 50 and 80% force, which was followed by a large decrease to near basal levels at 100% force. The authors concluded that the different mix of myosin isoforms and the differences in RLC phosphorylation in the bladder and urethra play significant roles in the phasic nature of the bladder and the tonic nature of the urethra.

Several studies have utilized bladder smooth muscle as the primary tissue in order to better understand the roles of myosin isoforms. One such study compared amounts of Sm1 to maximal force generation in adult and newborn bladders in mice (Wu et al. 2004). Sm1 expression was highest in the newborn animals, as was the maximal force generated by the muscle. Both Sm1 expression and maximal force decreased as the animals aged, suggesting a potential role of Sm1 in maximal force generation. Another

model used surgically-induced partial bladder outlet obstruction (PBOO) which has been studied in both mouse (Austin et al. 2004) and rabbit (Mannikarottu et al. 2005). Similar to previous findings, both studies showed a decrease of SM-B expression in tissues with PBOO when compared to sham controls which, in turn, was accompanied by an increase in SM-A expression. Both also reported an increase in the SM1:SM2 ratio, although Mannikarottu et al. (2005) showed more SM2 in control animals than Austin et al. (2004). Rabbit studies also showed an increase in LC17b in PBOO animals. In comparisons of different regions of the rabbit bladder, it was observed that the base region displayed a decrease in force and a more tonic-like contraction than the dome region. By comparison, mouse studies showed a higher volume for optimal pressure and a decreased rate of pressure change in severe PBOO animals when compared to sham controls. It was suggested from these studies that the SM-B isoform is a fast form of myosin and the SM-A isoform the slow form. A later study agreed with this assessment (Basha et al. 2006), in which a higher percentage of SM-B in rat vaginal wall smooth muscle correlated with a higher Vmax of the myosin molecule, with SM1 and SM2 showing no effect on the Vmax. These studies continue to imply that SM-B is the isoform that denotes a more phasic characteristic to smooth muscle. However, lower maximum force does not always correlate with increased Sm1 expression.

A mouse model with a knockout of SM-B was developed (Babu et al. 2004) and the tissues of mesenteric arteries and aorta were examined. The mesenteric vessels displayed higher force, stress, and time to 50% of peak contraction in knockout animals when compared to WT. No change in tail isoform or light chain expression was seen in the mesenteric vessels of knockout mice compared to either WT or heterozygous mice.

Wild type (WT) animals did not express SM-B in aorta. However, knockout animals still showed changes in the aorta muscle. Shortening velocity was decreased, but force generation was increased.  $K^+$  sensitivity was not changed in aorta, but sensitivity to phenylephrine was higher in the knockout animals. In aorta, expression of Sm1, Sm2, and RLC were all unchanged in the knockout animals, but the LC17a:LC17b ratio was decreased due to a relative increase in LC17b. The authors also observed an increase in calponin and a decrease in caldesmon in knockouts as well as an increase in ERK MAPK phosphorylation. They concluded that the loss of SM-B in mesenteric arteries leads to adaptive changes in other areas of the circulatory system. Changes in calponin, caldesmon, and MAPK activation could be evidence of those changes.

### **Fluorescence resonance energy transfer (FRET)**

The interaction of proteins is a very important aspect of cellular function. This interaction can be measured in several ways including co-immunoprecipitation and yeast 2 hybrid experiments. Another way of determining protein interaction is by fluorescence resonance energy transfer (FRET). FRET is one of the few tools for measuring distances and changes in distances on a nanometer scale (Selvin 2000). If a sensitive enough detector is used (e.g. a charge coupled device (CCD)) FRET can be measured on a pixel by pixel basis (Selvin 2000). This method utilizes fluorophores that are attached to the proteins in question. This has typically been performed in solution using a spectrophotometer and purified proteins with fluorescent molecules directly attached. However, fluorescent microscopes can also be used. FRET can extend the resolution of fluorescent microscopes and allow quantitative detection of protein-protein interactions

which is superior to standard colocalization measurements (Kenworthy 2001). The fluorophores used must be chosen according to specific criteria. One fluorophore, the donor, must have an emission spectrum that overlaps the excitation spectrum of the other, the acceptor. If this criteria is met and the fluorophores are within 10 nm of each other (Jares-Erijman and Jovin 2003), the excitation of the donor molecule will result in emission energy being transferred to the acceptor effectively decreasing donor fluorescence. The efficiency of this transfer can be calculated by an equation which views the efficiency as a function of the distance between the two fluorophores:

$$E=1/[1+(r/R_0)^6]$$

in which E stands for transfer efficiency, r is the distance separating the two fluorophores, and  $R_0$  is the Förster distance between donor and acceptor, typically 10-70 Å, and is a function of the spectral overlap of the donor emission and the acceptor excitation spectra. If the distance between donor and acceptor is  $>2 R_0$ , then FRET does not occur. The Förster distance is defined in the Förster equation (Kekic et al. 1996):  $E= R_0^6/( R_0^6+ R^6)$ , in which the Förster distance ( $R_0$ ) is the distance between the donor and acceptor when E is 50%. In this equation, R, the distance separating donor and acceptor probes, is defined by yet another equation:

$$R=9.78 \times 10^3 (J n^{-4} k^2 Q_0)^{1/6}.$$

In this equation, J is the overlap integral between the emission spectrum of the donor and the absorption spectrum of the acceptor, n is the refractive index of the medium with a range of values between 1/3 and 1/5,  $k^2$  is the dipolar orientation factor having a range of 0-4, but which is assumed to be 2/3 in most applications and  $Q_0$  is the quantum yield of the donor (Jares-Erijman and Jovin 2003). The equation we have adopted in our

laboratory is,  $E=1-(F_{da}/F_d)$ , in which  $F_{da}$  is the fluorescence of the donor in the presence of the acceptor (i.e. before photobleaching of the acceptor) and  $F_d$  is the fluorescence of the donor in the absence of the acceptor (i.e. after photobleaching). Hence the FRET method that we have employed utilizes the measurement of donor fluorescence quenching by the acceptor as an index of the cellular protein-protein interaction. For this to work well, the donor fluorophore must remain stable and the acceptor fluorophore should photobleach readily (Kenworthy 2001). Data acquisition requires acquiring an image of the activated donor before photobleaching of the acceptor, an image of the acceptor before photobleaching, photobleaching of the acceptor and viewing the acceptor to ensure it has been adequately photobleached, and then acquiring a second image of the donor. An appropriate negative control to perform is that of only labeling the donor and performing the above steps to view how the donor molecule is affected by the photobleaching process. A positive control that should be performed is placing both donor and acceptor labels on a single protein which should result in high transfer efficiency. These experiments can be performed with antibody labels without direct labeling of the proteins being examined (Kenworthy 2001) as demonstrated in our laboratory (Dykes et al. 2003). Our method of performing FRET can be considered novel because we not only use indirect labeling of the proteins in question, but we also are doing this labeling in order to examine protein-protein interaction within sections of smooth muscle tissue and isolated cells.

FRET and other similar techniques have been used widely to measure intramolecular distances within the myosin protein and intermolecular distances between myosin and other contractile proteins as well as changes in those distances. Distances



between the myosin heads bound to actin were found to be in the range of 6.0-6.3 nm (Ishiwata et al. 1997). The distance between the catalytic domain and the regulatory light chain domain of the myosin head was measured and without ATP bound the distance was determined to be 73 Å (Burmeister Getz et al. 1998). When ATP was bound to the active site the distance was increased. The authors state that the distances they measured correlate well with crystal structure measurements. Another group performed similar measurements and found that the distance between the catalytic and regulatory domain to be no longer than 85 Å (Palm et al. 1999). Examining the myosin II of an amoeba with FRET enabled Suzuki et al. (1998) to confirm that the power stroke occurs with the release of Pi. The hydrolyzation of ATP occurred during the recovery stroke (Suzuki et al. 1998). FRET studies of *Dictyostelium* myosin II suggests that this myosin has two distinct prestroke states which are both induced by the binding of ADP and Pi, but not the binding of ATP (Shih et al. 2000). The movement of myosin during the power stroke has also been examined with FRET. Binding of actin to myosin caused a conformational change in the myosin protein. The actin-dependent ADP swing caused an 18 Å change in distance between the 25/50 kDa loop in the catalytic domain and the RLC, which corresponds to a 23° swing of the light chain domain (Xiao et al. 2003). Palm et al. (1999) found that during the power stroke RLC was reoriented in respect to ELC and could contribute 22 Å to the power stroke. In scallop muscle fibers, it was found that the RLC domains moved closer together during contraction simulating a lever action (Lidke and Thomas 2002). The distances between the RLCs during three muscle conditions were determined. The distance during relaxation (85 Å) was greater than that of contracted (76.7 Å) and that of rigor (68 Å). Some of the apparent differences in these

studies could be related to where exactly the fluorophores were attached to the molecules being studied.

The light chain has been shown to move during the hydrolysis of ATP and the release of ADP and Pi during the power stroke (Reshetnyak and Andreev 2001; Mizukura and Maruta 2002). Examination of the S1 fragment of skeletal muscle found changes in flexibility upon hydrolysis of ATP which the authors suggested could be the mechanism of the transfer of the energy of ATP hydrolysis from the ATP-binding domain to the lever arm (Bodis et al. 2003).

Interaction of myosin with other molecules has also been examined. It was determined that the binding of myosin displaced several tropomyosin molecules from F-actin (Graceffa 1999). Indeed the tropomyosin molecules were “rolled” uniformly on the F-actin by saturating S1 heads (Bacchiocchi et al. 2004). Hence, FRET methodology has been widely employed and accepted as a valid tool in the study of myosin protein interactions.

## **References**

Austin, J. C., S. K. Chacko, M. DiSanto, D. A. Canning and S. A. Zderic (2004). "A male murine model of partial bladder outlet obstruction reveals changes in detrusor morphology, contractility and Myosin isoform expression." J Urol **172**(4 Pt 1): 1524-8.

Babij, P. (1993). "Tissue-specific and developmentally regulated alternative splicing of a visceral isoform of smooth muscle myosin heavy chain." Nucleic Acids Res **21**(6): 1467-71.

Babij, P., S. Kawamoto, S. White, R. S. Adelstein and M. Periasamy (1992). "Differential expression of SM1 and SM2 myosin isoforms in cultured vascular smooth muscle." Am J Physiol **262**(3 Pt 1): C607-13.

Babij, P., C. Kelly and M. Periasamy (1991). "Characterization of a mammalian smooth muscle myosin heavy-chain gene: complete nucleotide and protein coding sequence and analysis of the 5' end of the gene." Proc Natl Acad Sci U S A **88**(23): 10676-80.

Babij, P. and M. Periasamy (1989). "Myosin heavy chain isoform diversity in smooth muscle is produced by differential RNA processing." J Mol Biol **210**(3): 673-9.

Babu, G. J., G. J. Pyne, Y. Zhou, C. Okwuchukwasanya, J. E. Brayden, G. Osol, R. J. Paul, R. B. Low and M. Periasamy (2004). "Isoform switching from SM-B to SM-A myosin results in decreased contractility and altered expression of thin filament regulatory proteins." Am J Physiol Cell Physiol **287**(3): C723-9.

Babu, G. J., D. M. Warshaw and M. Periasamy (2000). "Smooth muscle myosin heavy chain isoforms and their role in muscle physiology." Microsc Res Tech **50**(6): 532-40.

Bacchiocchi, C., P. Graceffa and S. S. Lehrer (2004). "Myosin-induced movement of alphaalpha, alphabeta, and betabeta smooth muscle tropomyosin on actin observed by multisite FRET." Biophys J **86**(4): 2295-307.

Bahler, M. (2000). "Are class III and class IX myosins motorized signalling molecules?" Biochim Biophys Acta **1496**(1): 52-9.

Barany, M. (1996). Biochemistry of Smooth Muscle Contraction. San Diego, Academic Press, Inc.

Basha, M., S. Chang, E. M. Smolock, R. S. Moreland, A. J. Wein and S. Chacko (2006). "Regional differences in myosin heavy chain isoform expression and maximal shortening velocity of the rat vaginal wall smooth muscle." Am J Physiol Regul Integr Comp Physiol.

Battistella-Patterson, A. S., S. Wang and G. L. Wright (1997). "Effect of disruption of the cytoskeleton on smooth muscle contraction." Can J Physiol Pharmacol **75**(12): 1287-99.

Berg, J. S., B. C. Powell and R. E. Cheney (2001). "A millennial myosin census." Mol Biol Cell **12**(4): 780-94.

Bitar, K. N. (2003). "Function of gastrointestinal smooth muscle: from signaling to contractile proteins." Am J Med **115 Suppl 3A**: 15S-23S.

Bitar, K. N., M. S. Kaminski, N. Hailat, K. B. Cease and J. R. Strahler (1991). "Hsp27 is a mediator of sustained smooth muscle contraction in response to bombesin." Biochem Biophys Res Commun **181**(3): 1192-200.

Bodis, E., K. Szarka, M. Nyitrai and B. Somogyi (2003). "Dynamic reorganization of the motor domain of myosin subfragment 1 in different nucleotide states." Eur J Biochem **270**(24): 4835-45.

Borovikov, Y. S., A. Wrzosek, N. Kulikova, P. Vikhorev, N. Vikhoreva and R. Dabrowska (2004). "Behavior of caldesmon upon interaction of thin filaments with myosin subfragment 1 in ghost fibers." Biochim Biophys Acta **1699**(1-2): 183-9.

Brandt, D., M. Gimona, M. Hillmann, H. Haller and H. Mischak (2002). "Protein kinase C induces actin reorganization via a Src- and Rho-dependent pathway." J Biol Chem **277**(23): 20903-10.

Brophy, C. M., M. Dickinson and D. Woodrum (1999). "Phosphorylation of the small heat shock-related protein, HSP20, in vascular smooth muscles is associated with changes in the macromolecular associations of HSP20." J Biol Chem **274**(10): 6324-9.

Brophy, C. M., S. Lamb and A. Graham (1999). "The small heat shock-related protein-20 is an actin-associated protein." J Vasc Surg **29**(2): 326-33.

Brown, D., A. Dykes, J. Black, S. Thatcher, M. E. Fultz and G. L. Wright (2006). "Differential actin isoform reorganization in the contracting A7r5 cell." Can J Physiol Pharmacol **84**(8-9): 867-75.

Burmeister Getz, E., R. Cooke and P. R. Selvin (1998). "Luminescence resonance energy transfer measurements in myosin." Biophys J **74**(5): 2451-8.

Cavaille, F., C. Janmot, S. Ropert and A. d'Albis (1986). "Isoforms of myosin and actin in human, monkey and rat myometrium. Comparison of pregnant and non-pregnant uterus proteins." Eur J Biochem **160**(3): 507-13.

Chan, W. L., J. Silberstein and C. M. Hai (2000). "Mechanical strain memory in airway smooth muscle." Am J Physiol Cell Physiol **278**(5): C895-904.

Chrzanowska-Wodnicka, M. and K. Burridge (1996). "Rho-stimulated contractility drives the formation of stress fibers and focal adhesions." J Cell Biol **133**(6): 1403-15.

Cyr, J. L., R. A. Dumont and P. G. Gillespie (2002). "Myosin-1c interacts with hair-cell receptors through its calmodulin-binding IQ domains." J Neurosci **22**(7): 2487-95.

DiSanto, M. E., R. H. Cox, Z. Wang and S. Chacko (1997). "NH<sub>2</sub>-terminal-inserted myosin II heavy chain is expressed in smooth muscle of small muscular arteries." Am J Physiol **272**(5 Pt 1): C1532-42.

Diwan, J. J. (2006). "Myosin." Biochemistry of the Cell, from [www.rpi.edu/dept/bcbp/molbiochem/MBWeb/mb2/part1/myosin.htm](http://www.rpi.edu/dept/bcbp/molbiochem/MBWeb/mb2/part1/myosin.htm).

Dykes, A. C., M. E. Fultz, M. L. Norton and G. L. Wright (2003). "Microtubule-dependent PKC- $\alpha$  localization in A7r5 smooth muscle cells." Am J Physiol Cell Physiol **285**(1): C76-87.

Eddinger, T. J. and R. A. Murphy (1991). "Developmental changes in actin and myosin heavy chain isoform expression in smooth muscle." Arch Biochem Biophys **284**(2): 232-7.

Fujihara, H., L. A. Walker, M. C. Gong, E. Lemichez, P. Boquet, A. V. Somlyo and A. P. Somlyo (1997). "Inhibition of RhoA translocation and calcium sensitization by in vivo ADP-ribosylation with the chimeric toxin DC3B." Mol Biol Cell **8**(12): 2437-47.

Fultz, M. E., C. Li, W. Geng and G. L. Wright (2000). "Remodeling of the actin cytoskeleton in the contracting A7r5 smooth muscle cell." J Muscle Res Cell Motil **21**(8): 775-87.

Fultz, M. E. and G. L. Wright (2003). "Myosin remodelling in the contracting A7r5 smooth muscle cell." Acta Physiol Scand **177**(2): 197-205.

Gallagher, P. J., Y. Jin, G. Killough, E. K. Blue and V. Lindner (2000). "Alterations in expression of myosin and myosin light chain kinases in response to vascular injury." Am J Physiol Cell Physiol **279**(4): C1078-87.

Gerthoffer, W. T. and S. J. Gunst (2001). "Invited review: focal adhesion and small heat shock proteins in the regulation of actin remodeling and contractility in smooth muscle." J Appl Physiol **91**(2): 963-72.

Gong, M. C., H. Fujihara, A. V. Somlyo and A. P. Somlyo (1997). "Translocation of rhoA associated with Ca<sup>2+</sup> sensitization of smooth muscle." J Biol Chem **272**(16): 10704-9.

Gorenne, I., X. Su and R. S. Moreland (2004). "Caldesmon phosphorylation is catalyzed by two kinases in permeabilized and intact vascular smooth muscle." J Cell Physiol **198**(3): 461-9.

Graceffa, P. (1999). "Movement of smooth muscle tropomyosin by myosin heads." Biochemistry **38**(37): 11984-92.

Graceffa, P. and A. Mazurkie (2005). "Effect of caldesmon on the position and myosin-induced movement of smooth muscle tropomyosin bound to actin." J Biol Chem **280**(6): 4135-43.

Gusev, N. B. (2001). "Some properties of caldesmon and calponin and the participation of these proteins in regulation of smooth muscle contraction and cytoskeleton formation." Biochemistry (Mosc) **66**(10): 1112-21.

Guyton, A. C. and J. E. Hall (2000). Textbook of Medical Physiology. Philadelphia, PA, W. B. Saunders Company.

Hai, C. M. and H. R. Kim (2005). "An expanded latch-bridge model of protein kinase C-mediated smooth muscle contraction." J Appl Physiol **98**(4): 1356-65.

Hai, C. M. and R. A. Murphy (1992). "Adenosine 5'-triphosphate consumption by smooth muscle as predicted by the coupled four-state crossbridge model." Biophys J **61**(2): 530-41.

Hamada, Y., M. Yanagisawa, Y. Katsuragawa, J. R. Coleman, S. Nagata, G. Matsuda and T. Masaki (1990). "Distinct vascular and intestinal smooth muscle myosin heavy chain mRNAs are encoded by a single-copy gene in the chicken." Biochem Biophys Res Commun **170**(1): 53-8.

Hasson, T. and M. S. Mooseker (1996). "Vertebrate unconventional myosins." J Biol Chem **271**(28): 16431-4.

Helper, D. J., J. A. Lash and D. R. Hathaway (1988). "Distribution of isoelectric variants of the 17,000-dalton myosin light chain in mammalian smooth muscle." J Biol Chem **263**(30): 15748-53.

Herrera, A. M., K. H. Kuo and C. Y. Seow (2002). "Influence of calcium on myosin thick filament formation in intact airway smooth muscle." Am J Physiol Cell Physiol **282**(2): C310-6.

Herrera, A. M., B. E. McParland, A. Bienkowska, R. Tait, P. D. Pare and C. Y. Seow (2005). "'Sarcomeres' of smooth muscle: functional characteristics and ultrastructural evidence." J Cell Sci **118**(Pt 11): 2381-92.

Hoya, K., A. Asai, T. Sasaki, K. Nagata, K. Kimura and T. Kirino (2003). "Expression of myosin heavy chain isoforms by smooth muscle cells in cerebral arteriovenous malformations." Acta Neuropathol (Berl) **105**(5): 455-61.



Hypolite, J. A., M. E. DiSanto, Y. Zheng, S. Chang, A. J. Wein and S. Chacko (2001). "Regional variation in myosin isoforms and phosphorylation at the resting tone in urinary bladder smooth muscle." Am J Physiol Cell Physiol **280**(2): C254-64.

Hyvelin, J. M., C. O'Connor and P. McLoughlin (2004). "Effect of changes in pH on wall tension in isolated rat pulmonary artery: role of the RhoA/Rho-kinase pathway." Am J Physiol Lung Cell Mol Physiol **287**(4): L673-84.

Ishiwata, S., M. Miki, I. Shin, T. Funatsu, K. Yasuda and C. G. dos Remedios (1997). "Interhead distances in myosin attached to F-actin estimated by fluorescence energy transfer spectroscopy." Biophys J **73**(2): 895-904.

Itoh, S., S. Umemoto, M. Hiromoto, Y. Toma, Y. Tomochika, S. Aoyagi, M. Tanaka, T. Fujii and M. Matsuzaki (2002). "Importance of NAD(P)H oxidase-mediated oxidative stress and contractile type smooth muscle myosin heavy chain SM2 at the early stage of atherosclerosis." Circulation **105**(19): 2288-95.

Jares-Erijman, E. A. and T. M. Jovin (2003). "FRET imaging." Nat Biotechnol **21**(11): 1387-95.

Kawabata, S., J. Usukura, N. Morone, M. Ito, A. Iwamatsu, K. Kaibuchi and M. Amano (2004). "Interaction of Rho-kinase with myosin II at stress fibres." Genes Cells **9**(7): 653-60.

Kawamoto, S. and R. S. Adelstein (1987). "Characterization of myosin heavy chains in cultured aorta smooth muscle cells. A comparative study." J Biol Chem **262**(15): 7282-8.

Kekic, M., W. Huang, P. D. Moens, B. D. Hambly and C. G. dos Remedios (1996). "Distance measurements near the myosin head-rod junction using fluorescence spectroscopy." Biophys J **71**(1): 40-7.

Kelley, C. A. and R. S. Adelstein (1990). "The 204-kDa smooth muscle myosin heavy chain is phosphorylated in intact cells by casein kinase II on a serine near the carboxyl terminus." J Biol Chem **265**(29): 17876-82.

Kelley, C. A., J. R. Sellers, P. K. Goldsmith and R. S. Adelstein (1992). "Smooth muscle myosin is composed of homodimeric heavy chains." J Biol Chem **267**(4): 2127-30.

Kelley, C. A., M. Takahashi, J. H. Yu and R. S. Adelstein (1993). "An insert of seven amino acids confers functional differences between smooth muscle myosins from the intestines and vasculature." J Biol Chem **268**(17): 12848-54.

Kendrick-Jones, J., T. P. Hodge, I. M. B. Lister, R. C. Roberts and F. Buss. (2001). "Myosin Superfamily."

Kenworthy, A. K. (2001). "Imaging protein-protein interactions using fluorescence resonance energy transfer microscopy." Methods **24**(3): 289-96.

Khaitlina, S. Y. (2001). "Functional specificity of actin isoforms." Int Rev Cytol **202**: 35-98.

Kuo, K. H. and C. Y. Seow (2004). "Contractile filament architecture and force transmission in swine airway smooth muscle." J Cell Sci **117**(Pt 8): 1503-11.

Kuro-o, M., R. Nagai, H. Tsuchimochi, H. Katoh, Y. Yazaki, A. Ohkubo and F. Takaku (1989). "Developmentally regulated expression of vascular smooth muscle myosin heavy chain isoforms." J Biol Chem **264**(31): 18272-5.

Li, C., M. E. Fultz, J. Parkash, W. B. Rhoten and G. L. Wright (2001). "Ca<sup>2+</sup>-dependent actin remodeling in the contracting A7r5 cell." J Muscle Res Cell Motil **22**(6): 521-34.

Lidke, D. S. and D. D. Thomas (2002). "Coordination of the two heads of myosin during muscle contraction." Proc Natl Acad Sci U S A **99**(23): 14801-6.

Liu, J., T. Wendt, D. Taylor and K. Taylor (2003). "Refined model of the 10S conformation of smooth muscle myosin by cryo-electron microscopy 3D image reconstruction." J Mol Biol **329**(5): 963-72.

Lohn, M., D. Kampf, C. Gui-Xuan, H. Haller, F. C. Luft and M. Gollasch (2002). "Regulation of arterial tone by smooth muscle myosin type II." Am J Physiol Cell Physiol **283**(5): C1383-9.

Low, R. B., J. Mitchell, J. Woodcock-Mitchell, A. S. Rovner and S. L. White (1999). "Smooth-muscle myosin heavy-chain SM-B isoform expression in developing and adult rat lung." Am J Respir Cell Mol Biol **20**(4): 651-7.

Lowey, S. and K. M. Trybus (1995). "Role of skeletal and smooth muscle myosin light chains." Biophys J **68**(4 Suppl): 120S-126S; discussion 126S-127S.

Mannikarottu, A. S., J. A. Hypolite, S. A. Zderic, A. J. Wein, S. Chacko and M. E. Disanto (2005). "Regional alterations in the expression of smooth muscle myosin isoforms in response to partial bladder outlet obstruction." J Urol **173**(1): 302-8.

Meer, D. P. and T. J. Eddinger (1997). "Expression of smooth muscle myosin heavy chains and unloaded shortening in single smooth muscle cells." Am J Physiol **273**(4 Pt 1): C1259-66.

Mehta, D. and S. J. Gunst (1999). "Actin polymerization stimulated by contractile activation regulates force development in canine tracheal smooth muscle." J Physiol **519 Pt 3**: 829-40.

Mehta, D., M. F. Wu and S. J. Gunst (1996). "Role of contractile protein activation in the length-dependent modulation of tracheal smooth muscle force." Am J Physiol **270**(1 Pt 1): C243-52.

Mizukura, Y. and S. Maruta (2002). "Analysis of the conformational change of myosin during ATP hydrolysis using fluorescence resonance energy transfer." J Biochem (Tokyo) **132**(3): 471-82.

Morgan, K. G. and S. S. Gangopadhyay (2001). "Invited review: cross-bridge regulation by thin filament-associated proteins." J Appl Physiol **91**(2): 953-62.

Nabeshima, Y., Y. Nabeshima, Y. Nonomura and Y. Fujii-Kuriyama (1987). "Nonmuscle and smooth muscle myosin light chain mRNAs are generated from a single gene by the tissue-specific alternative RNA splicing." J Biol Chem **262**(22): 10608-12.

Nagai, R., M. Kuro-o, P. Babij and M. Periasamy (1989). "Identification of two types of smooth muscle myosin heavy chain isoforms by cDNA cloning and immunoblot analysis." J Biol Chem **264**(17): 9734-7.

Nagai, R., D. M. Larson and M. Periasamy (1988). "Characterization of a mammalian smooth muscle myosin heavy chain cDNA clone and its expression in various smooth muscle types." Proc Natl Acad Sci U S A **85**(4): 1047-51.

Numaguchi, K., S. Eguchi, T. Yamakawa, E. D. Motley and T. Inagami (1999). "Mechanotransduction of rat aortic vascular smooth muscle cells requires RhoA and intact actin filaments." Circ Res **85**(1): 5-11.

Owens, G. K. and M. M. Thompson (1986). "Developmental changes in isoactin expression in rat aortic smooth muscle cells in vivo. Relationship between growth and cytodifferentiation." J Biol Chem **261**(28): 13373-80.

Palm, T., K. Sale, L. Brown, H. Li, B. Hambly and P. G. Fajer (1999). "Intradomain distances in the regulatory domain of the myosin head in prepower and postpower stroke states: fluorescence energy transfer." Biochemistry **38**(40): 13026-34.

Paul, R. J. (1983). "Functional compartmentalization of oxidative and glycolytic metabolism in vascular smooth muscle." Am J Physiol **244**(5): C399-409.

Pratusevich, V. R., C. Y. Seow and L. E. Ford (1995). "Plasticity in canine airway smooth muscle." J Gen Physiol **105**(1): 73-94.

Reshetnyak, Y. K. and O. A. Andreev (2001). "The interdomain motions in myosin subfragment 1." Biophys Chem **94**(1-2): 41-6.

Rovner, A. S., P. M. Fagnant, S. Lowey and K. M. Trybus (2002). "The carboxyl-terminal isoforms of smooth muscle myosin heavy chain determine thick filament assembly properties." J Cell Biol **156**(1): 113-23.

Rovner, A. S., P. M. Fagnant and K. M. Trybus (2006). "Phosphorylation of a single head of smooth muscle myosin activates the whole molecule." Biochemistry **45**(16): 5280-9.

Rovner, A. S., M. M. Thompson and R. A. Murphy (1986). "Two different heavy chains are found in smooth muscle myosin." Am J Physiol **250**(6 Pt 1): C861-70.

Schildmeyer, L. A. and C. L. Seidel (1989). "Quantitative and qualitative heterogeneity in smooth muscle myosin heavy chains." Life Sci **45**(18): 1617-25.

Selvin, P. R. (2000). "The renaissance of fluorescence resonance energy transfer." Nat Struct Biol **7**(9): 730-4.

Seow, C. Y. (2005). "Myosin filament assembly in an ever-changing myofilament lattice of smooth muscle." Am J Physiol Cell Physiol **289**(6): C1363-8.

Sherwood, J. J. and T. J. Eddinger (2002). "Shortening velocity and myosin heavy- and light-chain isoform mRNA in rabbit arterial smooth muscle cells." Am J Physiol Cell Physiol **282**(5): C1093-102.

Shih, W. M., Z. Gryczynski, J. R. Lakowicz and J. A. Spudich (2000). "A FRET-based sensor reveals large ATP hydrolysis-induced conformational changes and three distinct states of the molecular motor myosin." Cell **102**(5): 683-94.

Smolensky, A. V., S. H. Gilbert, M. Harger-Allen and L. E. Ford (2007). "Inhibition of myosin light-chain phosphorylation inverts the birefringence response of porcine airway smooth muscle." J Physiol **578**(Pt 2): 563-8.

Somara, S. and K. N. Bitar (2004). "Tropomyosin interacts with phosphorylated HSP27 in agonist-induced contraction of smooth muscle." Am J Physiol Cell Physiol **286**(6): C1290-301.

Spudich, J. A. (1989). "In pursuit of myosin function." Cell Regul **1**(1): 1-11.

Suzuki, Y., T. Yasunaga, R. Ohkura, T. Wakabayashi and K. Sutoh (1998). "Swing of the lever arm of a myosin motor at the isomerization and phosphate-release steps." Nature **396**(6709): 380-3.

Sweeney, H. L. (1998). "Regulation and tuning of smooth muscle myosin." Am J Respir Crit Care Med **158**(5 Pt 3): S95-9.

- Szymanski, P. T., T. K. Chacko, A. S. Rovner and R. K. Goyal (1998). "Differences in contractile protein content and isoforms in phasic and tonic smooth muscles." Am J Physiol **275**(3 Pt 1): C684-92.
- Trybus, K. M., T. W. Huiatt and S. Lowey (1982). "A bent monomeric conformation of myosin from smooth muscle." Proc Natl Acad Sci U S A **79**(20): 6151-5.
- Trybus, K. M. and S. Lowey (1984). "Conformational states of smooth muscle myosin. Effects of light chain phosphorylation and ionic strength." J Biol Chem **259**(13): 8564-71.
- Tyska, M. J., D. E. Dupuis, W. H. Guilford, J. B. Patlak, G. S. Waller, K. M. Trybus, D. M. Warshaw and S. Lowey (1999). "Two heads of myosin are better than one for generating force and motion." Proc Natl Acad Sci U S A **96**(8): 4402-7.
- VanBuren, P., S. S. Work and D. M. Warshaw (1994). "Enhanced force generation by smooth muscle myosin in vitro." Proc Natl Acad Sci U S A **91**(1): 202-5.
- Vorotnikov, A. V., M. A. Krymsky and V. P. Shirinsky (2002). "Signal transduction and protein phosphorylation in smooth muscle contraction." Biochemistry (Mosc) **67**(12): 1309-28.
- Wagner, P. D. (1981). "Formation and characterization of myosin hybrids containing essential light chains and heavy chains from different muscle myosins." J Biol Chem **256**(5): 2493-8.
- Webb, R. C. (2003). "Smooth muscle contraction and relaxation." Adv Physiol Educ **27**(1-4): 201-6.

White, S., A. F. Martin and M. Periasamy (1993). "Identification of a novel smooth muscle myosin heavy chain cDNA: isoform diversity in the S1 head region." Am J Physiol **264**(5 Pt 1): C1252-8.

White, S. L., M. Y. Zhou, R. B. Low and M. Periasamy (1998). "Myosin heavy chain isoform expression in rat smooth muscle development." Am J Physiol **275**(2 Pt 1): C581-9.

Worth, N. F., G. R. Campbell, J. H. Campbell and B. E. Rolfe (2004). "Rho expression and activation in vascular smooth muscle cells." Cell Motil Cytoskeleton **59**(3): 189-200.

Wright, G. and E. Hurn (1994). "Cytochalasin inhibition of slow tension increase in rat aortic rings." Am J Physiol **267**(4 Pt 2): H1437-46.

Wu, H. Y., S. A. Zderic, A. J. Wein and S. Chacko (2004). "Decrease in maximal force generation in the neonatal mouse bladder corresponds to shift in myosin heavy chain isoform composition." J Urol **171**(2 Pt 1): 841-4.

Xiao, M., J. G. Reifenberger, A. L. Wells, C. Baldacchino, L. Q. Chen, P. Ge, H. L. Sweeney and P. R. Selvin (2003). "An actin-dependent conformational change in myosin." Nat Struct Biol **10**(5): 402-8.

### **Internet References**

[fig.cox.miami.edu/~cmallery/150/neuro/c49x33muscle-cycle.jpg](http://fig.cox.miami.edu/~cmallery/150/neuro/c49x33muscle-cycle.jpg)

[www.cella.cn/book/09/images/image009.jpg](http://www.cella.cn/book/09/images/image009.jpg)



## Chapter II

# FRET Analysis of Actin/Myosin Interaction in Contracting Rat Aortic Smooth Muscle

**J. Black<sup>1</sup>, A. Dykes<sup>1</sup>, S. Thatcher<sup>1</sup>, D. Brown<sup>1</sup>, E.C. Bryda<sup>2</sup>, and G.L. Wright<sup>1</sup>**

<sup>1</sup>The Joan C. Edwards School of Medicine, Department of Pharmacology, Physiology and Toxicology, Marshall University, Huntington, WV 25704, USA

<sup>2</sup>Department of Veterinary Pathobiology, University of Missouri, Columbia, MO 65211, USA

**Correspondence to:**

Gary L. Wright  
Professor of Pharmacology, Physiology and Toxicology  
The Joan Edwards School of Medicine  
Marshall University  
Huntington, WV 25704 USA  
Phone: 304 696 7368  
Fax: 304 696 7381  
E-mail: [wrightg@marshall.edu](mailto:wrightg@marshall.edu)

**Running title:** Actin/myosin association in smooth muscle

**Key Words:** actin isoforms, cytoskeleton, podosome, remodeling

## Abstract

**AIM:** We examined the interaction of smooth muscle myosin with  $\alpha$ -actin and  $\beta$ -actin isoforms during the contraction of A7r5 smooth muscle cells and rat aortic smooth muscle. **METHODS:** The techniques of confocal microscopy and fluorescence resonance energy transfer were utilized in examining A7r5 cells and rat aortic rings contracted with phorbol-12, 13-dibutyrate. **RESULTS:** Visual evaluation of confocal images of A7r5 smooth muscle cells contracted by phorbol-12, 13-dibutyrate indicated significant disassociation of myosin from  $\alpha$ -actin but not  $\beta$ -actin. Whole cell fluorescence resonance energy transfer analysis confirmed these observations ( $\alpha$ -actin/myosin, -67%;  $\beta$ -actin/myosin, -2%). Time course studies further showed that  $\alpha$ -actin/myosin complex increased significantly (40%) within 1.5 minutes after the addition of phorbol-12, 13-dibutyrate and then declined as contraction progressed. Fluorescence resonance energy transfer analysis of rat aortic rings at different intervals of contraction indicated significant increases in  $\alpha$ -actin/myosin at the initiation (79%) and plateau (67%) in force development but not during the intermediate period of slowly developing tension (-4%). By comparison,  $\beta$ -actin/myosin complex was unchanged except during slow force development where the association was significantly decreased (-30%). Similar to  $\alpha$ -actin/myosin, Alexa 488-phalloidin staining fluorescence indicated increased tissue F-actin content at initiation (21%) and the plateau (62%) in force. Fluorescence resonance energy transfer images indicated the development of thickened cables and patches of  $\alpha$ -actin/myosin in tissue throughout the interval of contraction. **CONCLUSION:** The results provide direct evidence of dynamic remodeling of the

contractile protein during vascular smooth muscle contraction and suggest that fluorescence resonance energy transfer analysis may be a powerful tool for assessment of tissue protein-protein associations.

### **Introduction**

A number of the contractile properties exhibited by smooth muscle are not readily explained by unmodified sliding filament theory. For example, smooth muscle has the ability to slowly develop force and then to sustain maximal tension for extended intervals at low energy cost (22). Moreover, there is evidence suggesting that force development and sustained tension (6) as well as velocity of shortening (20) are disassociated from myosin ATPase activity (32) in smooth muscle. Hence, there is growing recognition that mechanisms exist to modify the contractile properties of smooth muscle from that predicted solely on the basis of actin/myosin interaction within a static sarcomere arrangement.

One hypothesis gaining interest is that the contractile apparatus remodels in response to cell loading and during force development with cell shortening. Based on studies of isolated cells in which it was demonstrated that the length-tension relationship was altered by changing the initial length at which the cells were activated, Harris and Warshaw (1991) first suggested a disassociation of cell length and contractile element length. Gunst et al. (1993) subsequently showed that the velocity of shortening decreased as the tissue was activated at increasing lengths suggesting their results were consistent

with an earlier hypothesis (13) that decreased velocity could reflect an internal load created by compression of the cytoskeleton. They further suggested (11) that the inverse relationship between tissue length and velocity of shortening could be due to reorganization of the cytoskeleton serving to optimize contractile responses at each length. In a similar vein, Shen et al. (1997) concluded that the depression of force seen during oscillation of smooth muscle could be due to resetting of contractile element length due to stretch. Based on the observation that cytochalasin inhibition of actin polymerization blocked slow force development in rat aortic smooth muscle, our laboratory proposed that dynamic remodeling within the actin cytoskeleton was obligatory for this mode of contraction (30). This conclusion has been supported by the finding that inhibition of actin polymerization depresses force development without affecting myosin light chain phosphorylation, suggesting that actin remodeling contributes directly to force development (19).

It has also been suggested that remodeling of myosin could play a primary role in determining the contractile properties of smooth muscle by increasing the length of individual filaments and/or the number of contractile units in series (8, 23). The proposed series-to-parallel transition in myosin thick filament arrangement could potentially explain potentiation of isometric force and the inverse relationship between force and velocity of shortening (24).

Although there is increasing acceptance of the importance of cytoskeletal remodeling in smooth muscle contraction, the exact nature of the reorganization and manner in which

this impacts on contractility remains a matter of speculation. A number of studies have reported evidence of actin polymerization in tissues contracted with acetylcholine (19, 26), histamine (1) and norepinephrine (27). In addition, there is evidence to suggest that the number of myosin filaments is increased in contracted anococcygeus muscle (31). Studies of A7r5 smooth muscle cells contracted with phorbol esters further suggests that contractile remodeling may be unexpectedly complex. Initial findings indicate that  $\alpha$ - and  $\beta$ -actin, the dominant isoforms in these cells, remodel differently during contraction (10, 18) suggesting they could be subject to different regulatory influence. In addition, myosin was observed to undergo extensive relocalization in association with  $\alpha$ -actin during phorbol-induced contraction of these cells (9). However, it is not certain to what extent these findings in cultured cells apply to preloaded, highly differentiated smooth muscle cells within their tissue matrix. In the present study we have utilized confocal microscopy and fluorescence resonance energy transfer (FRET) analysis to compare actin/myosin association in A7r5 cells and rat aortic tissue at different time points during contraction. The results support actin isoform specific changes in association with myosin and alteration of actin/myosin structure during contraction.

## Methods

**Animals.** All procedures were performed in accordance with the Guide for the Care and Use of Laboratory Animals as approved by the Council of the American Physiological Society and the Animal Use Review Board of Marshall University. Male 12 week-old Sprague Dawley rats were housed on wood chip bedding in rooms

maintained at  $23 \pm 2^\circ\text{C}$  with a 12h light cycle. Purina Rat Chow and tap water were freely available.

**Tissue Preparation.** Rats were anesthetized with a ketamine-xylazine mixture (21:9 mg  $\text{kg}^{-1}$ ) and the thoracic aorta was surgically removed into buffer, cleaned of adherent tissue, and cut into 0.3 cm rings. Tissues were denuded of endothelium and then mounted under 5.0g of passive tension in glass organ baths containing Krebs buffer [(in mM) 118 NaCl, 4.7 KCl, 1.5  $\text{CaCl}_2$ , 25  $\text{NaHCO}_3$ , 1.1  $\text{MgCl}_2$ , 1.2  $\text{KH}_2\text{PO}_4$ , and 5.6 glucose; pH 7.4] maintained at  $37^\circ\text{C}$  and aerated with 5%  $\text{CO}_2$  in  $\text{O}_2$ . The tissues were equilibrated for a minimum of 2h before contraction by addition of  $10^{-7}\text{M}$  phorbol-12, 13-dibutyrate (PDBu). Isometric tension was measured using a grass FT03 force-displacement transducer and a Grass model 7D polygraph. Rings removed from the bath at selected intervals of contraction (Fig. 1) were cut longitudinally, placed adventitia down on aluminum foil and snap frozen in liquid nitrogen. Samples were maintained at  $-70^\circ\text{C}$  until sectioned.

**Cell Culture.** A7r5 smooth muscle cells derived from embryonic rat aorta and shown to maintain the ability to contract to phorbol esters (21, 10), were obtained from American Type Culture Collection (Manassas, VA). Cells were plated on  $75\text{ cm}^2$  flasks and grown to approximately 80% confluence at  $37^\circ\text{C}$  in a humidified atmosphere of 5%  $\text{CO}_2$  in air. The cells were maintained in Dulbecco's modified Eagles medium (DMEM) supplemented with 10% fetal calf serum, 100 units  $\text{ml}^{-1}$  penicillin G, and  $100\ \mu\text{g}\ \text{ml}^{-1}$

streptomycin. Media was changed every other day and cells were passaged at least once a week.

**Confocal Microscopy.** Cells were seeded onto glass coverslips, placed in 6 well culture plates and returned to the incubator to allow for attachment and spreading. After treatment with PDBu ( $10^{-7}$  M) the cells were immediately fixed and permeabilized by addition of ice-cold acetone for 1.0 minute. The cells were then washed several times with phosphate-buffered saline (PBS) containing 0.5% TWEEN-20 (PBS-T), pH 7.5, followed by a 60 minute incubation in blocking solution containing 5% nonfat dry milk in PBS. Aortic rings from individual rats were selected for study at the onset of PDBu-induced force development (0.3g tension), approximately midway through the contraction (2.5g tension), and 15 minutes after the plateau in tension (Fig. 1). Tissues were sectioned at 8  $\mu$ m longitudinally on an IEC cryotome and placed on poly-L-lysine coated slides. Sections were then fixed and permeablized by addition of ice-cold acetone for 1.0 minute. The slides were rinsed (3X) with PBS-T and preblocked with 5% nonfat dry milk in PBS. Cell and tissue samples were stained for myosin by incubation with a monoclonal, clone C5C.S2 pan-anti-myosin IgM primary antibody (Covance, Berkeley, CA) followed by an anti-IgM Alexa 546 secondary antibody (Molecular Probes, Eugene, OR).  $\alpha$ -Actin and  $\beta$ -actin were visualized using monoclonal anti- $\alpha$ -smooth muscle actin, clone 1A4 (IgG2a) and anti- $\beta$ -actin, clone AC-15 (IgG1) primary antibodies (Sigma, Saint Louis, MO), respectively, followed by Alexa 488 anti-IgG secondary antibody (Molecular Probes). In many experiments, tissues were also stained with TO-PRO-3

iodide (Molecular Probes) to enable visualization of the cell nucleus in combination with FRET images. Cells were viewed at 600X magnification and tissue sections were viewed at 1000x. The numerical aperture of the objective was 1.4. The thickness of the section analyzed was 0.5  $\mu\text{m}$ .

To evaluate F-actin content, tissue sections from each group were stained with phalloidin conjugated with an Alexa 488 fluorophore (Molecular Probes, Eugene, OR). Sections from all groups were imaged at constant confocal settings and the fluorescence plot was obtained using Image J (NIH) software. The area under the curve was determined using PeakFit (Systat Software, Inc., Richmond, CA) and the fluorescence calculated per unit area surveyed.

**FRET analysis.** In the present study, we utilized the approach of measuring donor molecule quenching in the presence of acceptor as an index of FRET (reviewed in 16). This approach to FRET evaluation is amenable to immunostaining and confocal imaging of fixed biological samples. It must be noted, however, that the method as presently employed assumes that such factors as the absorption coefficient of the acceptor, the quantum yield of the donor, relative antibody binding affinity and the relative orientation of donor/acceptor antibody complexes, remain constant between treatment groups. Cell and tissue samples were imaged with a Nikon Diaphot Microscope and confocal microscopy performed with a BioRad Model 1024 scanning system with a krypton/argon laser. Within a FRET system two fluorophores with overlapping emission and excitation spectra are utilized. Here actin isoforms were labeled with Alexa 488 (excitation, 488



nm; emission, 520 nm) and served as the donor component of the system. Myosin was labeled with Alexa 546 (excitation, 546 nm; emission, 580 nm) and served as the acceptor component. The donor molecule ( $\alpha$ - or  $\beta$ -actin, Alexa 488) was directly excited and the resulting emission was obtained with a 522 DF32 band pass filter. However, a portion of the energy of emission was not released as light but was transferred to neighboring Alexa 546 fluorophore resulting in emission which was captured on a second channel with an HQ 598/40 band-pass filter. Subsequently, the image was excited at the 568 nm laser line at 100% power to photobleach the acceptor molecule (myosin) and a second image of the cell or tissue was acquired again at the 488 nm laser line excitation with the multichannel filter set to obtain actin fluorescence (522 DF32) and to verify the absence of myosin label Alexa 546 emission (HQ 598/40). An intensity profile was generated for each sample (Image J Software, NIH) and the resulting plot was analyzed with Peakfit V4.11 software (SPSS Science, Richmond, CA) to obtain the area under the curve. The values were then used to calculate the percent increase in fluorescence emission after photobleaching. Resonance energy transfer can only occur if the donor and acceptor molecules are close enough to each other for the transfer to occur efficiently. Hence, the resulting values were analyzed in comparisons of control and PDBu-treated A7r5 cells and aortic tissue samples as an index of the association between actin and myosin during PDBu-induced contraction.

In addition to the evaluation of experimental samples, FRET analysis of A7r5 cells was conducted in two control conditions. In an initial experiment, FRET analysis of  $\alpha$ -actin/myosin association was performed in the absence of anti- $\alpha$  smooth muscle actin

clone 1A4 primary antibody. This negative control tested for the magnitude of effect of non-specific binding of the donor Alexa 488 labeled secondary antibody in its contribution to the increase in fluorescence intensity after photobleaching of the Alexa 546 labeled myosin. In a second experiment, unstimulated and PDBu-treated cells were stained only for myosin using the monoclonal, clone C5C.S2 pan anti-myosin primary antibody. This was followed by incubation with a 1:1 mixture of mouse anti-IgM antibodies conjugated to Alexa 488 or Alexa 546 fluorophores. Because the primary antibody binding epitope is the S2 head region of myosin, it was expected that the FRET index of increased fluorescence after acceptor fluorophore photobleaching would not be altered by PDBu treatment as occurred with actin/myosin association.

**Statistics.** Differences in the index of actin/myosin association were analyzed by ANOVA followed by Student's t-test (Sigma Stat 2.03, SPSS Science). Differences were considered significant if  $P < 0.05$  in all cases. Data are presented as means  $\pm$  SEM throughout the text.

## **Results**

**A7r5 Smooth Muscle Cells.** Figure 2 shows control and PDBu-treated ( $10^{-7}$  M) cells with dual staining for  $\alpha$ -actin and myosin. Similar to previous findings (10), colocalization imaging indicated myosin association with  $\alpha$ -actin stress fibers in unstimulated control cells. PDBu stimulation resulted in a loss of  $\alpha$ -actin stress fibers with relocation of  $\alpha$ -actin at podosomes in the cell periphery. Myosin was observed to be

associated with  $\alpha$ -actin in podosomes and in the remaining stress fibers but also showed diffuse staining in the perinuclear region, suggesting substantial disassociation of myosin from  $\alpha$ -actin in the contracted cell. Figure 3 shows FRET analysis of the same cells including fluorescence before and after acceptor (myosin) photobleaching. In addition to enabling the calculation of an index of  $\alpha$ -actin/myosin association (Table 1A), the difference between these two images may provide a high resolution method for imaging specific sites of protein interaction not completely clear from colocalization images. For example, FRET images show clearly the intermittent nature of  $\alpha$ -actin/myosin association in stress fibers and indicate strong  $\alpha$ -actin/myosin association on the cytosolic side of podosomes (Fig. 3).

Unlike  $\alpha$ -actin,  $\beta$ -actin remained in stress fibers in PDBu-treated cells (Fig. 4). Myosin appeared to be colocalized with  $\beta$ -actin stress fibers as well as perinuclear structure not observed in  $\alpha$ -actin stained cells. FRET analysis indicated  $\beta$ -actin/myosin association in stress fibers but further suggested a diffuse, network-like arrangement of  $\beta$ -actin/myosin structure in some cells (Fig. 5).

FRET analysis yielded significant indices of myosin association with  $\alpha$ -actin ( $73.3 \pm 6.0$ ) and  $\beta$ -actin ( $74.5 \pm 5.2$ ) in control A7r5 cells (Table 1A). Consistent with visual evaluations of colocalization images suggesting myosin disassociation at near completion of cell contraction, the index of myosin association with  $\alpha$ -actin decreased by approximately 70% in PDBu-treated cells (Table 1A). By comparison, the FRET index of myosin association with  $\beta$ -actin was unchanged in PDBu-treated cells. A detailed

FRET evaluation of the time course of  $\alpha$ -actin/myosin association further indicated a significant increase in the interaction of these proteins within the 5.0 min interval following the addition of PDBu which then declined with cell contraction (Table 1B). FRET analysis of  $\alpha$ -actin/myosin association in the absence of anti- $\alpha$ -smooth muscle actin primary antibody indicated insignificant non-specific binding of donor Alexa 488 labeled secondary antibody (<1% control). As expected the increase in Alexa 488 fluorophore fluorescence after photobleaching of the acceptor Alexa 546 fluorophore was not different between control ( $17.8 \pm 3.4\%$ ) and PDBu-stimulated ( $22.5 \pm 1.7\%$ ) cells. Taken together, the results with A7r5 cells suggest a highly dynamic remodeling of the actin/myosin contractile protein during contraction. They further suggest that FRET analysis is a valuable tool in determining cell protein-protein associations.

**Aortic Vascular Smooth Muscle.** Dual staining with phalloidin and TO-PRO-3 iodide shows the parallel and densely packed arrangement of vascular smooth muscle cells (Fig. 6). This figure emphasizes the differences in cell plane of section and lack of detailed structure which make difficult the interpretation of images from tissue sections.

Actin/myosin colocalization imaging (Fig. 7) shows the confusion of structure typically obtained with immunostaining of these proteins in tissue, while indicating significant colocalization of the two proteins. FRET analysis greatly simplified the tissue images of actin/myosin structure (Fig. 8), and indicated that  $\alpha$ -actin/myosin complex was increased at the beginning (79%) and at the plateau (67%) in force development, but was unchanged from control midway through the PDBu-induced contraction (Table 2). By comparison,  $\beta$ -actin/myosin association was not significantly different from controls

except at mid-contraction where an approximate 30% decrease was recorded. The results suggest extensive isoform specific remodeling of the actin/myosin contractile protein in contracting vascular smooth muscle tissue.

Evaluation of actin/myosin structural changes in intact tissues remains problematic. The small cell size, variance in cell orientation in the plane of sectioning, difficulty in achieving correct orientation of tissues for sectioning, and the relatively low magnification of confocal microscopy each contribute to the random nature of actin/myosin structural organization seen in tissue. Nevertheless, we report one change in  $\alpha$ -actin/myosin consistently observed in contracting but not control tissue. Notable at each stage of contraction was the coalescence of  $\alpha$ -actin and myosin, which when viewed in relation to nuclei, appeared as thickened cables or patches (Fig. 9). We estimate that cable-like structures in tissues range at 0.6 to 1.0  $\mu\text{m}$  in diameter and are comparable in size to stress fibers observed in A7r5 cells (1.0-2.2  $\mu\text{m}$ )

Quantitation of phalloidin staining fluorescence suggested that the F-actin content of tissue slightly increased (21%) at the beginning of force development and was significantly elevated (62%) at the plateau in tension (Table 3). F-actin was reduced (-17%) midway through the contraction but this was not significantly different from the control value.

## Figures

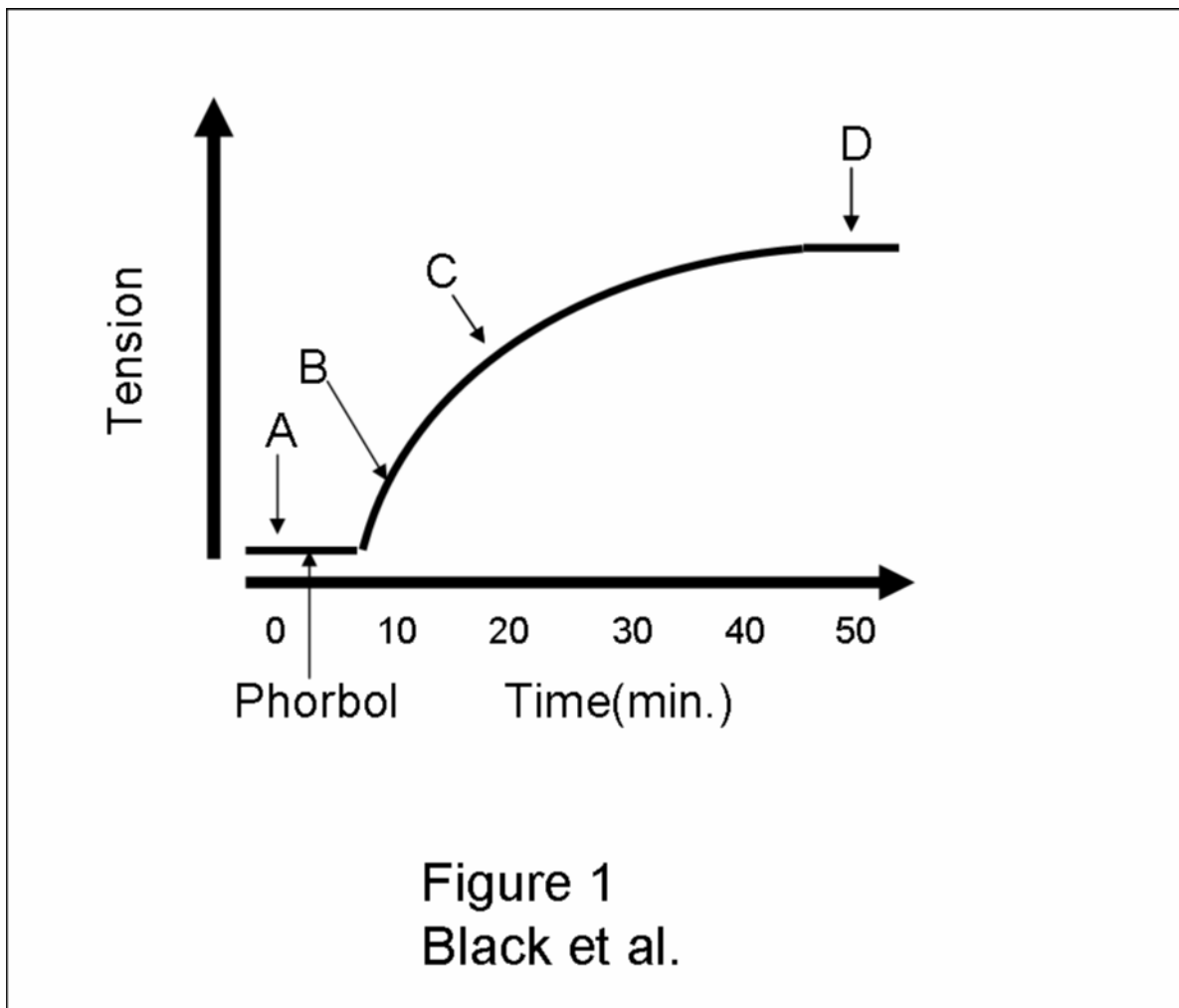


**Figure 1.** Time intervals selected for FRET analysis of rat aortic smooth muscle. Aortic rings were mounted in glass organ baths at a preload of 5.0g and equilibrated for 2 hours. They were then contracted by the addition of  $10^{-7}$  M phorbol 12, 13 dibutyrate (PDBu) and removed at time 0 (A), at the start of force development (B), approximately midway through the contraction (C), and at 15 minutes after the plateau in tension (D). The tissues were then frozen in liquid nitrogen for sectioning. A set of aortic segments obtained at each interval was taken from an individual animal.

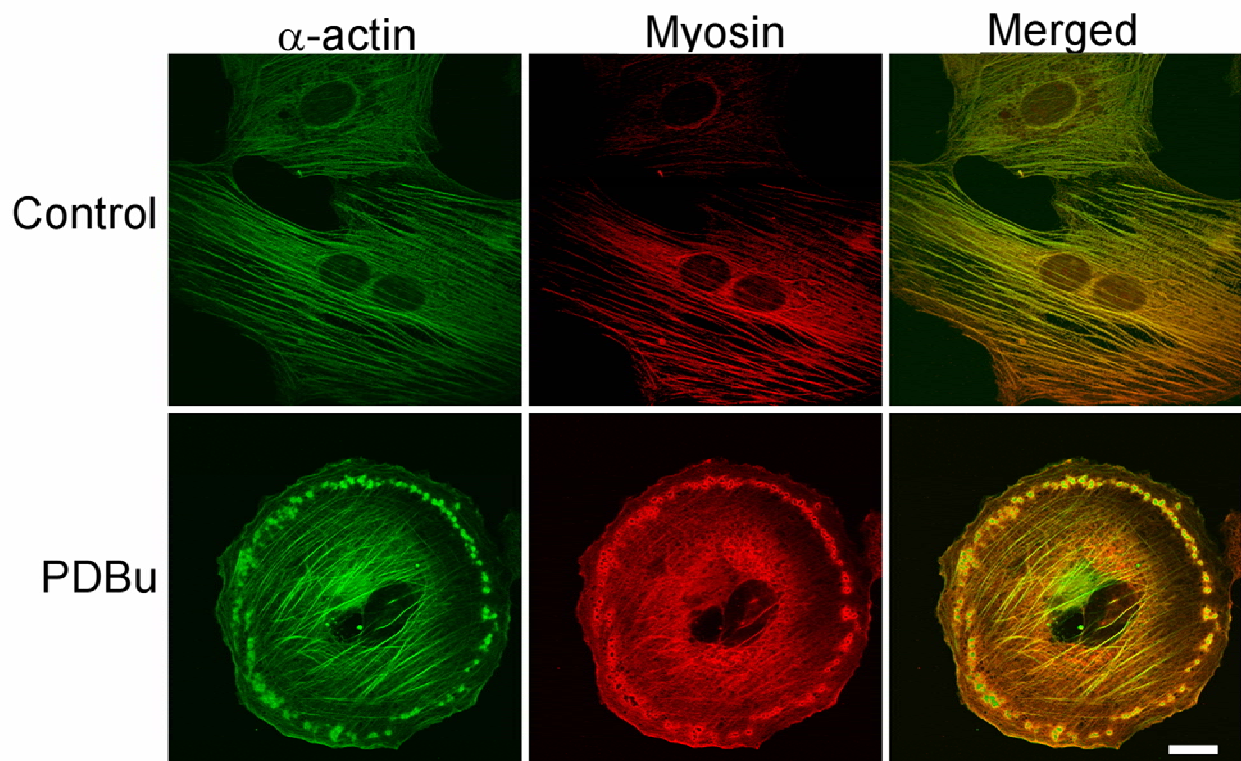


Figure 2  
Black et al.

**Figure 2.** Dual immunostaining of  $\alpha$ -actin and myosin in unstimulated (Control) and PDBu-activated A7r5 cells. At 20 minutes after PDBu ( $10^{-7}$  M) addition, cells were fixed with acetone and prepared for confocal imaging.  $\alpha$ -Actin was visualized with a monoclonal anti- $\alpha$ -smooth muscle actin, clone 1A4 antibody. Myosin was visualized with a monoclonal, clone C5C.52 pan-anti-myosin antibody. Yellow color indicates colocalization of the two proteins. The white bar indicates 20  $\mu$ m.

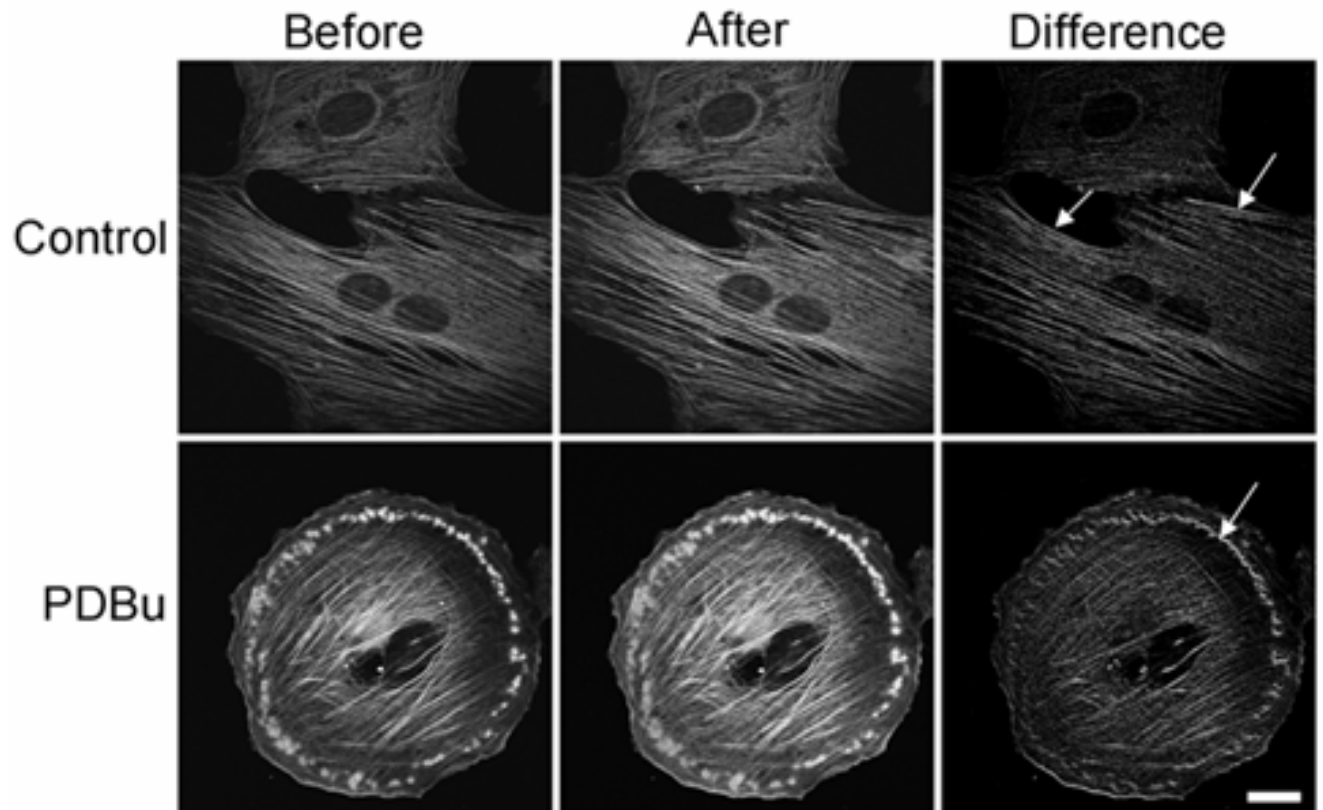


Figure 3  
Black et al.

**Figure 3.** FRET analysis of  $\alpha$ -actin/myosin complex in control and PDBu-activated A7r5 cells shown in Figure 2.  $\alpha$ -Actin was labeled with Alexa Fluor 488 and served as the donor component. Myosin was labeled with Alexa Fluor 546 and served as the acceptor component. Images show  $\alpha$ -actin fluorescence before and after photobleaching of the acceptor fluorophore. The difference in fluorescence between the before and after images was determined using Paint Shop Pro software. Arrows point to stress fibers in control cells showing clear intermittent  $\alpha$ -actin/myosin association and to indicate the localization of  $\alpha$ -actin/myosin complex on the cytosolic side of podosomes.



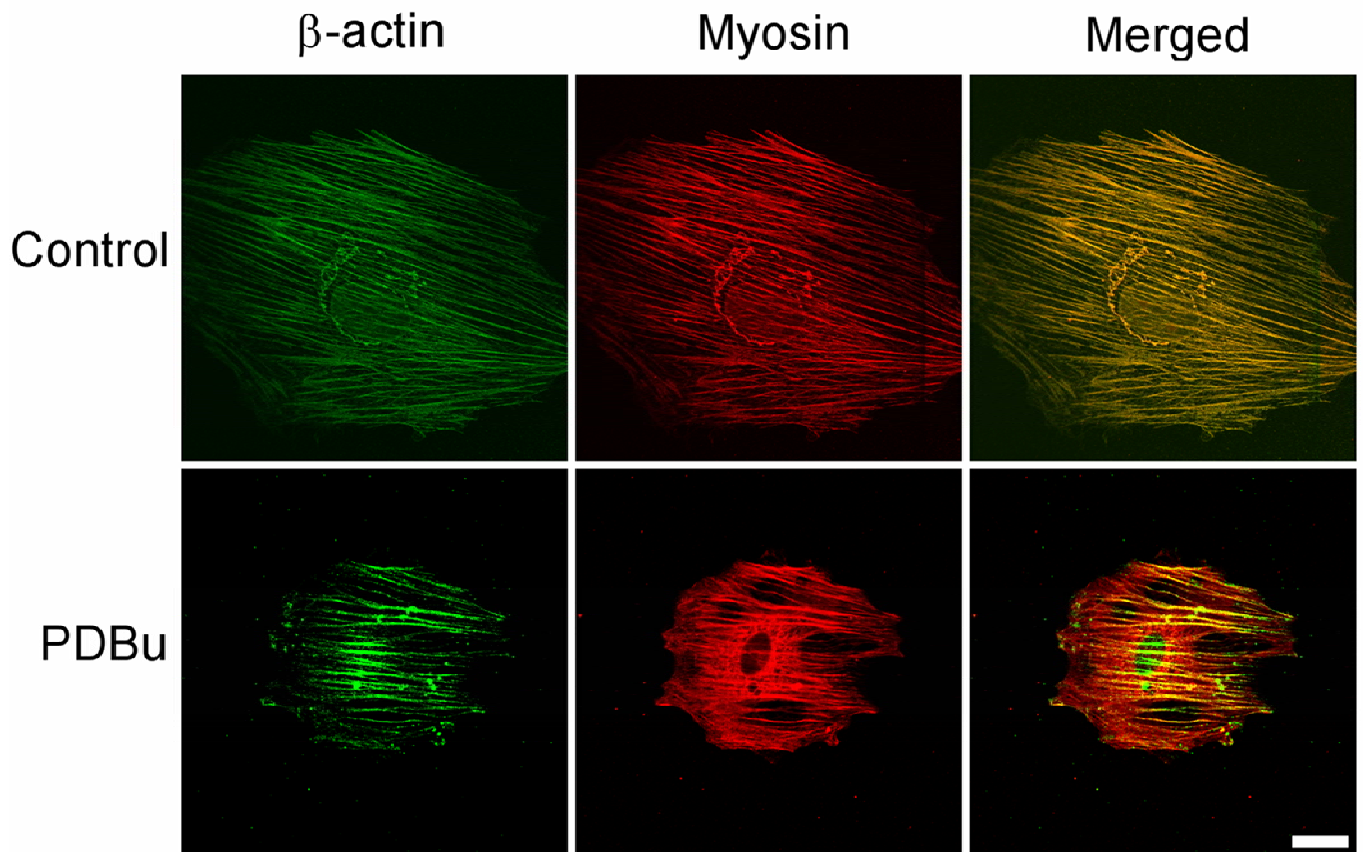


Figure 4  
Black et al.

**Figure 4.** Dual immunostaining of  $\beta$ -actin and myosin in control and PDBu-activated A7r5 cells. Twenty minutes after the addition of PDBu, cells were fixed with acetone and prepared for confocal microscopy.  $\beta$ -Actin was visualized with a monoclonal anti- $\beta$ -actin, clone AC-15 antibody. Myosin was visualized with a monoclonal, clone C5C.52 pan-anti-myosin antibody. Yellow color indicates colocalization of the two proteins. The bar in the lower right panel indicates 20  $\mu$ m.

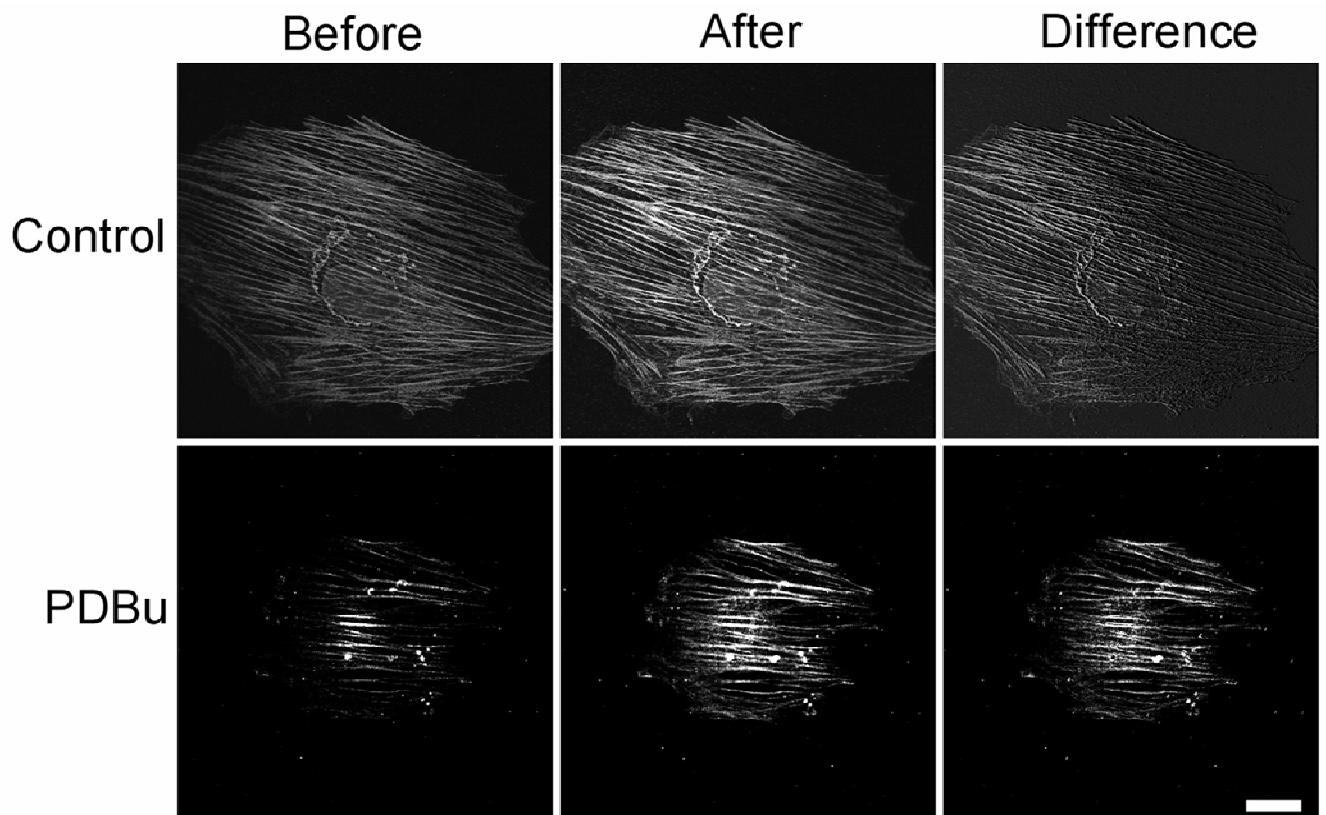
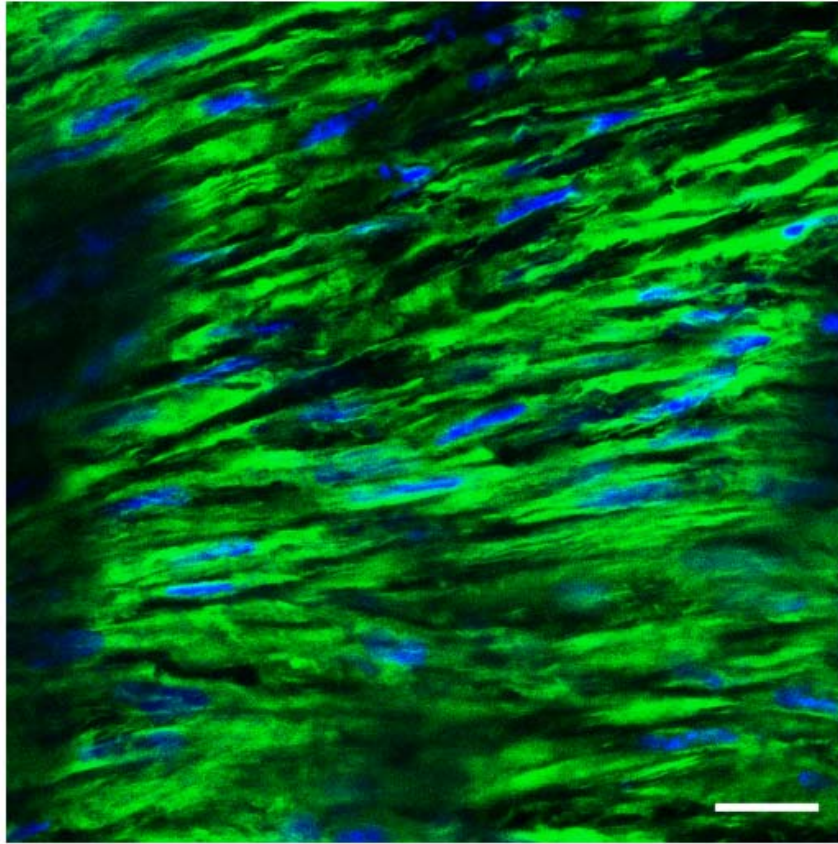


Figure 5  
Black et al.

**Figure 5.** FRET analysis of  $\beta$ -actin/myosin complex in control and PDBu-activated A7r5 cells shown in Figure 4.  $\beta$ -Actin was labeled with Alexa Fluor 488 and served as the donor component. Myosin was labeled with Alexa Fluor 546 and served as the acceptor component of the system. Images show  $\beta$ -actin fluorescence before and after photobleaching of the acceptor fluorophore. The difference in fluorescence was then determined using Paint Shop Pro software.



## Figure 6

### Black et al.

**Figure 6.** Rat aortic smooth muscle dual stained with phalloidin (F-actin) and TO-PRO-3 iodide (nuclei) to demonstrate the parallel and densely packed arrangement of cells in tissue. Note the variance of cells within the plane of section and the lack of intracellular structural detail typically seen in these sections. The bar at the lower right of the panel indicates 10  $\mu\text{m}$ .

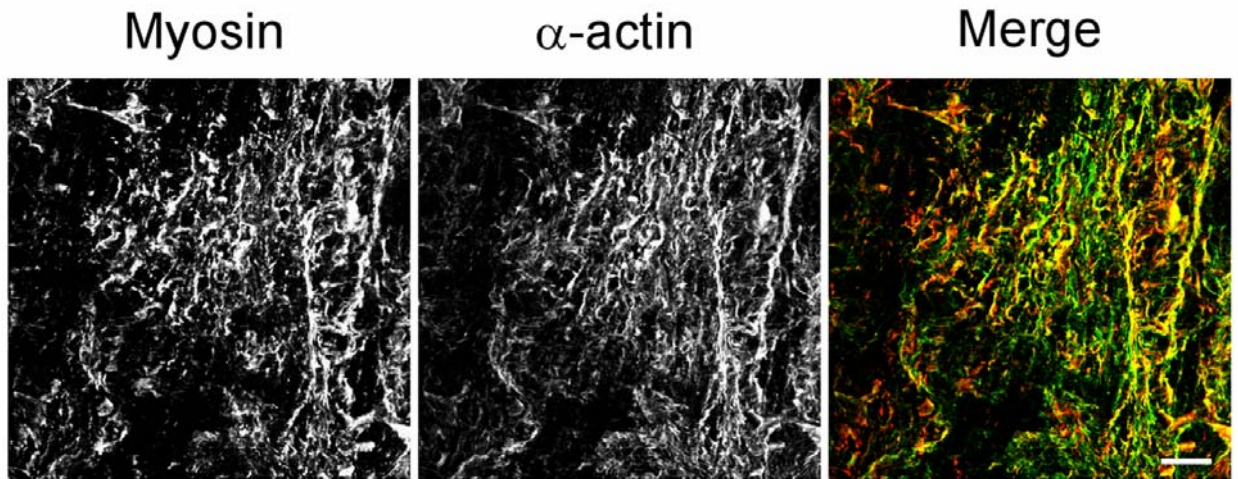


Figure 7  
Black et al.

**Figure 7.** Dual staining of a control tissue section for  $\alpha$ -actin and myosin. Sections were immunostained for  $\alpha$ -actin using a monoclonal anti- $\alpha$ -smooth muscle actin, clone 1A4 antibody while myosin was visualized using a monoclonal, clone C5C.52 pan-anti-myosin antibody. Yellow color indicates  $\alpha$ -actin and myosin colocalization. The white bar in the lower right hand panel indicates 10  $\mu$ m. The image emphasizes the confusion of structure obtained with colocalization staining of tissue sections.

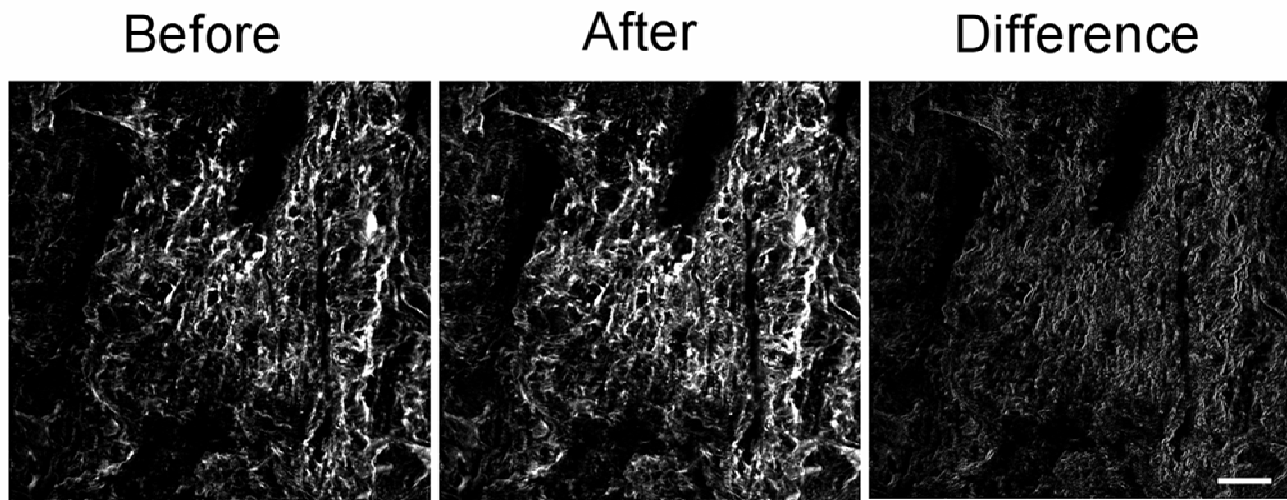


Figure 8  
Black et al.

**Figure 8.** FRET analysis of  $\alpha$ -actin/myosin in aortic tissue sections shown in Figure 7.  $\alpha$ -Actin was labeled with Alexa Fluor 488 and served as the donor component. Myosin was labeled with Alexa Fluor 546 and served as the acceptor component. Images show  $\alpha$ -actin fluorescence before and after photobleaching of the acceptor fluorophore. The difference between the before and after images was then determined using Paint Shop Pro software. This panel demonstrates the simplification of the image engendered by visualization of only  $\alpha$ -actin/myosin complex.

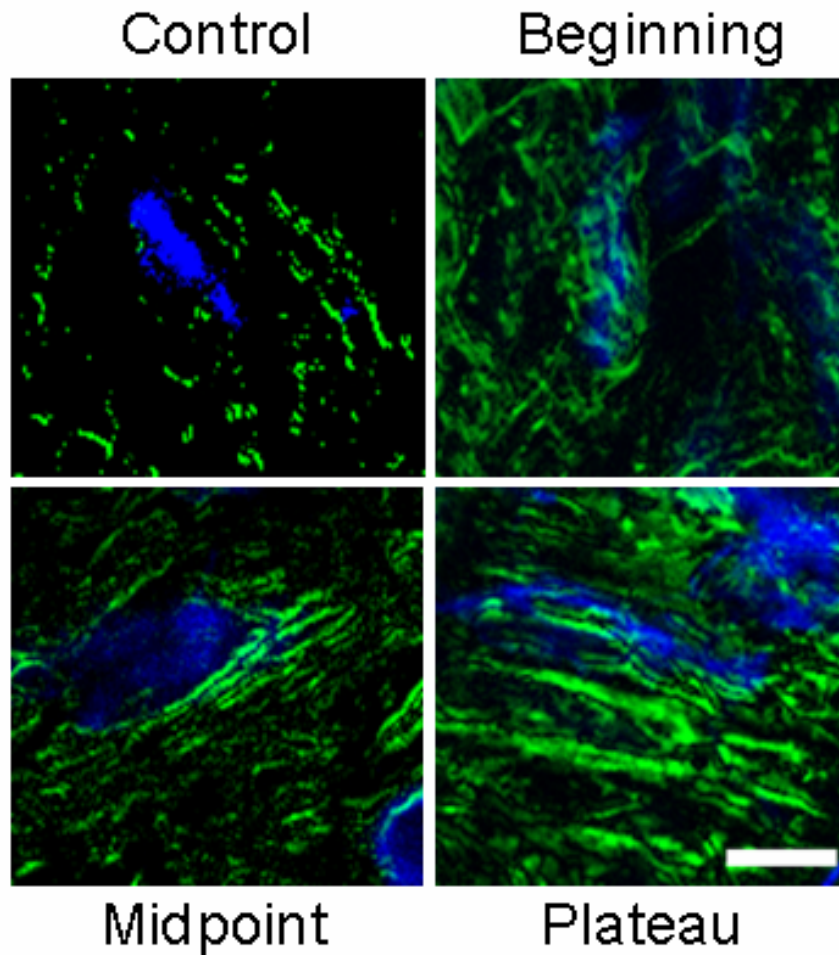


Figure 9  
Black et al.

**Figure 9.** FRET images showing  $\alpha$ -actin/myosin structure in relation to cell nuclei at the various intervals during contraction. Tissue sections were immunostained for FRET analysis as indicated above and were additionally stained with TO-PRO-3 iodide to visualize cell nuclei (blue). Differences between before and after images were obtained with Paint Shop Pro and merged with nuclear stain images. The images are typical of sections showing limited structure in controls with the development of thick  $\alpha$ -actin/myosin cables and patches at each stage of contraction examined.

## Tables

**Table 1.** Fluorescence resonance energy transfer (FRET) analysis of the association of myosin with  $\alpha$ - and  $\beta$ -actin in Control and PDBu-stimulated A7r5 cells. A) The index of association between actin isoforms and myosin for control cells and those at an advanced stage of contraction (20 min.). B) The association index of  $\alpha$ -actin and myosin at selected time intervals after PDBu addition with data presented as percentage of the control value. Myosin was visualized using a monoclonal, clone C5C.52 pan-anti-myosin antibody.  $\alpha$ -Actin and  $\beta$ -actin were visualized with monoclonal anti- $\alpha$  smooth muscle actin clone 1A4 and anti- $\beta$ -actin clone AC-15 antibodies, respectively. Values represent the average of a minimum of 10 cells.

### A. FRET Association Index

<u>Treatment</u>	<u><math>\alpha</math>-actin</u>	<u><math>\beta</math>-actin</u>
Control	73.3 $\pm$ 6.0	74.5 $\pm$ 5.2
PDBu (20 min.)	24.4 $\pm$ 2.8*	73.0 $\pm$ 4.5

### B. Time course

<u>Time, min.</u>	<u><math>\alpha</math>-Actin/Myosin Association Index<sup>+</sup></u>
0	100.0 $\pm$ 8.2
1.5	139.8 $\pm$ 8.2*
5	133.4 $\pm$ 9.3*
10	112.1 $\pm$ 8.0
20	33.2 $\pm$ 3.8*

<sup>+</sup>Data presented as % of Control. An asterisk (\*) indicates significant difference from the control value, P < 0.05 or greater.

**Table 2.** FRET analysis of the association of myosin with  $\alpha$ - and  $\beta$ -actin in rat aortic smooth muscle. Aortic rings were mounted in glass organ baths and contracted by the addition of  $10^{-7}$  M PDBu. Tissue were removed for analysis before PDBu addition (Control), at the first indication of force development (Start), approximately midway through the contraction, and well after the establishment of the plateau in force development. Values represent the average of 10 determinations from different tissues and are presented as percent of control.

<u>Sample Time</u>	<u><math>\alpha</math>-actin</u>	<u><math>\beta</math>-actin</u>
Control	100.0 $\pm$ 15.0	100.0 $\pm$ 8.7
Start	179.2 $\pm$ 18.8*	139.0 $\pm$ 13.1
Midway	96.2 $\pm$ 15.0	70.1 $\pm$ 6.1*
Plateau	167.9 $\pm$ 11.3*	94.7 $\pm$ 10.5

An asterisk (\*) indicates a significant difference from the control value,  $P < 0.05$  or better.



**Table 3.** F-actin content of tissue sections obtained from aortic segments before contraction with  $10^{-7}$  M PDBu (Control), at the beginning of force development, approximately midway through the contraction, and after the plateau in force development. Tissue sections were stained with phalloidin and fluorescence obtained at constant confocal settings for all tissue groups. Values represent the average of 8 to 10 sections from individual vessels and are presented in ratio to the control value.

<b><u>Treatment</u></b>	<b><u>Fluorescence/Unit Area</u></b>
Control	$1.00 \pm 0.07$
Start	$1.21 \pm 0.11$
Midway	$0.83 \pm 0.08$
Plateau	$1.62 \pm 0.18^*$

An asterisk indicates significant difference from the Control value,  $P < 0.05$  or better.

## Discussion

Phorbol esters, as analogues of diacylglycerol, act through PKC to induce a robust, slowly developed contraction in vascular smooth muscle. In A7r5 smooth muscle cells, phorbol 12, 13 dibutyrate (PDBu) has been demonstrated to induce contraction in the absence of an increase in  $[Ca^{2+}]_i$  and is thought to act by both calcium-dependent and independent mechanisms (21). At advanced stages of the PDBu contraction there is a loss in  $\alpha$ -actin stress fibers (10) as  $\alpha$ -actin remodels to podosomes at the cell periphery (10, 12). In contrast,  $\beta$ -actin remained in stress fibers during the interval of  $\alpha$ -actin reorganization. Most surprising, confocal images suggest decreased actin/myosin association in contracting A7r5 cells during podosome formation (9).

Whole cell FRET analysis has been successfully used to evaluate microtubule-PKC- $\alpha$  complexes in PDBu-contracted A7r5 cells (7). Because the donor/acceptor proteins must be within 100 angstroms distance from each other for efficient energy transfer (5, 16) this technique provides a measure of protein-protein distances compatible with molecular interaction. The present results using FRET analysis indicate dynamic changes in the  $\alpha$ -actin/myosin contractile protein throughout the course of PDBu-induced A7r5 cell contraction (Table 1). Associated  $\alpha$ -actin/myosin increased significantly at the initiation of contraction but declined to an estimated 70% loss in the contractile protein during the interval of visible loss in  $\alpha$ -actin stress fibers and podosome formation. Furthermore, FRET images provided clear resolution of  $\alpha$ -actin/myosin structure, showing the intermittent arrangement of the complex in stress fibers and that  $\alpha$ -actin/myosin

association was primarily localized on the cytosolic side of podosomes (Fig. 3). By comparison, FRET analysis indicated  $\beta$ -actin/myosin association remained stable during the interval of  $\alpha$ -actin/myosin disassociation and showed well defined perinuclear structure not observed in  $\alpha$ -actin/myosin images. The results confirm earlier conclusions regarding the isoform-specific remodeling of the cytoskeleton in PDBu-contracted A7r5 cells and indicate the potential use of FRET analysis in whole cell evaluation of protein-protein associations.

In recent work, Kuo et al. (2003) have correlated myosin filament density with isometric force, shortening velocity, power output, and the ATPase rate in tracheal smooth muscle adapted to different lengths prior to contraction with acetylcholine. Based on findings of increased myosin filament density and changes in contractile function at increased tissue preload, they proposed cytoskeletal remodeling to increase actin/myosin units in series at increased tissue length. Consistent with this model, a number of reports have indicated increased tissue F-actin content in contracted smooth muscle (15, 19, 1, 27, 28, 29). The present results support previous conclusions of increased F-actin and actin/myosin association in vascular smooth muscle contracted by PDBu. However, our findings further suggest that the contractile cytoskeleton undergoes variable remodeling during the course of contraction. We report evidence for both increased F-actin and  $\alpha$ -actin/myosin association at the initiation and the plateau in force development but not in the intermediate interval of force development. One explanation is that slow force development represents a period of significant reorganization of the contractile apparatus with activity similar to the previously proposed “asynchronous” remodeling (2, 18) in

which a portion of the cytoskeleton remodels to sustain force development while the remainder serves to preserve tension gains. Similar to findings in A7r5 cells (10, 18) tissue smooth muscle showed a dichotomy in  $\alpha$ -versus  $\beta$ -actin association with myosin during the interval of contraction (Table 2). The  $\beta$ -actin/myosin complex appeared less labile than that of  $\alpha$ -actin but was observed to decrease significantly midway through the contraction further suggesting significant remodeling during shortening and re-alignment of the contractile apparatus.

Probably due to a number of technical difficulties including the relatively low magnification power available with confocal microscopy, FRET images of control tissue sections revealed little detail of cellular actin/myosin structure. However, the formation of thickened patches and cable-like  $\alpha$ -actin/myosin structures were observed in contracted tissue (Fig. 9). These structures argue against homogeneous distribution of contractile protein in the contracting cell, a finding consistent with earlier observations of myosin segregation to the periphery of cross-sectional profiles in stretched guinea pig taenia coli smooth muscle (4). On the other hand, heterogenous distribution might be reasonably expected in cells undergoing cytoskeletal remodeling in response to changes in cytoskeletal strain resulting from internal tension development as well as that imposed by adjacent cell activity.

In summary, the results show that in unloaded A7r5 cells, PDBu-induced contraction resulted in isoform-specific remodeling of the actin cytoskeleton with increased  $\alpha$ -actin/myosin structure at the start of contraction followed by loss of  $\alpha$ -actin stress fibers

and myosin disassociation with advanced contraction. In preload aortic segments, PDBu-induced contraction resulted in isoform-specific changes in association with myosin. Hence, the remodeling characteristics of both cells and tissues suggest that the regulation and potentially the contractile function of these isoforms may differ. Both the tissue F-actin content and  $\alpha$ -actin/myosin complex increased at the initiation of force development and during the plateau phase of tension maintenance but was at the control level during the interval of slowly developing force midway through contraction. The work of Chrzanowska-Wadnicka and Burridge (1996) has provided compelling evidence that cytoskeletal strain is obligatory for stress fiber formation. Based on their findings, the results of the present study may reflect predominantly actin/myosin polymerization in response to strain on established contractile protein during the initiation and plateau in force development. However, midway through the contraction, the internal shortening of the contractile apparatus and development of external strain due to adjacent cell activity would be expected to alter vectors of force imposed on the cytoskeleton. Hence, it may be reasonable to speculate that during this interval, concurrent contractile protein polymerization/depolymerization serves to constantly address changes of internal strain with realignment of the contractile cytoskeleton for optimal force development.

### References

1. Barany M, Barron JT, Gu L and Barany K (2001) Exchange of the actin bound nucleotide in intact arterial smooth muscle. *J Biol Chem* **276(51)**: 48398-48403.

2. Battistella-Patterson AS, Wang S and Wright GL (1997) Effect of disruption of the cytoskeleton on smooth muscle contraction. *Can J Physiol Pharmacol* **75**: 1287-1299.
3. Chrzanowska-Wodnika M and Burridge K (1996) Rho-stimulated contractility drives the formation of stress fibers and focal adhesions. *J Cell Biol* **133(6)**: 1403-1415.
4. Cooke PH and Fay FS (1972) Correlation between fiber length, ultrastructure, and the length-tension relationship of mammalian smooth muscle. *J Cell Biol* **52**: 105-116.
5. Dos Remedios CG, Miki M and Barden JA (1987) Fluorescence resonance energy transfer measurements of distances in actin and myosin. A critical evaluation. *J Muscle Res Cell Motil* **8**: 97-117.
6. Driska SP, Aksoy MO and Murphy RA (1981) Myosin light chain phosphorylation associated with contraction in arterial smooth muscle. *Am J Physiol* **240**: C222-C223.
7. Dykes AC, Fultz ME, Norton ML and Wright GL (2003) Microtubule-dependent PKC- $\alpha$  localization in A7r5 smooth muscle cells. *Am J Cell Physiol* **285**: C76-C87.
8. Ford LE, Seow CY and Pratusевич VR (1994) Plasticity in smooth muscle. *Can J Physiol Pharmacol* **72**: 1320-1324.
9. Fultz ME and Wright GL (2003) Myosin remodeling in the contracting A7r5 cell. *Acta Physiol Scand* **177**: 197-205.
10. Fultz ME, Li C, Geng W and Wright GL (2000) Remodeling of the actin cytoskeleton in the contracting A7r5 smooth muscle cell. *J Mus Res Cell Motil* **21(8)**: 775-787.

11. Gunst SJ, Wu MF and Smith DD (1993) Contraction history modulates isotonic shortening velocity in smooth muscle. *Am J Physiol* **265(34)**: C467-C476.
12. Hai CM, Hahne P, Harrington EO and Gimona M (2002) Conventional PKC mediates phorbol dibutyrate-induced cytoskeletal remodeling in A7r5 smooth muscle cells. *Exp Cell Res* **280**: 64-74.
13. Harris DE and Warshaw DM (1990) Slowing of velocity during isotonic shortening in isolated smooth muscle cells. *J Gen Physiol* **96**: 581-601.
14. Harris DE and Warshaw DM (1991) Length vs. active force relationship in single isolated smooth muscle cells. *Am J Physiol* **260(29)**: C1104-C1112.
15. Hirshman CA, Togashi H, Shao D and Emala CW. (1998)  $G\alpha_{i-2}$  is required for carbachol-induced stress fiber formation in human airway smooth muscle cells. *Am J Physiol* **275(Lung Cell Mol Physiol 19)**: L911-L916.
16. Kenworthy AK (2001) Imaging protein-protein interactions using fluorescence resonance energy transfer microscopy. *Methods* **24**: 289-296.
17. Kuo K-H, Herrera AM, Wang L, Paré PD, Ford LE, Stephen NL and Seow CY. (2003) Structure function correlation in airway smooth muscle adapted to different lengths. *Am J Physiol Cell Physiol* **285**: C384-C390.
18. Li C, Fultz ME, Parkash J, Rhoten WB and Wright GL (2001)  $Ca^{2+}$ -dependent actin remodeling in the contracting A7r5 cell. *J Mus Res Cell Motil* **22**: 521-534.
19. Mehta D and Gunst SJ (1999) Actin polymerization stimulated by contractile activation regulates force development in canine tracheal smooth muscle. *J Physiol (Lond)* **519(3)**: 829-840.

20. Merkel L, Gerthoffer WT and Torphy TJ (1990) Disassociation between myosin phosphorylation and shortening velocity in canine trachea. *Am J Physiol* **258**: C524-C532.
21. Nakajima S, Fujimoto M and Veda M (1993) Spatial changes of  $[Ca^{2+}]_i$  and contraction caused by phorbol esters in vascular smooth muscles. *Am J Physiol* **265(4)**: C1138-C1145.
22. Paul RJ (1983) Functional compartmentalization of oxidative and glycolytic metabolism in vascular smooth muscle. *Am J Physiol* **244**: C399-C409.
23. Pratusевич VR, Seow CY and Ford LE (1995) Plasticity in canine airway smooth muscle. *J Gen Physiol* **105**: 73-94.
24. Seow CY, Pratusевич VR and Ford LE (2000) Series-to parallel transition in the filament lattice of airway smooth muscle. *J Appl Physiol* **89**: 869-876.
25. Shen X, Wu MF, Tepper RS and Gunst SJ (1997) Mechanisms for mechanical response of airway smooth muscle to length oscillation. *J Appl Physiol* **83(3)**: 731-738.
26. Tang DD and Gunst SJ (2004) The small GTPase Cdc42 regulates actin polymerization and tension development during contractile stimulation of smooth muscle. *J Biol Chem* **279(50)**: 51722-51728.
27. Tang DD and Tan J (2003) Downregulation of profilin with antisense oligodeoxynucleotides inhibits force development during stimulation of smooth muscle. *Am J Physiol Heart Circ Physiol* **285**: H1528-H1536.



28. Tang DD, Turner CE and Gunst SJ (2003) Expression of non-phosphorylatable paxillin mutants in canine tracheal smooth muscle inhibits tension development. *J Physiol* **553(1)**: 21-35.
29. Tang DD, Zhang W and Gunst SJ (2005) The adapter protein CrkII regulates neuronal Wiskott-Aldrich syndrome protein, actin polymerization, and tension development during contractile stimulation of smooth muscle. *J Biol Chem* **280(4)**: 23380-23389.
30. Wright GL and Hurn E (1994) Cytochalasin inhibition of slow tension increase in rat aortic rings. *Am J Physiol* **267(36)**: H1437-H1447.
31. Xu J-Q, Gillis J-M and Craig R (1997) Polymerization of myosin on activation of rat anococcygeus smooth muscle. *J Mus Res Cell Motil* **18**: 381-393.
32. Zhang Y and Moreland RS (1994) Regulation of Ca<sup>2+</sup>-dependent ATPase activity in detergent-skinned vascular smooth muscle. *Am J Physiol* **267**: H1032-H1039.

## Chapter III

# Myosin isoform interaction with actin isoforms in A7r5 cells and rat aorta smooth muscle

J. Black<sup>1</sup>, S. Thatcher<sup>1</sup>, E.C. Bryda<sup>2</sup>, and G.L. Wright<sup>1</sup>

<sup>1</sup>The Joan C. Edwards School of Medicine, Department of Pharmacology, Physiology and Toxicology, Marshall University, Huntington, WV 25704, USA

<sup>2</sup>Department of Veterinary Pathobiology, University of Missouri, Columbia, MO 65211, USA

**Correspondence to:**

Gary L. Wright  
Professor of Pharmacology, Physiology and Toxicology  
The Joan Edwards School of Medicine  
Marshall University  
Huntington, WV 25704 USA  
Phone: 304 696 7368  
Fax: 304 696 7381  
E-mail: [wrightg@marshall.edu](mailto:wrightg@marshall.edu)

**Running title:** Myosin/actin isoform association

**Key words:** myosin isoforms, actin isoforms, cytoskeletal remodeling

## Abstract

Actin and smooth muscle myosin have several different isoforms. How these different isoforms interact and remodel during smooth muscle contraction is still unknown. We used fluorescence resonance energy transfer (FRET) and co-immunoprecipitation to examine the interactions of the myosin tail isoforms SM1 and SM2 with  $\alpha$ -actin and  $\beta$ -actin in an A7r5 embryonic rat aorta smooth muscle cell model and in intact adult rat aorta tissue. Confocal images of A7r5 cells showed little colocalization of SM2 or SM1 with either actin isoform in either control cells or cells contracted with phorbol-12, 13-dibutyrate. Although FRET transfer efficiencies were higher for SM1, no significant difference was seen between control and contracted cells. In tissue, higher colocalization was visible between the myosin isoforms and the actin isoforms. However, FRET showed slight changes in myosin association with  $\alpha$ -actin during contraction with a significant decrease seen with SM1 and  $\alpha$ -actin interaction at the midpoint of contraction. Both myosin isoforms showed significant decreases in their interaction with  $\beta$ -actin between control and most time points of contraction. Co-immunoprecipitation of tissue lysate showed the same trends as the results of FRET experiments. These results suggest that SM1 and SM2 interact differently with  $\alpha$ -actin and  $\beta$ -actin during contraction and that these two actin isoforms remodel in different ways during contraction with phorbol. Finally, FRET results were confirmed by co-immunoprecipitation suggesting that this technique can be used in tissue sections to accurately determine protein-protein interactions.

## Introduction

Smooth muscle contraction is an integral part of mammalian physiology. However, the mechanisms underlying force development in this muscle type are still not completely known. The lack of a skeletal muscle-like sarcomere has caused much debate over how the contractile apparatus forms and functions. One hypothesis put forth is that controlled cytoskeletal remodeling could maintain the contractile apparatus at optimal mechanical advantage and serve to maintain contraction with little energy expenditure (Paul 1983). Several papers have been published discussing the potential role of both actin remodeling (Fultz et al. 2000; Herrera et al. 2004; Brown et al. 2006) and myosin remodeling (Herrera et al. 2002; Fultz and Wright 2003) in smooth muscle contraction.

Two major actin isoforms have been reported to occur in the smooth muscle cell.  $\alpha$ -Actin has been used as a marker for smooth muscle and is thought to be a major component of the contractile apparatus, while  $\beta$ -actin is proposed to serve a role in cytoskeletal structure (North et al. 1994). Both isoforms have been found to remodel in distinctly different ways when the A7r5 embryonic smooth muscle cell is caused to contract by phorbol-12, 13-dibutyrate (PDBu) (Fultz et al. 2000; Brown et al. 2006).  $\beta$ -Actin has been found to remain in stress fibers at lower PDBu concentrations ( $<10^{-7}$  M) as  $\alpha$ -actin is seen to relocate to structures known as podosomes at these lower concentrations. At higher concentrations of PDBu,  $\beta$ -actin has been reported to also migrate to the podosomes (Brown et al. 2006).

Smooth muscle myosin is a very diverse molecule with several isoforms found within smooth muscle (White et al. 1998). The different carboxy isoforms were first reported by Rovner et al. (1986), based on the discovery of two myosin heavy chains on a denaturing polyacrylamide gel using protein extracts from several smooth muscle tissues. They first used the terms Sm1 and Sm2 to denote the heavier (204kDa) isoform and the lighter (200kDa) isoform, respectively. These isoforms are formed by alternative splicing of the same myosin gene (Babij and Periasamy 1989; Nagai et al. 1989) resulting in Sm1, with 43 unique amino acids at its carboxyl end and another, Sm2, with 9 unique amino acids at the carboxyl end. Rovner et al. (1986) noted a 1:1 ratio of Sm1 to Sm2 but could not determine if Sm1 and Sm2 formed homodimers or heterodimers. Subsequently (Kelley et al. 1992), it was determined that Sm1 and Sm2 form homodimers dominantly, but that under certain conditions thick filaments may contain both Sm1 and Sm2 myosin molecules (Rovner et al. 2002). The difference in function between the two myosin tail isoforms is not well understood.

In addition to the tail isoforms, the myosin heavy chain has other isoforms (White et al. 1998; Low et al. 1999) generated by alternative splicing in the head region leading to a seven amino acid insert near the actin-activated  $Mg^{2+}$ -ATPase (Babij et al. 1991; Babij 1993) and it is this isoform that is thought to convey faster myosin enzymatic activity (Kelley et al. 1993; DiSanto et al. 1997; Rovner et al. 1997; Austin et al. 2004). It is now generally believed that the head isoforms determine enzymatic differences; whereas the tail isoforms play a role in structural differences. Cells from rat arteries were found to have differing final cell length after contraction which correlated significantly with the

Sm2/Sm1 ratio with length decreasing as the amount of Sm2 increased (Meer and Eddinger 1997). Sm1 and Sm2 show differences in filament formation (Rovner et al. 2002) suggesting that, similar to actin, the myosin isoforms could remodel differently in contracting cells.

We examined the association of myosin tail isoforms with  $\alpha$ -actin and  $\beta$ -actin using fluorescence resonance energy transfer (FRET) and co-immunoprecipitation. The results show that myosin isoforms undergo changes in association with actin during the interval of contraction studied suggesting the force generating activity due to actin-myosin interaction declines in the later stages of contraction as the tissue approaches a plateau in tension.

## **Methods**

**Animals.** All procedures were performed in accordance with the Guide for the Care and Use of Laboratory Animals as approved by the Council of the American Physiological Society and the Animal Use Review Board of Marshall University. Male 12 week-old Sprague Dawley rats were housed on wood chip bedding in rooms maintained at  $23 \pm 2^\circ\text{C}$  with a 12h light cycle. Purina Rat Chow and tap water were freely available.

**Tissue preparation.** Rats were anesthetized with a ketamine-xylazine mixture (21:9 mg kg<sup>-1</sup>) and the thoracic aorta was surgically removed into buffer, cleaned of adherent tissue, and cut into 0.3 cm rings. Tissues were denuded of endothelium and then mounted under 5.0g of passive tension in glass organ baths containing Krebs buffer [(in mM) 118 NaCl, 4.7 KCl, 1.5 CaCl<sub>2</sub>, 25 NaHCO<sub>3</sub>, 1.1 MgCl<sub>2</sub>, 1.2 KH<sub>2</sub>PO<sub>4</sub>, and 5.6 glucose; pH 7.4] maintained at 37°C and aerated with 5% CO<sub>2</sub> in O<sub>2</sub>. The tissues were equilibrated for a minimum of 2h before contraction by addition of 10<sup>-7</sup>M phorbol-12, 13-dibutyrate (PDBu). Isometric tension was measured using a Grass FT03 force-displacement transducer and a Grass model 7D polygraph. Rings were removed from the bath at selected intervals of contraction and cut longitudinally, placed adventitia down on aluminum foil and snap frozen in liquid nitrogen. Samples were maintained at -70°C until sectioned.

**Cell culture.** A7r5 smooth muscle cells derived from embryonic rat aorta and shown to maintain the ability to contract to phorbol esters (Fultz et al. 2000), were obtained from American Type Culture Collection (Manassas, VA). Cells were plated on 75 cm<sup>2</sup> flasks and grown to approximately 80% confluence at 37°C in a humidified atmosphere of 5% CO<sub>2</sub> in air. The cells were maintained in Dulbecco's modified Eagles medium (DMEM) supplemented with 10% fetal calf serum, 100 units ml<sup>-1</sup> penicillin G, and 100 µg ml<sup>-1</sup> streptomycin. Media was changed every other day and cells were passaged at least once a week.

**Confocal microscopy.** Cells were seeded onto glass coverslips, placed in 6 well culture plates and returned to the incubator to allow for attachment and spreading. After treatment with PDBu ( $10^{-7}$  M) the cells were immediately fixed and permeabilized by addition of ice-cold acetone for 1.0 minute. The cells were then washed several times with phosphate-buffered saline (PBS) containing 0.5% TWEEN-20 (PBS-T), pH 7.5, followed by a 60 minute incubation in blocking solution containing 5% nonfat dry milk in PBS. Aortic rings from individual rats were selected for study at the onset of PDBu-induced force development (0.3g tension), approximately midway through the contraction (2.5g tension), and 15 minutes after the plateau in tension. Tissues were sectioned at 8  $\mu$ m longitudinally on an IEC cryotome and placed on poly-L-lysine coated slides. Sections were then fixed and permeablized by addition of ice-cold acetone for 1.0 minute. The slides were rinsed (3X) with PBS-T and preblocked with 5% nonfat dry milk in PBS. Antibodies against SM1 and SM2 were obtained from Seikagaku America of the Associates of Cape Cod, Inc. (East Falmouth, MA). Alexa-conjugated secondary antibodies were obtained from Molecular Probes, Inc. (Eugene, OR). Samples were blocked with 5% non-fat milk in PBS. Washings between steps were performed with 0.5% Tween-20 in PBS. Samples were incubated overnight in a solution of SM1 or SM2 antibodies in PBS. This was followed with incubation with secondary anti-mouse antibodies conjugated with Alexa-488.  $\alpha$ -Actin and  $\beta$ -actin were visualized using monoclonal anti- $\alpha$ -smooth muscle actin, clone 1A4 (IgG2a) and anti- $\beta$ -actin, clone AC-15 (IgG1) primary antibodies (Sigma, St. Louis, MO), respectively, followed by Alexa 546 anti-IgG secondary antibody (Molecular Probes). Cell and tissue samples were imaged with a Nikon Diaphot Microscope and confocal microscopy performed with a



BioRad Model 1024 scanning system with a krypton/argon laser. Cells were viewed at 600X magnification and tissue sections were viewed at 1000x. The numerical aperture of the objective was 1.4. The thickness of the section analyzed was 0.5  $\mu\text{m}$ . Controls to test for non-specific binding of primary antibodies and secondary antibodies were performed and no significant non-specific binding was visible.

**FRET analysis.** In the present study, we utilized the approach of measuring donor molecule quenching in the presence of acceptor fluorophore as an index of FRET (Kenworthy 2001). This approach to FRET evaluation is amenable to immunostaining and confocal imaging of fixed biological samples (Dykes et al. 2003). It must be noted, however, that the method as presently employed assumes that such factors as the absorption coefficient of the acceptor, the quantum yield of the donor, relative antibody binding affinity and the relative orientation of donor/acceptor antibody complexes, remain constant between treatment groups. Within a FRET system two fluorophores with overlapping emission and excitation spectra are utilized. Here myosin isoforms were labeled with Alexa 488 (excitation, 488 nm; emission, 520 nm) and served as the donor component of the system. Actin isoforms were labeled with Alexa 546 (excitation, 546 nm; emission, 580 nm) and served as the acceptor component. The donor molecule (SM1 or SM2, Alexa 488) was directly excited and the resulting emission was obtained with a 522DF32 band pass filter. However, a portion of the energy of emission was not released as light but was transferred to neighboring Alexa 546 fluorophore resulting in emission which was captured on a second channel with an HQ 598/40 band-pass filter. Subsequently, the image was excited at the 568 nm laser line at 100% power to

photobleach the acceptor molecule (actin) and a second image of the cell or tissue was acquired again at the 488 nm laser line excitation with the multichannel filter set to obtain myosin fluorescence (522DF32) and to verify the absence of actin label Alexa 546 emission (HQ 598/40). An intensity profile was generated for each sample (Image J Software, NIH) and the resulting plot was analyzed with Peakfit V4.11 software (SPSS Science, Richmond, CA) to obtain the area under the curve. The values were then used to calculate the percent increase in fluorescence emission after photobleaching.

Resonance energy transfer can only occur if the donor and acceptor molecules are close enough to each other for the transfer to occur efficiently. Hence, the resulting values were analyzed in comparisons of control and PDBu-treated A7r5 cells and aortic tissue samples as an index of the association between actin and myosin during PDBu-induced contraction.

**Protein collection.** Aorta smooth muscle samples were pooled from each of the specific time points from specific days of collection. Tissue samples were placed in lysis buffer (10mM MOPS, 1% NP-40, 5mM EDTA, 0.0mM EGTA, 1mM DTT, 50mM MgCl<sub>2</sub>, 300mM NaCl, 1mM PMSF, 50µg/mL leupeptin, chymostatin, and pepstatin A) and ground using a glass-on-glass Con-Torque Power Unit motorized homogenizer (Eberbach, Corp., Ann Harbor, MI) and then sonicated for 3-4 times for 10 seconds each time with an ultrasonic homogenizer (Cole-Power Instrument Co., Chicago, IL). Protein concentration was determined by bicinchoninic acid (BCA) protein assay (Pierce, Rockford, IL) or spectroscopically by measuring at the 280 nm wavelength.

**Co-immunoprecipitation.** Equal amounts of protein from pooled samples of tissue lysate at each of the time points of contraction were incubated with either  $\alpha$ -actin or  $\beta$ -actin antibodies overnight. The antibodies complexes were then cross-linked with Protein A/G beads (Pierce) for over two hours. Samples were washed extensively (6X) in PBS and protein was removed from beads by adding SDS-PAGE sample buffer (125mM Tris-HCl, 4% SDS, 20% glycerol, 10% 2-mercaptoethanol, 0.004% bromophenol blue) and heating at 100°C for 10 minutes. Samples were then stored at 4°C.

**Gel electrophoresis and Western Blot analysis.** Equal volumes of samples from the co-immunoprecipitation experiment were boiled for five minutes and centrifuged for five minutes to bring the protein beads to the bottom of the tube. Equal amounts of supernatant (20-50 $\mu$ L) were run on a 5% polyacrylamide gel for over 4 hours at 30 mAmps in order to separate the myosin heavy chain isoforms. Protein was then transferred to PVDF membrane (Amersham Pharmacia Biotech, Piscataway, NJ) for one hour with a Mini-Trans blot apparatus (BioRad, Hercules, CA). Membranes were blocked in 5% non-fat powdered milk in PBS. Membranes were incubated with an IgM anti-pan myosin antibody (Covance, Berkeley, CA). After washing with 0.1% Tween-20 in PBS (3X), membranes were incubated with an anti-IgM secondary antibody conjugated with horseradish peroxidase (Kirkegaard & Perry Laboratories, Gaithersburg, MD). Bands were visualized with ECL or ECL Plus (Amersham). Densitometry of bands was determined with ImageJ.

**Statistics.** Differences in the index of actin/myosin association were analyzed by ANOVA followed by Student's t-test (Sigma Stat 2.03, SPSS Science). Differences were considered significant if  $P < 0.05$  in all cases. Data are presented as means  $\pm$  SEM throughout the text.

## **Results**

**A7r5 Smooth Muscle Cells.** Confocal images of A7r5 cells were examined to determine the association of  $\alpha$ -actin with SM2 (Figure 1). Similar to previous findings (Fultz and Wright 2003) actin stress fibers were visible in the control cell with which myosin has been shown to colocalize. SM2 was highly visible in the vicinity of the nucleus in the control cell but generally absent from stress fibers. PDBu ( $10^{-7}$ M) treated cells showed fewer stress fibers with  $\alpha$ -actin translocated to the brightly fluorescing podosomes. There appeared to be little or no colocalization of SM2 with  $\alpha$ -actin in the contracted cell. It has been shown previously that  $\beta$ -actin remodels differently than  $\alpha$ -actin (Fultz et al. 2000; Brown et al. 2006), with  $\beta$ -actin remaining in stress fibers at physiological levels of contractile stimulation. Similar to these previous findings,  $\beta$ -actin was observed in stress fibers of both control and PDBu-treated cells. However, there was little or no evidence of significant SM2 colocalization with  $\beta$ -actin in either condition (Figure 2). Consistent with colocalization results FRET analysis indicated little association between SM2 and either of the actin isoforms (Table 1).

Control A7r5 cells that were dual stained for  $\alpha$ -actin (Figure 3) or  $\beta$ -actin (Figure 4) and SM1 show little evidence of colocalization. Contracted cells show the formation of

podosomes with obvious colocalization of  $\alpha$ -actin and SM1 at these structures. FRET analysis (Table 2) suggests a somewhat higher association of SM1 than SM2 with each actin isoform tested. Despite the apparent colocalization of SM1 with  $\alpha$ -actin in podosomes there was a tendency for a decrease in association in the contracted cell, although this decrease was not statistically significant.

**Aortic Vascular Smooth Muscle.** Rat aorta smooth muscle tissue was examined in order to determine the amount of association between  $\alpha$ -actin and  $\beta$ -actin and the tail isoforms of smooth muscle myosin, SM1 and SM2. Tissues dual stained for  $\alpha$ -actin and SM2 (Figure 5) shows the confusion of structure typically seen in these studies. However, colocalization of  $\alpha$ -actin and SM2 is visible in both control and contracted (Endpoint) tissue (Figure 5). In comparison to cultured cells, SM2 is much more visible which would be consistent with earlier reports that SM2 becomes more highly expressed in differentiated adult tissue (Kuro-o et al. 1989). Tissue dual stained for  $\beta$ -actin and SM2 (Figure 6) showed strong colocalization which appeared to be higher in control tissue than contracted tissue. FRET analysis (Table 3) indicated relatively strong association in controls with a trend for disassociation of SM2 from each of the actin isoforms during the course of contraction, although decreasing significantly only in SM2- $\beta$ -actin interaction.

Based on the review of ten or more sections per time point, the colocalization of SM1 with  $\alpha$ -actin (Figure 7) and  $\beta$ -actin (Figure 8) appeared to be stronger in control than in contracted tissue. FRET analysis suggests that the association of SM1 with  $\alpha$ -actin was

greater than for  $\beta$ -actin in controls. However, similar to SM2, the SM1 association with actin isoforms showed decline during contraction (Table 4). This was particularly dramatic in the SM1-  $\beta$ -actin interaction in which decreases of 88% to 95% were observed in the later phases of contraction. Our results could reflect cytoskeletal remodeling and rearrangement of the contractile apparatus as reported by others (Seow et al. 2000; Herrera et al. 2004; Herrera et al. 2005) but further suggest that active actin/myosin interaction declines as the contraction progresses.

Co-immunoprecipitation experiments verified the results of FRET studies indicating a tendency for actin and myosin isoforms change association during contraction (Table 5, Figure 9). Very similar to FRET results, co-immunoprecipitation indicated reductions in  $\beta$ -actin-myosin association to non-detectable levels during contraction (Figure 10).

## Figures

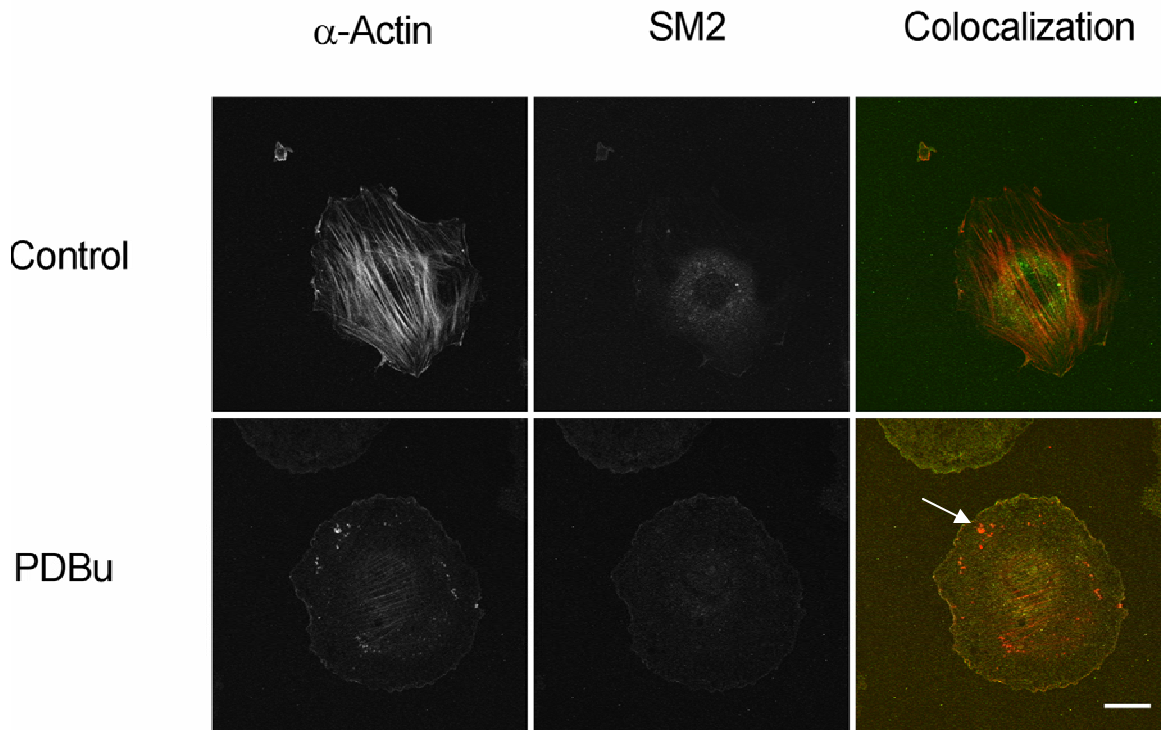


**Figure 1**  
Black et al.

**Figure 1.** Dual immunostaining of  $\alpha$ -actin and SM2 in unstimulated (Control) and PDBu-activated A7r5 cells. At 30 minutes after PDBu ( $10^{-7}$  M) addition, cells were fixed with acetone and prepared for confocal imaging.  $\alpha$ -Actin was visualized with a monoclonal anti- $\alpha$ -smooth muscle actin, clone 1A4 antibody. SM2 was visualized with a monoclonal anti-SM2 antibody, clone 3F8. Yellow color indicates colocalization of the two proteins. Arrow is pointing out a patch of podosomes. The white bar indicates 20  $\mu$ m.

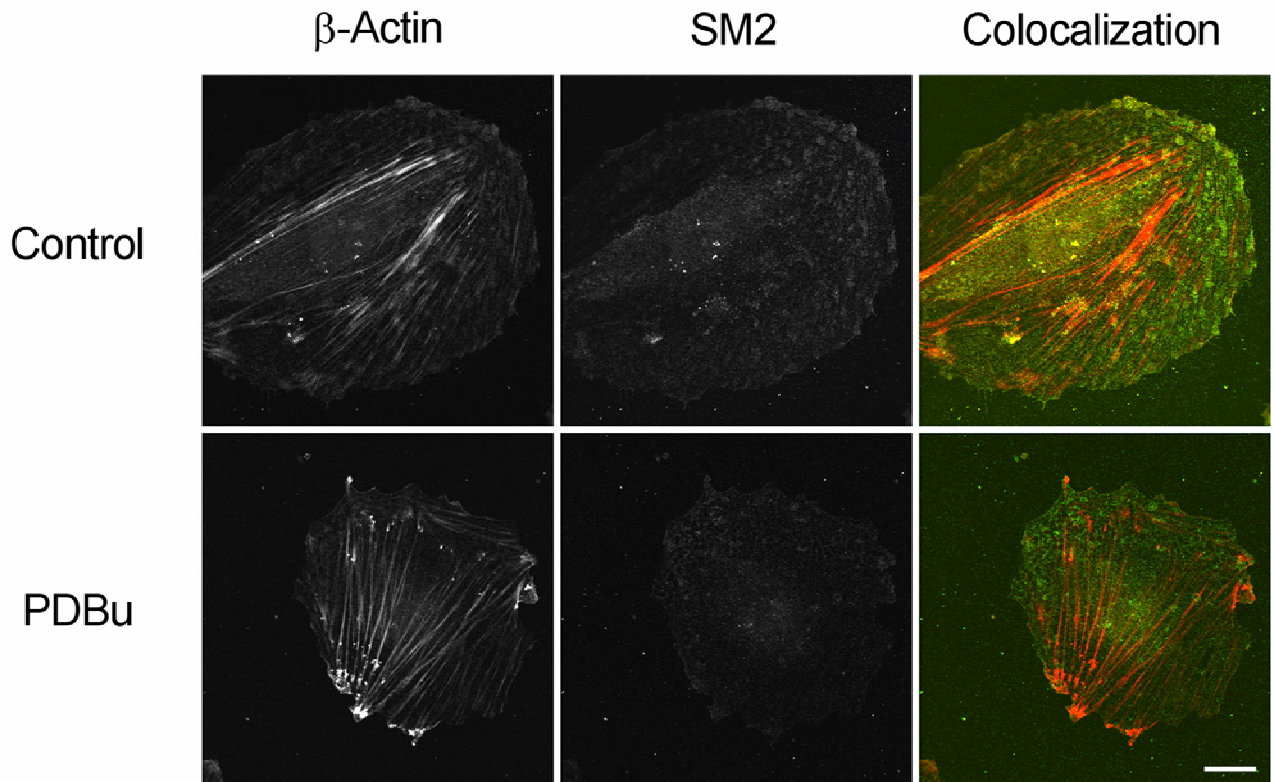


**Figure 2**  
Black et al.

**Figure 2.** Dual immunostaining of  $\beta$ -actin and SM2 in unstimulated (Control) and PDBu-activated A7r5 cells. At 30 minutes after PDBu ( $10^{-7}$  M) addition, cells were fixed with acetone and prepared for confocal imaging.  $\beta$ -Actin was visualized with a monoclonal anti- $\beta$ -smooth muscle actin, clone AC-15 antibody. SM2 was visualized with a monoclonal anti-SM2 antibody, clone 3F8. Yellow color indicates colocalization of the two proteins. The white bar indicates 20  $\mu$ m.



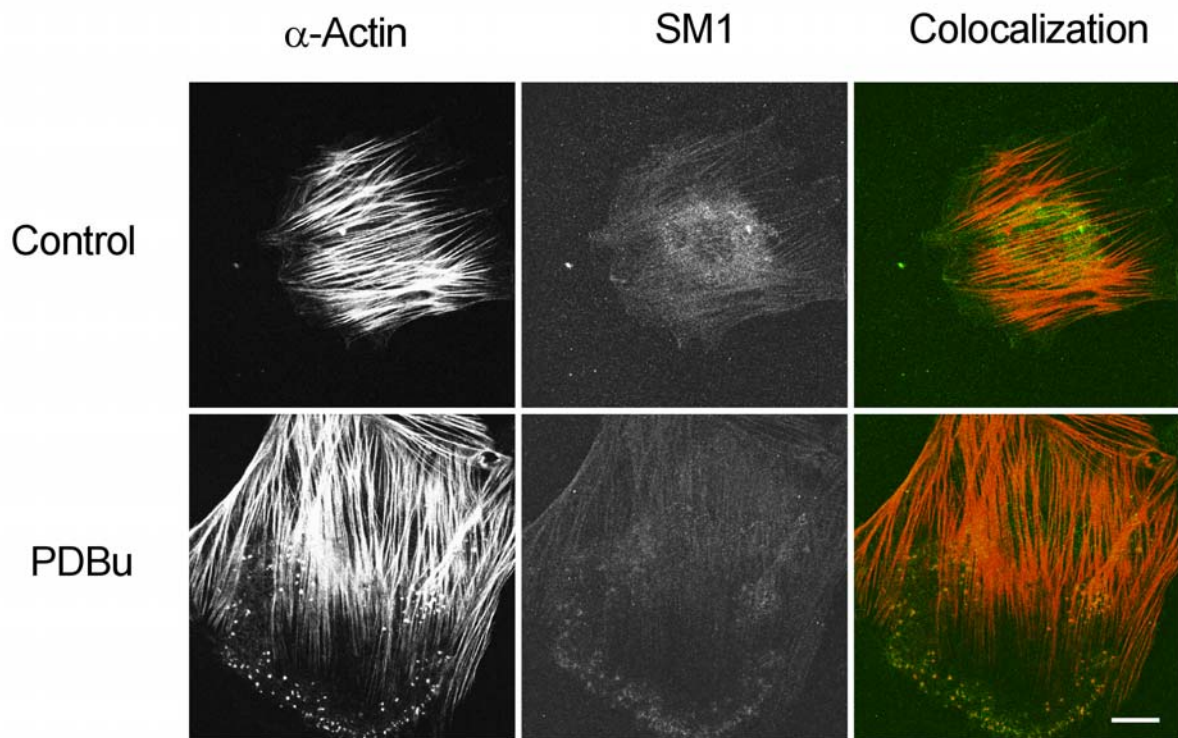


**Figure 3**  
Black et al.

**Figure 3.** Dual immunostaining of  $\alpha$ -actin and SM1 in unstimulated (Control) and PDBu-activated A7r5 cells. At 30 minutes after PDBu ( $10^{-7}$  M) addition, cells were fixed with acetone and prepared for confocal imaging.  $\alpha$ -Actin was visualized with a monoclonal anti- $\alpha$ -smooth muscle actin, clone 1A4 antibody. SM1 was visualized with a monoclonal anti-SM1 antibody, clone 1G12. Yellow color indicates colocalization of the two proteins. The white bar indicates 20  $\mu$ m.

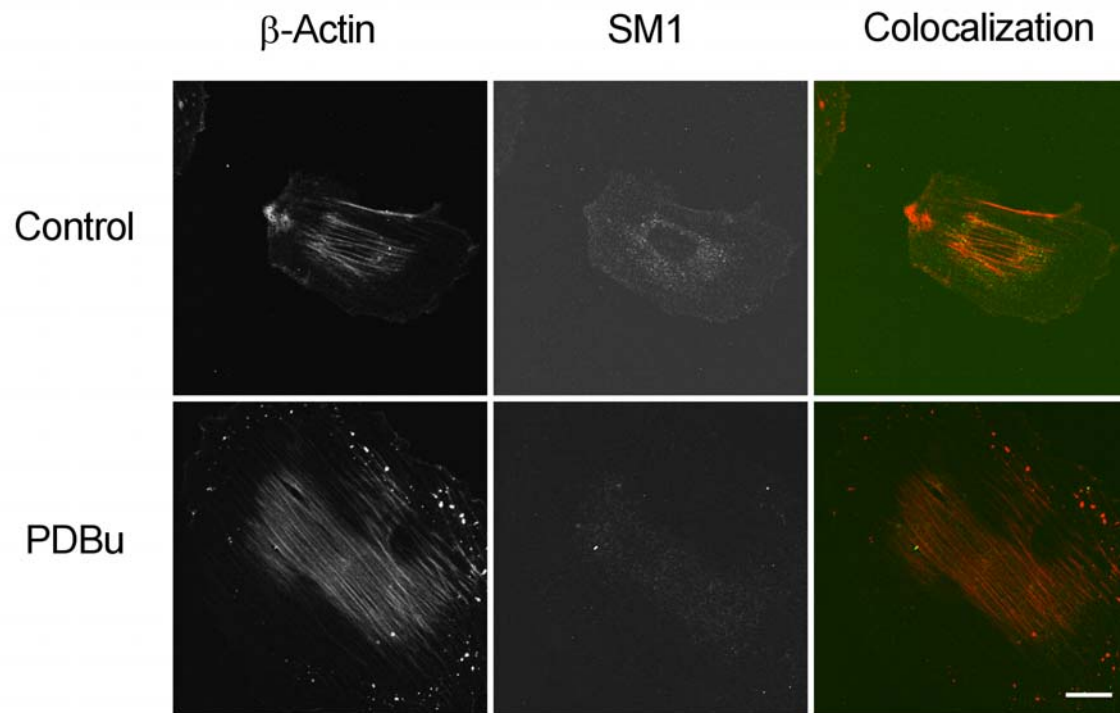


**Figure 4**  
Black et al.

**Figure 4.** Dual immunostaining of  $\beta$ -actin and SM1 in unstimulated (Control) and PDBu-activated A7r5 cells. At 30 minutes after PDBu ( $10^{-7}$  M) addition, cells were fixed with acetone and prepared for confocal imaging.  $\beta$ -Actin was visualized with a monoclonal anti- $\beta$ -smooth muscle actin, clone AC-15 antibody. SM1 was visualized with a monoclonal anti-SM1 antibody, clone 1G12. Yellow color indicates colocalization of the two proteins. The white bar indicates 20  $\mu$ m.

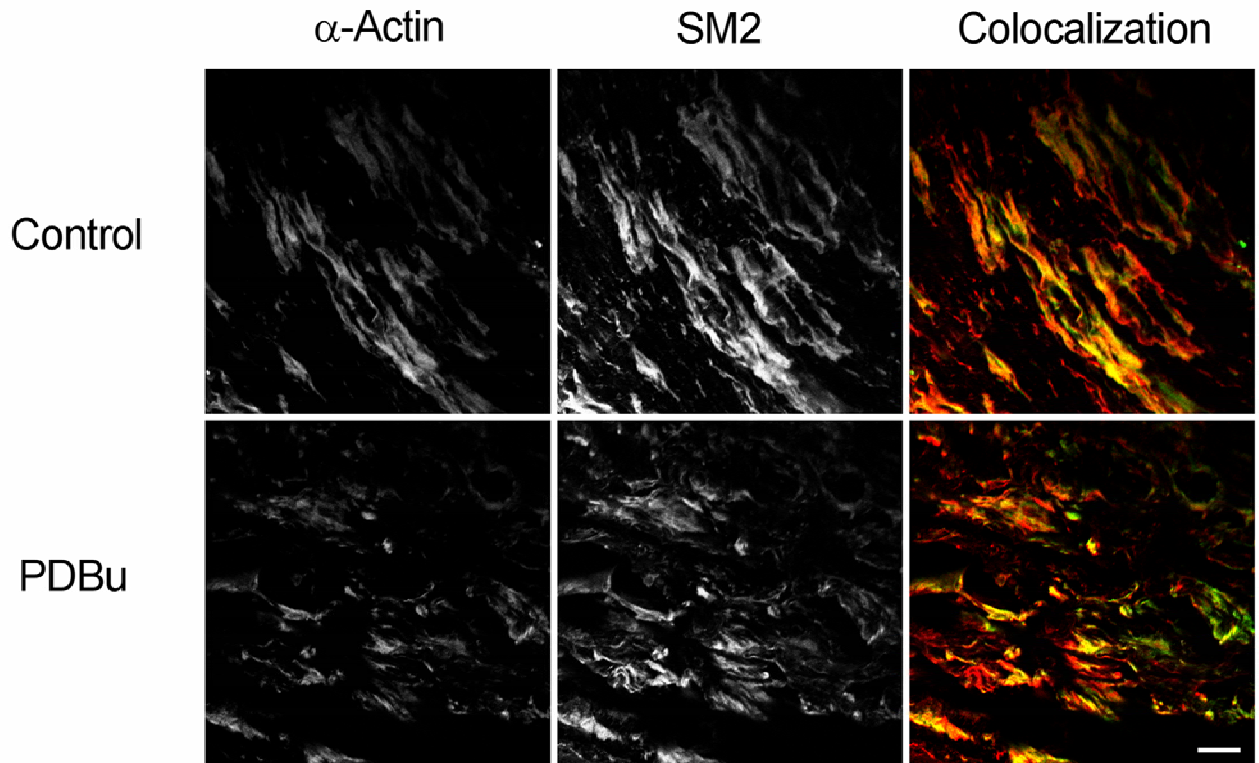


**Figure 5**  
Black et al.

**Figure 5.** Dual immunostaining of  $\alpha$ -actin and SM2 in unstimulated (Control) and PDBu-activated aorta tissue. Sections were fixed with ice cold acetone.  $\alpha$ -Actin was visualized with a monoclonal anti- $\alpha$ -smooth muscle actin, clone 1A4 antibody. SM2 was visualized with a monoclonal anti-SM2 antibody, clone 3F8. Yellow color indicates colocalization of the two proteins. The white bar indicates 10  $\mu$ m.

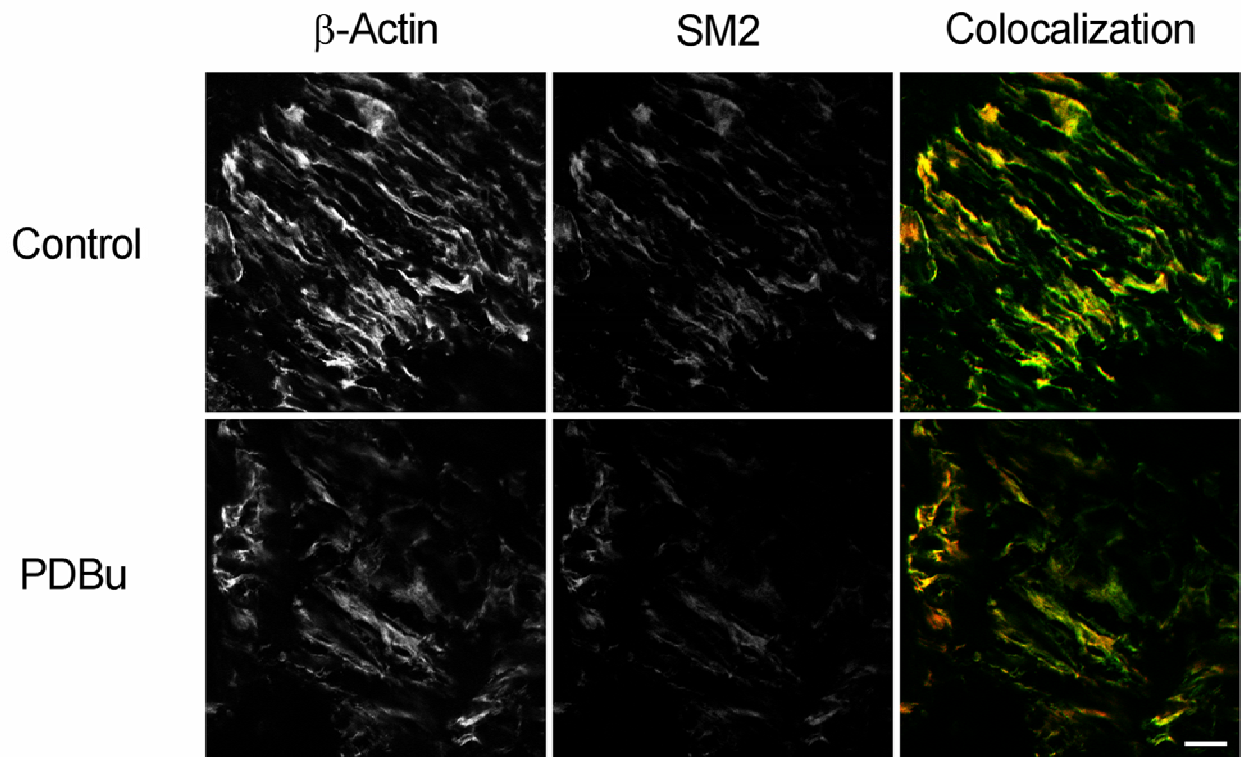


**Figure 6**  
Black et al.

**Figure 6.** Dual immunostaining of  $\beta$ -actin and SM2 in unstimulated (Control) and PDBu-activated aorta tissue. Sections were fixed with ice cold acetone.  $\beta$ -Actin was visualized with a monoclonal anti- $\beta$ -smooth muscle actin, clone AC-15 antibody. SM2 was visualized with a monoclonal anti-SM2 antibody, clone 3F8. Yellow color indicates colocalization of the two proteins. The white bar indicates 10  $\mu$ m.

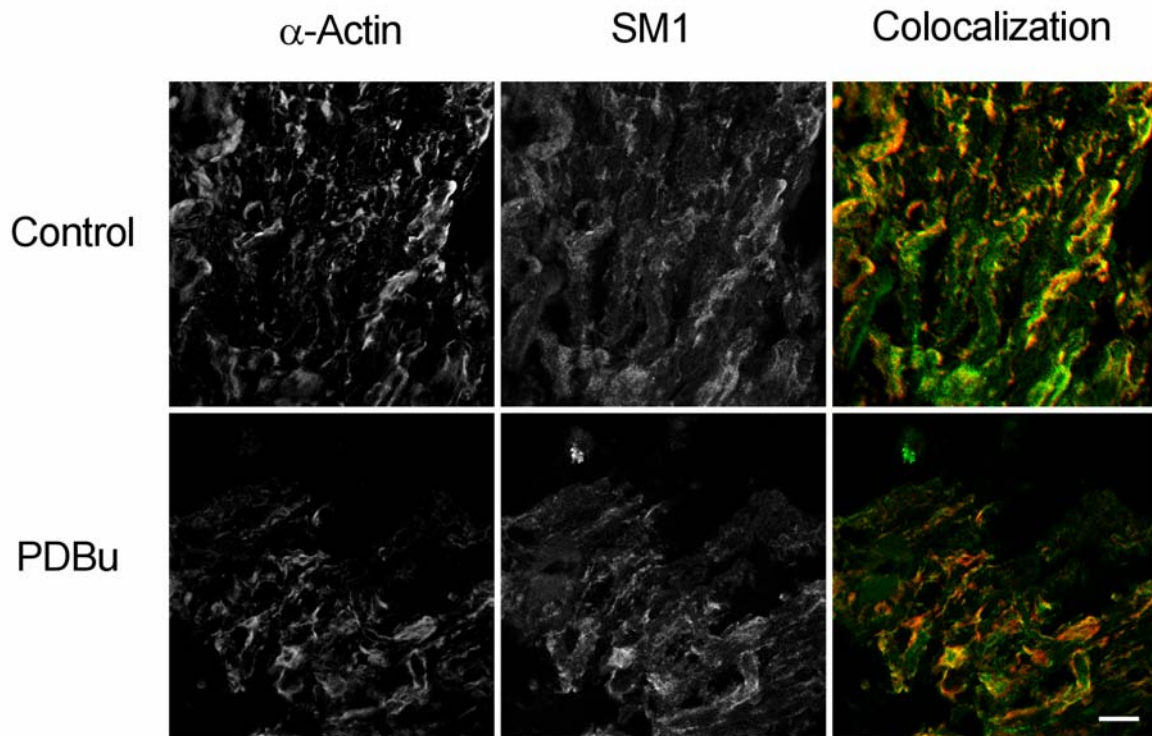


**Figure 7**  
Black et al.

**Figure 7.** Dual immunostaining of  $\alpha$ -actin and SM1 in unstimulated (Control) and PDBu-activated aorta tissue. Sections were fixed with ice cold acetone.  $\alpha$ -Actin was visualized with a monoclonal anti- $\alpha$ -smooth muscle actin, clone 1A4 antibody. SM1 was visualized with a monoclonal anti-SM1 antibody clone 1G12. Yellow color indicates colocalization of the two proteins. The white bar indicates 10  $\mu$ m.

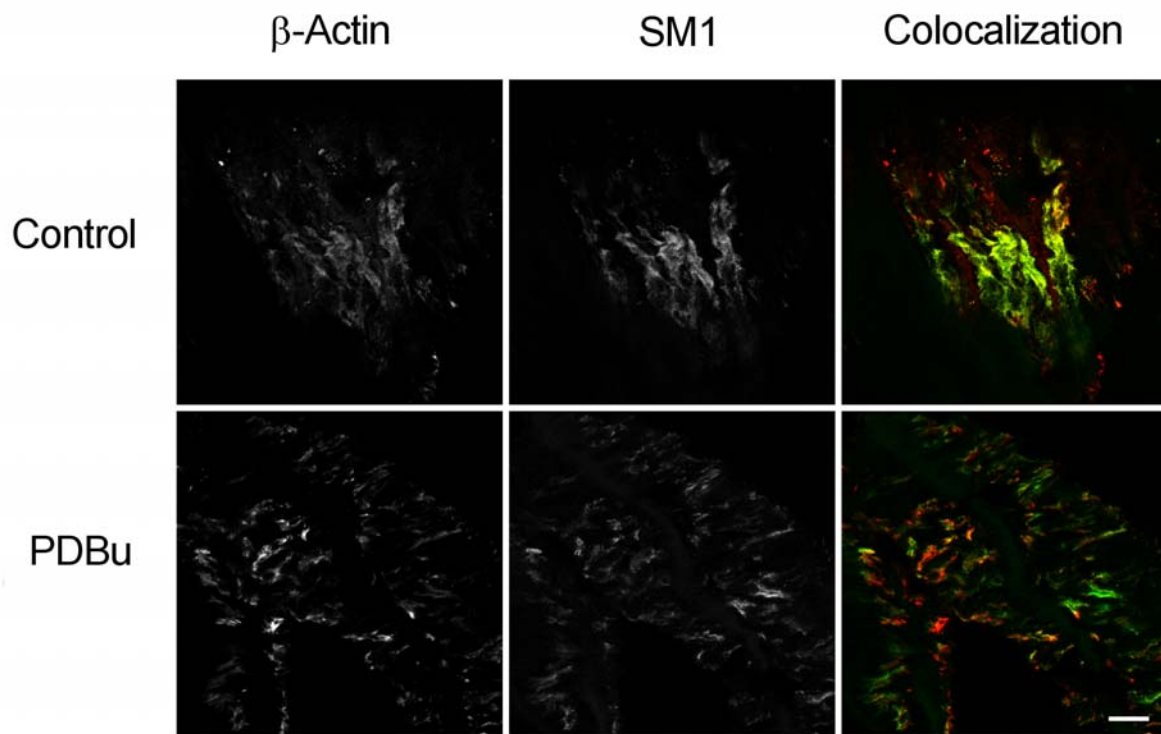


**Figure 8**  
Black et al.

**Figure 8.** Dual immunostaining of  $\beta$ -actin and SM1 in unstimulated (Control) and PDBu-activated aorta tissue. Sections were fixed with ice cold acetone.  $\beta$ -Actin was visualized with a monoclonal anti- $\beta$ -smooth muscle actin, clone AC-15 antibody. SM1 was visualized with a monoclonal anti-SM1 antibody clone 1G12. Yellow color indicates colocalization of the two proteins. The white bar indicates 10  $\mu$ m.

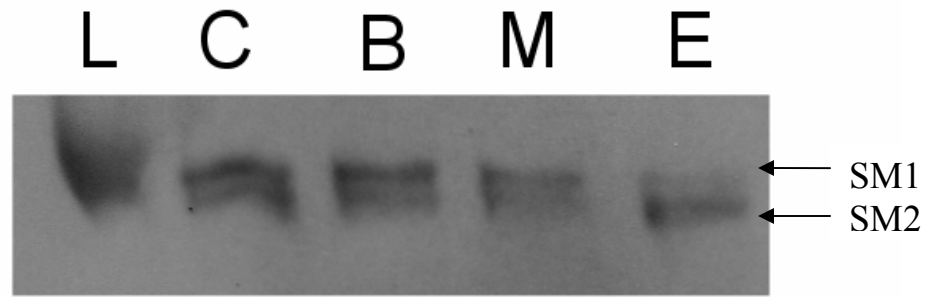


## Figure 9 Black et al.

**Figure 9.** Representative gel image of Western blot analysis of samples co-immunoprecipitated with anti- $\alpha$ -smooth muscle actin, clone 1A4 antibody. Myosin bands were visualized with an IgM-pan-myosin antibody and an anti-IgM secondary antibody conjugated with horseradish peroxidase. Upper band is the 204kDa SM1 and the lower is 200kDa SM2. L: Kaleidoscope ladder (Bio-Rad) (Myosin band is visible); C: Control; B: Beginning of contraction; M: Midpoint of contraction; E: Endpoint of contraction.

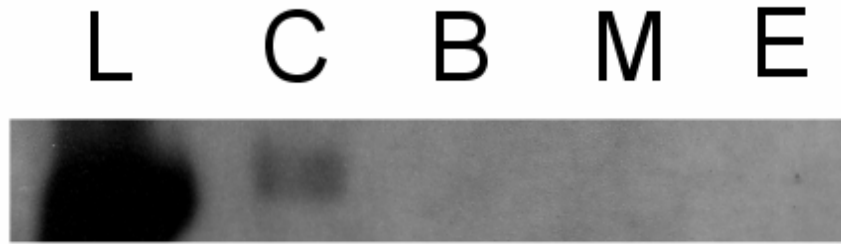


## Figure 10 Black et al.

**Figure 10.** Western blot analysis of samples co-immunoprecipitated with anti- $\beta$ -smooth muscle actin, clone AC-15 antibody. Myosin bands were visualized with an IgM-pan-myosin antibody and an anti-IgM secondary antibody conjugated with horseradish peroxidase. Upper band is the 204kDa SM1 and the lower is 200kDa SM2. L: Kaleidoscope ladder (Bio-Rad) (Myosin band is visible); C: Control; B: Beginning of contraction; M: Midpoint of contraction; E: Endpoint of contraction.



## Tables

**Table 1.** Fluorescence resonance energy transfer (FRET) analysis of the association of SM2 myosin with  $\alpha$ - and  $\beta$ -actin in Control and PDBu-stimulated A7r5 cells. The SM2 myosin isoform was visualized using monoclonal anti-SM2 antibodies.  $\alpha$ -Actin and  $\beta$ -actin were visualized with monoclonal anti- $\alpha$  smooth muscle actin clone 1A4 and anti- $\beta$ -actin clone AC-15 antibodies, respectively. Values represent the average of a minimum of 20 cells and reflect the percent increase in the fluorescence of the donor fluorophore (SM2) after photobleaching the acceptor fluorophore actin.

<b><u>Actin Isoform</u></b>	<b><u>Control</u></b>	<b><u>Contracted</u></b>
$\alpha$ -Actin	5.8 $\pm$ 1.8 %	8.8 $\pm$ 1.2 %
$\beta$ -Actin	9.6 $\pm$ 1.2 %	7.5 $\pm$ 1.3 %

**Table 2.** Fluorescence resonance energy transfer (FRET) analysis of the association of SM1 myosin with  $\alpha$ - and  $\beta$ -actin in Control and PDBu-stimulated A7r5 cells. The SM1 myosin isoform was visualized using monoclonal anti-SM1 antibodies.  $\alpha$ -Actin and  $\beta$ -actin were visualized with monoclonal anti- $\alpha$  smooth muscle actin clone 1A4 and anti- $\beta$ -actin clone AC-15 antibodies, respectively. Values represent the average of a minimum of 20 cells and reflect the percent increase in the fluorescence of the donor fluorophore (SM1) after photobleaching the acceptor fluorophore actin.

<b><u>Actin Isoform</u></b>	<b><u>Control</u></b>	<b><u>Contracted</u></b>
$\alpha$ -Actin	13.9 $\pm$ 1.9 %	9.6 $\pm$ 1.4 %
$\beta$ -Actin	17.7 $\pm$ 2.0 %	11.6 $\pm$ 2.1 %

**Table 3.** Fluorescence resonance energy transfer (FRET) analysis of the association of SM2 with  $\alpha$ - and  $\beta$ -actin in Control, Beginning, Midpoint, and Endpoint time points of PDBu-stimulated rat aorta smooth muscle tissue. SM2 was visualized using monoclonal anti-SM2 antibodies.  $\alpha$ -Actin and  $\beta$ -actin were visualized with monoclonal anti- $\alpha$  smooth muscle actin clone 1A4 and anti- $\beta$ -actin clone AC-15 antibodies, respectively. Values represent the average of a minimum of 10 sections and reflect the percent increase in fluorescence of the donor fluorophore (SM2) after photobleaching the acceptor fluorophore actin. \* Denotes  $p < 0.05$  when compared to control.

<b><u>Actin Isoform</u></b>	<b><u>Control</u></b>	<b><u>Beginning</u></b>	<b><u>Midpoint</u></b>	<b><u>Endpoint</u></b>
$\alpha$ -Actin	20.7 $\pm$ 2.1 %	15.0 $\pm$ 3.1 %	14.0 $\pm$ 4.5 %	11.0 $\pm$ 4.8 %
$\beta$ -Actin	21.1 $\pm$ 4.6 %	2.6 $\pm$ 3.3 %*	15.6 $\pm$ 3.0 %	7.9 $\pm$ 3.4 %*

**Table 4.** Fluorescence resonance energy transfer (FRET) analysis of the association of SM1 with  $\alpha$ - and  $\beta$ -actin in Control, Beginning, Midpoint, and Endpoint time points of PDBu-stimulated rat aorta smooth muscle tissue. SM1 was visualized using monoclonal anti-SM1 antibodies.  $\alpha$ -Actin and  $\beta$ -actin were visualized with monoclonal anti- $\alpha$  smooth muscle actin clone 1A4 and anti- $\beta$ -actin clone AC-15 antibodies, respectively. Values represent the average of a minimum of 10 sections and reflect the percent increase in fluorescence of the donor fluorophore (SM1) after photobleaching the acceptor fluorophore actin. \* Denotes  $p < 0.05$  when compared to control.

<b><u>Actin Isoform</u></b>	<b><u>Control</u></b>	<b><u>Beginning</u></b>	<b><u>Midpoint</u></b>	<b><u>Endpoint</u></b>
$\alpha$ -Actin	34.3 $\pm$ 5.4 %	28.7 $\pm$ 3.2 %	21.8 $\pm$ 2.6 %*	23.9 $\pm$ 3.7 %
$\beta$ -Actin	15.0 $\pm$ 2.8 %	5.8 $\pm$ 3.7 %	0.08 $\pm$ 3.3 %*	1.9 $\pm$ 2.2 %*

**Table 5.** Co-immunoprecipitation experiment results. Equal protein concentrations from aorta tissue lysate were treated with monoclonal anti- $\alpha$  smooth muscle actin clone 1A4. SDS-PAGE was performed on each sample and Western blots were performed using clone C5C.52 pan-anti-myosin antibody. Densitometry was performed on visualized bands and results were normalized to control levels.

<b><u>Myosin Isoform</u></b>	<b><u>Control</u></b>	<b><u>Beginning</u></b>	<b><u>Midpoint</u></b>	<b><u>Endpoint</u></b>
SM1	100 %	72 $\pm$ 27 %	29 $\pm$ 16 %	46 $\pm$ 39 %
SM2	100 %	81 $\pm$ 28 %	56 $\pm$ 54 %	100 $\pm$ 18 %

## **Discussion**

Our laboratory has reported that actin remodeling is an important element of contraction of aorta smooth muscle (Wright and Hurn 1994) and A7r5 embryonic rat aortic cells (Fultz et al. 2000). We have also shown that myosin remodels in the A7r5 cells during phorbol stimulated contraction (Fultz and Wright 2003). Such remodeling has also been verified by others (Mehta and Gunst 1999; Seow et al. 2000; Herrera et al. 2002; Burgstaller and Gimona 2004; Herrera et al. 2005). However, the exact nature of this remodeling, the mechanisms regulating it, and the means by which it conveys contractile properties to smooth muscle is still unknown. One centrally important question is how the different actin and myosin isoforms interact during remodeling. Our laboratory has shown that  $\alpha$ -actin and  $\beta$ -actin remodel differently in the A7r5 cell model when the cells are contracted with phorbol (Fultz et al. 2000; Brown et al. 2006). It is not certain to

what extent that actin and myosin remain associated during the dramatic reorganization of cytoskeletal actin (Fultz and Wright 2003).

There has been debate surrounding the different roles of the myosin tail isoforms, SM1 and SM2, in smooth muscle. Enzymatic activity differences in the myosin isoform have been attributed to the head isoforms (Rovner et al. 1997); whereas, it is thought that the tail isoforms are linked to structural differences in filaments and cell length (Meer and Eddinger 1997; Rovner et al. 2002) as well as to enzymatic activity (Martin et al. 1997). The present study focused on the tail isoforms and their associations with actin isoforms in the remodeling of the contractile apparatus in aorta smooth muscle. As a part of this investigation we utilized FRET analysis of protein-protein interaction. FRET is only effective when the fluorescent molecules are within 10nm of one another (Selvin 2000; Kenworthy 2001; Jares-Erijman and Jovin 2003). Because the SM1 and SM2 antibodies we used are specific for the different tail regions of myosin, the measurements we report are indicative of the association of myosin filaments containing these isoforms with thin filaments of  $\alpha$ -actin or  $\beta$ -actin which have been shown in the side-by-side arrangements in smooth muscle (Herrera et al. 2004; Herrera et al. 2005).

Selvin (2000) has suggested that FRET is better suited to the determination of changes in distance rather than absolute distances. For this reason, in our studies we have compared the differences (decreases/increases) of FRET values between samples at control and different time points in the contraction as an indicator of changes in actin-myosin association.

Studies with A7r5 smooth muscle cells verified previous findings (Fultz et al. 2000; Fultz and Wright 2003) regarding the extensive remodeling of the actin-myosin cytoskeletal system. FRET analysis suggested only minor levels of actin-myosin isoform association. There were no significant changes in FRET indices of association between control and PDBu-contracted cells although a trend for decreased interaction was noted for SM1 and actin isoforms of contracted cells (Table 1, 2).

By comparison, tissues showed evidence of highly significant levels of actin-myosin association (Tables 3, 4). Moreover, both SM2 and SM1 showed a strong tendency for decreased association with  $\alpha$ -actin and highly significant reductions in the association of these isoforms with  $\beta$ -actin during the course of the PDBu-induced contraction.

Differences between cells in culture and freshly isolated tissue could be due to differences in isoform expression, the fact that tissue cells are embedded in a matrix and are subject to cell-cell interaction, the loading (stretch) of tissues prior to contraction, or other differences between the two models. Although the apparent disassociation of actin and myosin during intervals of peak force development was unexpected these results were verified by co-immunoprecipitation experiments and are consistent with earlier confocal studies of actin-myosin colocalization in cells (Fultz and Wright 2003).

Importantly, these results are in direct opposition to the “latch” mechanism proposed by Hai and Murphy (1992) to explain the low energy cost of tension maintenance in smooth muscle. An alternate explanation is that during contractile remodeling cross-linking of actin filaments could hold the cell in the contracted configuration at low energy cost (Battistella-Patterson et al. 1997).

## References

Austin, J. C., S. K. Chacko, M. DiSanto, D. A. Canning and S. A. Zderic (2004). "A male murine model of partial bladder outlet obstruction reveals changes in detrusor morphology, contractility and Myosin isoform expression." J Urol **172**(4 Pt 1): 1524-8.

Babij, P. (1993). "Tissue-specific and developmentally regulated alternative splicing of a visceral isoform of smooth muscle myosin heavy chain." Nucleic Acids Res **21**(6): 1467-71.

Babij, P., C. Kelly and M. Periasamy (1991). "Characterization of a mammalian smooth muscle myosin heavy-chain gene: complete nucleotide and protein coding sequence and analysis of the 5' end of the gene." Proc Natl Acad Sci U S A **88**(23): 10676-80.

Babij, P. and M. Periasamy (1989). "Myosin heavy chain isoform diversity in smooth muscle is produced by differential RNA processing." J Mol Biol **210**(3): 673-9.

Battistella-Patterson, A. S., S. Wang and G. L. Wright (1997). "Effect of disruption of the cytoskeleton on smooth muscle contraction." Can J Physiol Pharmacol **75**(12): 1287-99.

Brown, D., A. Dykes, J. Black, S. Thatcher, M. E. Fultz and G. L. Wright (2006). "Differential actin isoform reorganization in the contracting A7r5 cell." Can J Physiol Pharmacol **84**(8-9): 867-75.

Burgstaller, G. and M. Gimona (2004). "Actin cytoskeleton remodelling via local inhibition of contractility at discrete microdomains." J Cell Sci **117**(Pt 2): 223-31.

DiSanto, M. E., R. H. Cox, Z. Wang and S. Chacko (1997). "NH<sub>2</sub>-terminal-inserted myosin II heavy chain is expressed in smooth muscle of small muscular arteries." Am J Physiol **272**(5 Pt 1): C1532-42.

Dykes, A. C., M. E. Fultz, M. L. Norton and G. L. Wright (2003). "Microtubule-dependent PKC- $\alpha$  localization in A7r5 smooth muscle cells." Am J Physiol Cell Physiol **285**(1): C76-87.

Fultz, M. E., C. Li, W. Geng and G. L. Wright (2000). "Remodeling of the actin cytoskeleton in the contracting A7r5 smooth muscle cell." J Muscle Res Cell Motil **21**(8): 775-87.

Fultz, M. E. and G. L. Wright (2003). "Myosin remodelling in the contracting A7r5 smooth muscle cell." Acta Physiol Scand **177**(2): 197-205.

Hai, C. M. and R. A. Murphy (1992). "Adenosine 5'-triphosphate consumption by smooth muscle as predicted by the coupled four-state crossbridge model." Biophys J **61**(2): 530-41.

Herrera, A. M., K. H. Kuo and C. Y. Seow (2002). "Influence of calcium on myosin thick filament formation in intact airway smooth muscle." Am J Physiol Cell Physiol **282**(2): C310-6.

Herrera, A. M., E. C. Martinez and C. Y. Seow (2004). "Electron microscopic study of actin polymerization in airway smooth muscle." Am J Physiol Lung Cell Mol Physiol **286**(6): L1161-8.

Herrera, A. M., B. E. McParland, A. Bienkowska, R. Tait, P. D. Pare and C. Y. Seow (2005). "'Sarcomeres' of smooth muscle: functional characteristics and ultrastructural evidence." J Cell Sci **118**(Pt 11): 2381-92.

- Jares-Erijman, E. A. and T. M. Jovin (2003). "FRET imaging." Nat Biotechnol **21**(11): 1387-95.
- Kelley, C. A., J. R. Sellers, P. K. Goldsmith and R. S. Adelstein (1992). "Smooth muscle myosin is composed of homodimeric heavy chains." J Biol Chem **267**(4): 2127-30.
- Kelley, C. A., M. Takahashi, J. H. Yu and R. S. Adelstein (1993). "An insert of seven amino acids confers functional differences between smooth muscle myosins from the intestines and vasculature." J Biol Chem **268**(17): 12848-54.
- Kenworthy, A. K. (2001). "Imaging protein-protein interactions using fluorescence resonance energy transfer microscopy." Methods **24**(3): 289-96.
- Kuro-o, M., R. Nagai, H. Tsuchimochi, H. Katoh, Y. Yazaki, A. Ohkubo and F. Takaku (1989). "Developmentally regulated expression of vascular smooth muscle myosin heavy chain isoforms." J Biol Chem **264**(31): 18272-5.
- Low, R. B., J. Mitchell, J. Woodcock-Mitchell, A. S. Rovner and S. L. White (1999). "Smooth-muscle myosin heavy-chain SM-B isoform expression in developing and adult rat lung." Am J Respir Cell Mol Biol **20**(4): 651-7.
- Martin, A. F., S. Bhatti and R. J. Paul (1997). "C-terminal isoforms of the myosin heavy chain and smooth muscle function." Comp Biochem Physiol B Biochem Mol Biol **117**(1): 3-11.
- Meer, D. P. and T. J. Eddinger (1997). "Expression of smooth muscle myosin heavy chains and unloaded shortening in single smooth muscle cells." Am J Physiol **273**(4 Pt 1): C1259-66.



Mehta, D. and S. J. Gunst (1999). "Actin polymerization stimulated by contractile activation regulates force development in canine tracheal smooth muscle." J Physiol **519 Pt 3**: 829-40.

Nagai, R., M. Kuro-o, P. Babij and M. Periasamy (1989). "Identification of two types of smooth muscle myosin heavy chain isoforms by cDNA cloning and immunoblot analysis." J Biol Chem **264**(17): 9734-7.

North, A. J., M. Gimona, Z. Lando and J. V. Small (1994). "Actin isoform compartments in chicken gizzard smooth muscle cells." J Cell Sci **107 ( Pt 3)**: 445-55.

Paul, R. J. (1983). "Functional compartmentalization of oxidative and glycolytic metabolism in vascular smooth muscle." Am J Physiol **244**(5): C399-409.

Rovner, A. S., P. M. Fagnant, S. Lowey and K. M. Trybus (2002). "The carboxyl-terminal isoforms of smooth muscle myosin heavy chain determine thick filament assembly properties." J Cell Biol **156**(1): 113-23.

Rovner, A. S., Y. Freyzon and K. M. Trybus (1997). "An insert in the motor domain determines the functional properties of expressed smooth muscle myosin isoforms." J Muscle Res Cell Motil **18**(1): 103-10.

Rovner, A. S., M. M. Thompson and R. A. Murphy (1986). "Two different heavy chains are found in smooth muscle myosin." Am J Physiol **250**(6 Pt 1): C861-70.

Selvin, P. R. (2000). "The renaissance of fluorescence resonance energy transfer." Nat Struct Biol **7**(9): 730-4.

Seow, C. Y., V. R. Pratushevich and L. E. Ford (2000). "Series-to-parallel transition in the filament lattice of airway smooth muscle." J Appl Physiol **89**(3): 869-76.

White, S. L., M. Y. Zhou, R. B. Low and M. Periasamy (1998). "Myosin heavy chain isoform expression in rat smooth muscle development." Am J Physiol **275**(2 Pt 1): C581-9.

Wright, G. and E. Hurn (1994). "Cytochalasin inhibition of slow tension increase in rat aortic rings." Am J Physiol **267**(4 Pt 2): H1437-46.

## Chapter IV

### Summary and Conclusion

**General Discussion.** Smooth muscle contraction has been a topic of investigation in our laboratory for well over a decade. Much work has focused on actin isoforms and the remodeling of actin and myosin during contraction. However, a major gap in the knowledge developed by our laboratory and others is in the relationship of actin and myosin during contraction in which both filament types are seen to undergo substantial reorganization. Secondly, it would be important to establish if cytoskeletal remodeling seen in isolated cells is comparable to that occurring in differentiated cells in tissue. In the studies presented in this dissertation, we have used both the A7r5 cell model and rat aorta rings to examine smooth muscle contraction in cells and tissue contracted with phorbol-12, 13-dibutyrate (PDBu). Confocal microscopy has been our primary method of observing the activity of cytoskeletal remodeling and contractile apparatus rearrangement at the cellular level. In addition, we have used a well-established technique, fluorescent resonance energy transfer (FRET) in a novel way to examine the myosin-actin protein interaction during contraction. Finally, we used another well-established technique, co-immunoprecipitation, to confirm the results of our FRET analysis.

We first examined the association of smooth muscle myosin with  $\alpha$ -actin and  $\beta$ -actin isoforms in A7r5 cells. Our results show that these associations are not static, but change throughout contraction. Comparison of endpoint to control showed a large decrease of myosin association with  $\alpha$ -actin, but association with  $\beta$ -actin remained unchanged. Time course studies showed that the association of myosin with  $\alpha$ -actin increased at the initiation of contraction but decreased as the contraction continued. Our studies in tissue showed similar results; however, the association of myosin with  $\alpha$ -actin increased at the endpoint of contraction. This difference between cells and tissue is an important

observation and can be attributed to the difference in the models. Isolated cells are not under constant tension, but are “unloaded”, whereas the aorta rings were maintained under constant tension. Perhaps more importantly, cells in tissue are embedded in a matrix and are subject to extensive cell-cell interaction. In tissue, myosin association with  $\beta$ -actin remained unchanged except for a significant decrease during the midpoint of contraction. By comparison association with  $\alpha$ -actin increased at the start and end but, similar to  $\beta$ -actin, decreased at the midpoint of contraction. Based on these data, we suggest that the midpoint of contraction is a significant time of remodeling of the contractile apparatus in which the association of myosin with each isoform of actin is decreased. Studies using phalloidin staining support this contention indicating that at the midpoint tissues had less F-actin content than seen in the beginning and end of contraction. We also report the occurrence of large actin fibers and patches throughout contraction of tissue. We concluded that these results suggest heterogeneous remodeling of the cytoskeleton and rearrangement of the contractile apparatus takes place during contraction of rat aorta smooth muscle, likely in response to heterogeneous strain resulting from internal force development. This reorganization and focus of contractile machinery at specific points of strain could explain how smooth muscle develops strong contractile force with relatively low levels of myosin.

Our next study examined the changes in interaction of the different myosin carboxyl isoforms, SM1 and SM2, with  $\alpha$ -actin and  $\beta$ -actin. Studies in A7r5 cells showed that the interaction of SM1 with each actin isoform tended to be decreased during contraction compared to control; whereas SM2 interaction with each actin isoform was unchanged, again indicating isoform specific remodeling. In tissue, the interaction of SM1 and SM2 with  $\alpha$ -actin was similar and tended to decrease with contraction. The interaction with  $\beta$ -actin was also similar with both myosin isoforms showing a dramatic decrease in

association once contraction began. Co-immunoprecipitation experiments showed similar trends as seen with FRET analysis.  $\beta$ -Actin association with each myosin isoform was shown to be undetectable at all time points of contraction, while the interaction with  $\alpha$ -actin was only slightly changed. These results confirm that significant remodeling of the contractile apparatus occurs with the actin isoforms interacting differently with myosin isoforms. In addition, these findings further suggest that the full complement of the actin-myosin complex is not utilized at peak points of force development.

These studies provide evidence against the suggestion that smooth muscle maintains tension with low energy output with slow cycling myosin-actin crossbridges, the “latch” hypothesis. What we see is not increased actin-myosin association at the endpoint of contraction, but the opposite. Myosin appears to disassociate from actin, yet tension is maintained. The hypothesis proposed by our laboratory has been that tension is maintained via cross-linking of the actin cytoskeleton. The actin fibers remodel and reorganize throughout smooth muscle contraction. These fibers are then cross-linked, possibly by myosin, and the apparatus is in essence “locked-up” at its contracted length. This enables the cell to remain contracted with very low energy expenditure. These studies provide evidence that supports this hypothesis.

**Future work.** Ideally, FRET should be performed with fluorescent molecules directly attached to the molecules under examination. Doing this with myosin and actin would be an important step in confirming these results. In such experiments one could examine both filament association as well as the interaction of the myosin head with actin. Another aspect that could be examined is the importance of the myosin head isoforms in this remodeling of the contractile apparatus. It has been reported that these isoforms affect the enzymatic activity of myosin, but they could also contribute to a structural

role. Finally, using a modified cell model with aorta cells cultured in a collagen matrix could allow a more detailed view of the influence of the matrix and cell-cell interaction on results. Of great interest is the finding that actin-myosin association declines during contraction. This observation provides direct evidence against the “latch” hypothesis of tension maintenance and supports our early contention that the low energy cost of this activity could be due to locking of the cytoskeleton in the contracted configuration by cross-linking of filaments. Future studies of cross-linking activity during contraction would, therefore be interesting in testing this hypothesis.

## Jason E. Black

### Contact Information:

Department of Pharmacology, Physiology, and Toxicology  
Joan C. Edwards School of Medicine  
Marshall University  
1542 Spring Valley Drive  
Huntington, WV 25704  
Lab Phone (304) 696-7363  
Cell Phone (304) 208-6443  
black46@marshall.edu

### Education:

Doctoral Candidate, Biomedical Sciences (expected Graduation July 2007), Joan C. Edwards School of Medicine, Marshall University, August-December 1999, August 2000-present.

B.S. Biochemistry, Ohio Northern University, May 1995.

### Awards and Honors:

Clyde & Frances Augsburger Scholarship for high academic performance, 1994, 1993, 1992

Chemistry Alumni Scholarship for high performance in chemistry, 1993

Phi Eta Sigma, Freshman honorary, 1992

### Research:

August 2000-Present, Graduate Student, Ph.D. Program, Joan C. Edwards School of Medicine, Huntington, WV; "Myosin and Myosin Isoforms in Smooth Muscle Contraction," Co-advisors: Gary L. Wright, Department of Pharmacology, Physiology and Toxicology and Elizabeth C. Bryda, Department of Microbiology, Immunology and Molecular Genetics

### Publications:

Peer Reviewed

Effect of experimental hyperhomocysteinemia on cardiac structure and function in the rat, Ernest Walker, Jason Black, *et al.*, *Annals of Clinical & Laboratory Science*, vol.34, no.2, pp.175-180, 2004.

Differential actin isoform reorganization in the contracting A7r5 cell, D. Brown, A. Dykes, J. Black, S. Thatcher, M.E. Fultz, and G.L. Wright, *Canadian Journal of Physiology and Pharmacology*, vol.84, no.8-9, pp. 867-875, August/September 2006.

## Manuscripts under Review

FRET analysis of actin/myosin interaction in contracting aortic smooth muscle, J. Black, *et al.*

## Manuscripts in Preparation

Interaction of smooth muscle myosin II isoforms with actin isoforms in A7r5 cells and rat aortic tissue, J. Black, *et al.*

MLCK/actin interaction in contracting rat aortic smooth muscle, S.E. Thatcher, J. Black, H. Tanaka, and G.L. Wright.

MMP-2 and MMP-9 localization in the contracting A7r5 smooth muscle cell, S.E. Thatcher, J. Black, D. Brown, and G.L. Wright.

## Abstracts Presented:

### National Meetings

Experimental Biology (Washington, D.C.), 2007

Poster Presentation: FRET analysis of Sm2 interaction with actin isoforms in rat aorta smooth muscle cells and tissue, J.E. Black and G.L. Wright.

The American Society of Cell Biology (San Diego, CA), 2006

Poster Presentation: SM2 Interaction with Actin Isoforms in Contracting Rat Aorta Smooth Muscle Cells and Tissue, J.E. Black and G.L. Wright.

Experimental Biology (San Francisco, CA), 2006

Poster Presentation: FRET analysis of actin/myosin association in aortic smooth muscle, J.E. Black and G.L. Wright.

The American Society of Cell Biology (San Francisco, CA), 2005

Poster Presentation: FRET analysis comparing myosin II isoforms in contracting A7r5 smooth muscle cells, J.E. Black and G.L. Wright.

### Local Meetings

Joan C. Edwards School of Medicine Research Day, (Huntington, WV), 2007

Poster Presentation: SM2 Interaction with Actin Isoforms in Contracting Rat Aorta Smooth Muscle Cells and Tissue, J.E. Black, *et al.*

Sigma Xi Research Day: Marshall University Chapter (Huntington, WV), 2003

Poster Presentation: Altered gene expression in rats due to increased levels of homocysteine, J.E. Black, *et al.*



Joan C. Edwards School of Medicine Research Day, (Huntington, WV), 2003  
Poster Presentation: Altered gene expression in rats due to increased levels of homocysteine, J.E. Black, *et al.*

Joan C. Edwards School of Medicine Research Day, (Huntington, WV), 2002  
Poster Presentation: Apolipoprotein regulation in a rat model of obesity, J.E. Black, *et al.*

### **Research Methods and Techniques:**

Whole animal (rat) studies and surgeries, Cell culture (A7r5), Bacterial culture, Molecular cloning, Restriction digest, Isolation of DNA, RNA, & Protein, Polymerase chain reaction, Real-time PCR, RT-PCR, Polyacrylamide gel electrophoresis, Two-dimensional PAGE, Western Blot analysis, Confocal Microscopy, Fluorescence resonance energy transfer, Echocardiography & Electrocardiography of rats, Tissue sectioning, MALDI-TOF mass spectrometry

### **Workshops Attended:**

WV-BRIN Bioinformatics Workshop: Introduction to Bioinformatics, Gene Mapping and Functional Genomics, June 2002, Marshall University, Huntington, WV

Grant Writing Workshop administered by Grant Writers' Seminars and Workshops, LLC, Stephen W. Russell and David C. Morrison, November 2002, Joan C. Edwards School of Medicine, Marshall University

### **Professional Societies:**

American Society of Cell Biology

### **Teaching:**

Guest lecture for Cell Physiology, "The Mammalian Cell Cycle: An Overview", 2005

Supervised an American Heart Association summer student, Stephen Peterson, 2003

Graduate Assistant: Tutored students in Math, Biology, and Chemistry as part of the Higher Education for Learning Problems program, August 2000- May 2002

Tutored Students in Chemistry and Physics, Fall 1993- Spring 1995

### **Academic Service:**

Biomedical Sciences Funding Committee, April 2005

**Community Service:**

Taught students in the Bath County Senior High School TAG program about DNA and protein and instructed them in experiments to collect DNA and to perform SDS-PAGE in summer of 2006.

Dissected rats for local fifth grade classes at Cammack Middle School in spring of 2002 and 2003 and for an eighth grade class at Our Lady of Fatima School in spring of 2004.

Elder, Treasurer, Small group director, and Small group leader of Crew Community Church in Huntington, WV, 2006-2007.

Taught Sunday school and Bible study classes at Crown City United Methodist Church 1996-March 2006.

**References:**

Gary L. Wright, Ph.D., Department of Pharmacology, Physiology and Toxicology, Joan C. Edwards School of Medicine, Marshall University, 1542 Spring Valley Drive, Huntington, WV 25704, (304) 696-7368

Elizabeth C. Bryda, Ph.D., Department of Veterinary Pathobiology, University of Missouri, Columbia, MO 65211, (573) 882-5504

William McCumbee, Ph.D., Department of Pharmacology, Physiology and Toxicology, Joan C. Edwards School of Medicine, Marshall University, 1542 Spring Valley Drive, Huntington, WV 25704, (304) 696-7366